The Dissertation Committee for Joohoon Kim certifies that this is the approved version of the following dissertation:

Development of Microdevices for Applications to Bioanalysis

Committee:

Richard M. Crooks, Supervisor

Andrew D. Ellington

Jennifer S. Brodbelt

John T. McDevitt

Lynn Loo

Development of Microdevices for Applications to Bioanalysis

by

Joohoon Kim, B.S.; M.S.

Dissertation

Presented to the Faculty of the Graduate School of

The University of Texas at Austin

in Partial Fulfillment

of the Requirements

for the Degree of

Doctor of Philosophy

The University of Texas at Austin

August, 2007

Dedication

Praise my God.

To my wife, Sunja Kim,

And my mother, Soonhwa Park.

But he knows the way that I take; when he has tested me, I will come forth as gold.

(JOB 23:10)

Acknowledgements

Development of Microdevices for Applications to Bioanalysis

Publication No._____

Joohoon Kim, Ph. D.

The University of Texas at Austin, 2007

Supervisor: Richard M. Crooks

The development of microdevices for applications related to bioanalysis is described. There are two types of microdevices involved in this study: DNA (or RNA) microarrays and bead-based microfluidic devices. First, a new method to fabricate DNA microarrays is developed: replication of DNA microarrays. It was shown that oligonucleotides immobilized on a glass master can hybridize with their biotin-modified complements, and then the complements can be transferred to a streptavidin-functionalized replica surface. This results in replication of the master DNA array. Several innovative aspects of replication are discussed. First, the zip code approach allows fabrication of replica DNA arrays having any configuration using a single, universal master array. It is demonstrated that this approach can be used to replicate master arrays having three different sequences (spot feature sizes as small as 100 μm) and that master arrays can be used to prepare multiple replicas. Second, it is shown that a surface T4 DNA polymerase reaction improves the DNA microarray replication method by removing the requirement for using presynthesizd oligonucleotides. This in-situ, enzymatic synthesis approach is used to replicate DNA master arrays consisting of 2304

spots and arrays consisting of different oligonucleotide sequences. Importantly, multiple replica arrays prepared from a single master show consistent functionality to hybridization-based application. It is also shown that RNA microarrays can be fabricated utilizing a surface T4 DNA ligase reaction, which eliminates the requirement of modified RNA in conventional fabrication schemes. This aspect of the work shows that the replication approach may be broadly applicable to bioarray technologies. A different but related aspect of this project focuses on biosensors consisting of microfluidic devices packed with microbeads conjugated to DNA capture probes. The focus here is on understanding the parameters affecting the hybridization of DNA onto the probe-conjugated microbeads under microfluidic flow conditions. These parameters include the surface concentration of the probe, the flow rate of the solution, and the concentration of the target. The simple microfluidic device packed with probe-conjugated microbeads exhibits efficient target capture resulting from the inherently high surface-area-to-volume ratio of the beads, optimized capture-probe surface density, and good mass-transfer characteristics. Furthermore, the bead-based microchip is integrated with a hydrogel preconcentrator enhancing the local concentration of DNA in a microchannel. The integration of the preconcentrator into the bead-based capture chip allows significantly lower limit of detection level (~10-fold enhancement in the sensitivity of the microbead-based DNA detection).

Table of Contents

List of Tables

List of Figures

List of Schemes

Chapter 1: Introduction

1.1 MOTIVATION AND OBJECTIVES

Miniaturized analytical systems have received much attention in chemistry primarily because of their unique advantages compared to traditional macro-scale analytical tools: short analysis times, small sample/reagent consumption, low waste production, portability, task integration and automation, disposability, and high-throughput analysis.[1-4] These benefits are especially useful for analysis of biological materials. For example, microarrays and microfluidic devices have demonstrated their potential for a number of bioanalysis applications. Specifically, DNA microarrays have revolutionized genetic analysis.[5-7] Traditional tools used to study genomics, such as gel electrophoresis[8] and high-performance liquid chromatography[9] (HPLC) for single-nucleotide polymorphism (SNP) detection, require tedious serial steps and result in low-throughput analysis. The advent of DNA microarrays, a highly parallel analysis technique, has enabled researchers to assay thousands of genes simultaneously using a single microarray.[10,11] In addition, highly integrated microfluidic devices (so called, lab-on-a-chip systems) have demonstrated the potential to replace bulky equipment and trained technicians with a single chip-sized device.[12,13]

Microdevices are fabricated using lithography, but this family of methods usually requires special clean room facilities and expensive lithographic tools, which add to the cost of the devices. For example, one of two existing approaches for fabricating DNA microarrays relies on sequential photolithographic and chemical coupling steps.[14-18] The other approach uses direct delivery of pre-synthesized oligonucleotides, but even this method requires an expensive robotic microarrayer to spot the DNA solutions.[5,19]

1

Therefore, it would be desirable to develop a new cost-effective approach. This issue will be addressed in Chapters 3-6 of this dissertation.

Miniaturized analytical devices often enable better performance, such as faster analysis time, because of their small size when compared to macro-scale devices. For instance, analyte molecules placed in a large volume will take more time to collide and to react with each other than if placed in a small and confined microchannel environment. Here, we assume the same number of analyte molecules in different volumes. The performance of microfluidic devices, however, depends on many other parameters. For example, the ability of surface-immobilized probes to capture analytes in microfluidic devices will depend on other factors like probe surface concentration, solution flow rate, and target concentration. Further study of these parameters is necessary for understanding and designing efficient microfluidic systems. Chapter 7 will address this issue.

Miniaturized devices enable processing of very small volumes of analytes, which can be useful for analysis of small quantities of biological materials. However, analysis of small sample quantities in microchips requires high detection sensitivity. For example, the demand for sensitive chip-based DNA detection has encouraged many researchers to enhance the sensitivity of DNA detection in several ways. Various approaches, including polymerase chain reaction (PCR) chips for simultaneous DNA amplification and detection,[20,21] electrokinetically controlled DNA chips,[22,23] and mixing-assisted DNA chips,[24-26] have been suggested for rapid and sensitive detection of DNA hybridization. However, amplification approaches without PCR steps on a chip, which would provide rapid and sensitive DNA detection with simpler chip design, have rarely been explored. Chapter 8 will address the sensitivity issue of bead-based microfluidic devices.

My dissertation studies have focused on understanding and optimizing microarrays and microfluidic devices. First, a new method to fabricate microarrays,

which is efficient in terms of fabrication time and cost, is discussed in Chapters 3-6.[27-29] Specifically, I will show that a single master microarray can be replicated multiple times through mechanical transfer of oligonucleotides from the master surface to a replica surface. Indeed, the oligonucleotides for the replica can even be synthesized directly on the master surface using surface enzymatic reactions. In this microarray fabrication approach, the synthesis and transfer of oligonucleotides proceeds in parallel, which is more efficient than serial methods based on spotting. Second, I have studied bead-based microfluidic devices for DNA sequence analysis. These experiments focused on a simple microfluidic device packed with probe DNA conjugated to polymeric microbeads to examine the parameters affecting hybridization of target DNA under microfluidic flow conditions (Chapter 7).[30] In some cases, these simple microfluidic chips incorporated a hydrogel-based preconcentrator to enhance the local concentration of DNA targets inside the microchannels, and thereby lower the limit of detection (Chapter 8).[31]

1.2 MICROARRAYS

Definition of Microarrays A microarray is a solid substrate having thousands of specific probe spots on its surface. A mixture of labeled analytes, called the targets, is introduced and may specifically bind to molecular recognition agents, called the probes, on the microarray surface. The specific recognition events can be identified because of the fixed spatial positions of probes. The microarray platform provides a number of independent assays performed under essentially identical conditions, which enables researchers to investigate a large number of targets simultaneously using a single microarray.

Microarrays can be classified depending on types of probes: nucleic acids (oligonucleotides or PCR products), proteins, and cells. DNA microarrays consist of

nucleic acids immobilized on supports. DNA microarray assays are based on hybridization of complementary sequences through Watson-Crick base pairing. The same general concepts used for DNA microarrays have been applied to protein microarrays consisting of antibodies (the probes) that recognize specific proteins. Protein microarrays are useful to directly investigate proteins that are translated from messenger RNA (mRNA). The applications of protein microarrays include high-throughput antibody screening[32,33] and the study of protein-protein interactions or protein-small molecule interactions.[34] In addition to nucleic acids and proteins, cells have also been immobilized onto substrates in a microarray format. Cell microarrays have advanced the study of cell-surface interactions and extracellular matrix (ECM) compositions, the discovery of new materials for tissue engineering, and the screening of small molecules for drug discovery.[35,36]

Although the different types of microarrays usually share many basic principles, physicochemical differences between probes lead to unique fabrication methods and assay practices.[37] For example, it is more difficult to fabricate protein and cell microarrays compared to DNA microarrays. This is because fragile proteins might lose their function and binding ability during printing and immobilization on the substrate. In addition, most protein microarrays are fabricated from a small library of proteins compared to DNA microarrays. This is due to challenges in sample preparation (synthesis, isolation, and purification of the protein probes). For instance, proteins cannot be easily amplified by the PCR process used for nucleic acids. Furthermore, unlike DNA, it is difficult to find probe antibodies having strong specific interactions with target proteins. This dissertation focuses mainly on DNA arrays, but it is likely that the general principles can be extended to other types of microarrays.

Importance of DNA Microarrays Progress in DNA microarray technology has enabled its use in various biological applications since it originated as a new technique for large-scale gene expression studies.[5] Researchers have applied microarray technology not only for gene expression profiling, but also for SNP genotyping,[38-40] resequencing,[41-43] pathogen detection,[44,45] and high-throughput screening for drug discovery.[46-48] The wide use of DNA microarrays is derived from the unique high-throughput analysis capability of microarrays. The parallel analysis capability comes from a spatially encoded array in which each probe spot is used to determine the amount of target in a biological sample. Because each assay at the numerous probe spots is carried out simultaneously on a single array surface, high-throughput analysis is typically highly reproducible and quantitative. In addition, the miniaturized array slides are fabricated in a standardized format (typically glass slides measuring 75 mm x 25 mm) and can be monitored using commercial laser scanners, both of which enhance automation.

Conventional Methods for Fabrication of DNA Microarrays Fabrication methods for DNA microarrays can be categorized mainly into two approaches: direct synthesis and delivery of pre-synthesized oligonucleotides.[37,49-51] Each category can be subclassified depending on the specific features of each method. For example, Table 1.1 classifies the techniques in each category as serial or parallel.

Each technique has its strengths and weaknesses. Direct synthesis approaches synthesize oligonucleotides (probes) in-situ on substrates through repetitive synthesis cycles. Each synthesis cycle consists of two steps as shown in Figure 1.1: the deprotection step and the coupling step. The deprotection steps can be spatially directed onto individual probe spots using light (photodeprotection: parallel), microelectrodes (electrochemical deprotection: parallel), or jet dispensers of reagents (chemical

5

Table 1.1 Microarray fabrication techniques.

Direct synthesis		Delivery	
Parallel	Serial	Parallel	Serial
Photolithographic mask	Jet dispenser	Microstamping	Pin-printing
Digital micromirror			Nano-tips
Electrode-directed synthesis			Jet-printing
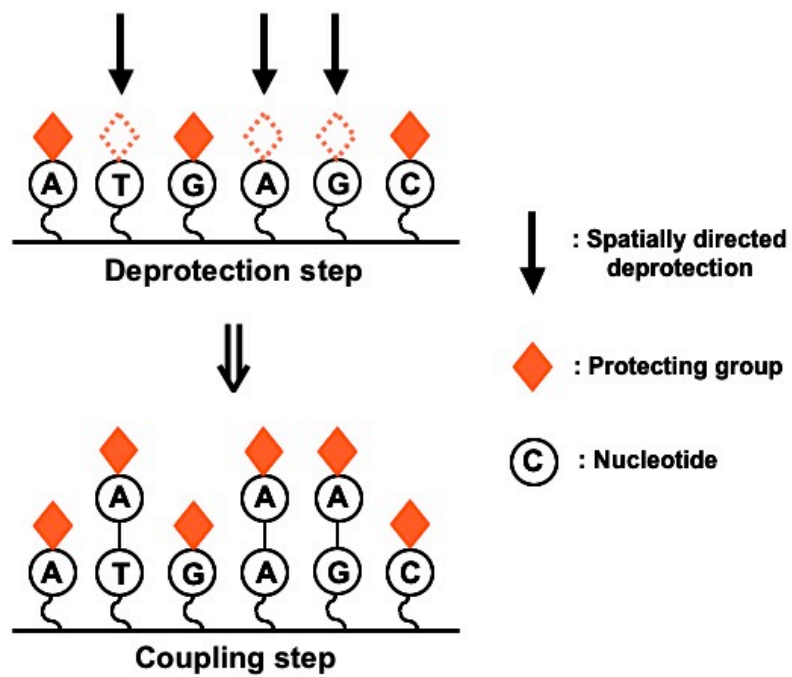
Figure 1.1. Schematic illustration of a synthesis cycle in direct synthesis approaches.

deprotection: serial). The coupling steps are performed at all deprotected sites simultaneously.

In the photolithographic technique[14,15,52] (commercialized by Affymetrix Inc., Santa Clara, CA), a surface is initially coated with linker molecules bearing removable photo-protecting groups. The photodeprotection can then be spatially directed using photolithographic masks. The deprotected areas are coupled to building blocks (base units with a photoprotecting group) that are exposed to the whole surface. This synthesis cycle is repeated to build up different oligonucleotide sequences at different sites. Even though this method enables synthesis of 4^l different sequences of length l in high-density array formats, it requires repetition of 4 x l synthesis cycles.[49] In practice, the efficiency of the overall synthesis cycles, which is the product of the yields of each individual step, becomes low as the cycles repeat because of the limited yield of individual steps. Therefore, the low yield limits the practical maximum length of oligonucleotides (for example, 25mers for the Affymetrix GeneChip Arrays). In addition, failure of photodeprotection or coupling reactions at any stage results in oligonucleotide sequence errors. The flexibility of the photomask-based technique is also limited by the large number of masks needed for synthesis of different oligonucleotide sequences. That is, many new photomasks are required for each unique chip layout (probe sequence).

Digital micromirror-based techniques (commercialized by NimbleGen Systems Inc., Madison, WI) allow more flexible on-chip synthesis by directing photodeprotection steps using digitally controlled micromirrors.[16-18] The function of the micromirror array is digitally programmable and replaces the static photomasks required in the photolithographic mask-based technique. Both the Affymetrix and NimbleGen approaches can achieve spot sizes down to 16 μm^2 and arrays having up to 400,000 probe spots on a 1.6 cm^2 area.[16,49]

In addition to guiding deprotection steps with light, chemical deprotection reagents can be delivered using jet dispensers, which are similar to those used in ink-jet printers.[53,54] The jet dispenser-based technique requires low volatility and high viscosity solvents having high surface tension to prevent evaporation and mixing of reagents at adjacent probe spots. In contrast to photolithographic or micromirror-based techniques, this method involves serial deprotection, and therefore it can be time consuming to fabricate high-density arrays. Another variant of the direct synthesis approach uses electrochemistry to facilitate in-situ synthesis of oligonucleotides (commercialized by CombiMatrix Corp., Mukilteo, WA).[55] Programmable microelectrodes situated at the spots produce acid locally to electrochemically induce deprotection, thus initiating DNA synthesis. The electrode-directed synthesis, however, still remains in its early development stage and involves expensive microelectrode fabrication schemes.

DNA microarrays can also be fabricated by delivering pre-synthesized oligonucleotides onto solid substrates. Compared to direct synthesis approaches, these methods have the advantage that the sequences of oligonucleotides delivered to the array are exactly those desired. The delivery of pre-synthesized oligonucleotides is performed either by contact or noncontact printing.

Contact printing methods include pin-printing, nano-tip printing, and microstamping techniques while jet-printing techniques are classified as noncontact printing methods. The pin-printing technique utilizes solid pins to deposit small amounts of the probe solution, usually, 50 pL - 100 nL corresponding to spot sizes in the range of 75 - 500 μm,[49] by contacting the pins with the microarray substrates. The pin-printing arrayer has evolved into a robotic arm system having an array of pins, which moves the pins among different probe solutions, array substrates, and a washing station (Figure 1.2). The technique is widely used in small laboratories to generate customized arrays having a
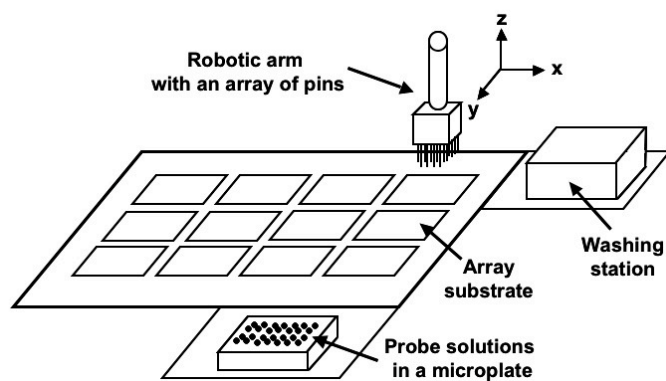
Figure 1.2. Schematic illustration of a pin-printing microarrayer.

moderate density of spots, because it is reasonably robust and affordable. The nano-tip printing technique is similar to pin-printing in terms of solution dispensing, but it employs an atomic force microscopy (AFM) nano-tip to deliver probes to the array substrate (this method is also known as dip-pen lithography).[56,57] When the AFM tip is brought into contact with the substrate, the probe solution flows from the tip to the substrate. The AFM tip can also be used to remove sections of a self-assembled monolayer (SAM) (in this case, molecules resisting biomolecule adsorption) on selected areas and simultaneously deposit another SAM of probe molecules. This method is known as AFM grafting.[58,59] The nano-tip printing technique can achieve nanoscale spot sizes and more complex shapes. The contact printing methods have some quality issues related to spot morphology. For example, ring-shaped spots are commonly observed in the contact printing methods. These result from formation of spots having greater probe density at the edges of the spots than in the middle. This phenomenon is explained in terms of simple physics: evaporation of a solution causes outward flow of molecules to spot edges, and physical contact with solid pins results in surface damage.[60,61] To avoid this problem, humidity control during probe immobilization must be maintained to prevent evaporation, and surface damage must be reduced. Noncontact, jet-printing techniques do not use pins or tips, but rather they employ piezoelectric or bubble jet nozzles.[62,63] Surface damage is avoided in the jet-printing technique, because there is no physical contact between the dispenser and the surface. These printing approaches, i.e. contact pin/nano-tip printing and noncontact jet-printing, require serial printing steps which can be time consuming and cause accumulation of printing errors such as missing and contamination of spots during the repetitive printing steps.

The microstamping method (also known as microcontact printing), along with other soft lithography techniques, was first developed by the Whitesides group.[64,65]

Microstamps are generally made from elastomeric materials, typically poly(dimethylsiloxane) (PDMS), which enables conformal contact to rough surfaces under an applied load. A probe sample is first adsorbed onto the patterned surface of a stamp and then transferred to a substrate through conformal contact. Unlike other delivery approaches, the microstamping technique is a parallel printing method that prints hundreds of spots in parallel, and thereby enables high-throughput microarray fabrication. However, there is no convenient means for loading many different probe solutions onto a stamp simultaneously, and this limits fabrication of high-density arrays composed of different probes. Note, however, that for small arrays microfluidic channels are sometimes used to pattern a stamp with different inks by introducing each sample solution into designated channels simultaneously.[66]

1.3 MICROFLUIDIC DEVICES

Definition of Microfluidic Devices Microfluidic analytical devices have demonstrated their potential in analytical chemistry, especially for separations-based analysis,[67,68] chemical and biochemical sensors,[69] genomic and proteomic analysis,[70,71] and chemical synthesis.[72,73] Microfluidic devices can be characterized by their fluidic structures, which are fabricated on the micrometer scale. These systems provide a unique set of potential advantages. For example, devices based on microfluidic operation commonly result in low consumption of samples and reagents and hence low assay costs. Other benefits of microfluidic-based systems include high-throughput analysis by parallel processing of samples in multiple microfluidic channels and high levels of system integration and automation by integrating several analysis steps into a single system. Highly integrated microfluidic devices are also known as micro total analysis systems (µTAS) or labs-on-a chip.[1] In addition, the efficient heat dissipation of microchannels

reduces the negative consequences of high electric fields, which provide fast separation times and high efficiencies per unit length of the separation channels in microfluidic devices based on electrophoresis.

Microfluidic devices can be fabricated from various materials using different techniques. Glass or silicon substrates are commonly used because of their well-understood chemical properties and the large number of available microfabrication methods, such as photolithography[74,75] and reactive ion/plasma etching techniques,[76] developed by the microelectronic industry. Glass substrates are especially attractive because of their well-defined surface characteristics and good optical properties which are desirable for commonly used fluorescence detection methods. However, the fabrication processes involved are usually time consuming and require special processing facilities. Polymers are an appealing alternative to rigid inorganic materials, because of the vast range of mechanical and chemical properties they encompass and because of their low processing costs.[77] The fluidic networks on polymer substrates can be fabricated using a variety of techniques including soft lithography, direct micromilling techniques, and laser ablation.[78]

Figure 1.3 shows a typical procedure for fabrication of microfluidic devices using soft lithography.[79-83]. Once the mold master is fabricated using conventional lithographic techniques, a solution containing the PDMS prepolymer and curing agent is cast against the mold. After casting, the cross-linked PDMS is removed from the mold and contains the reverse-duplicate network of microfluidic features. Once the microfluidic network is formed, a cover substrate can be sealed to the fluidic PDMS substrate to enclose the channels.

Importance of Microfluidic Devices   Microfluidic devices complement conventional two-dimensional (2-D) microarrays by providing the following benefits:

13
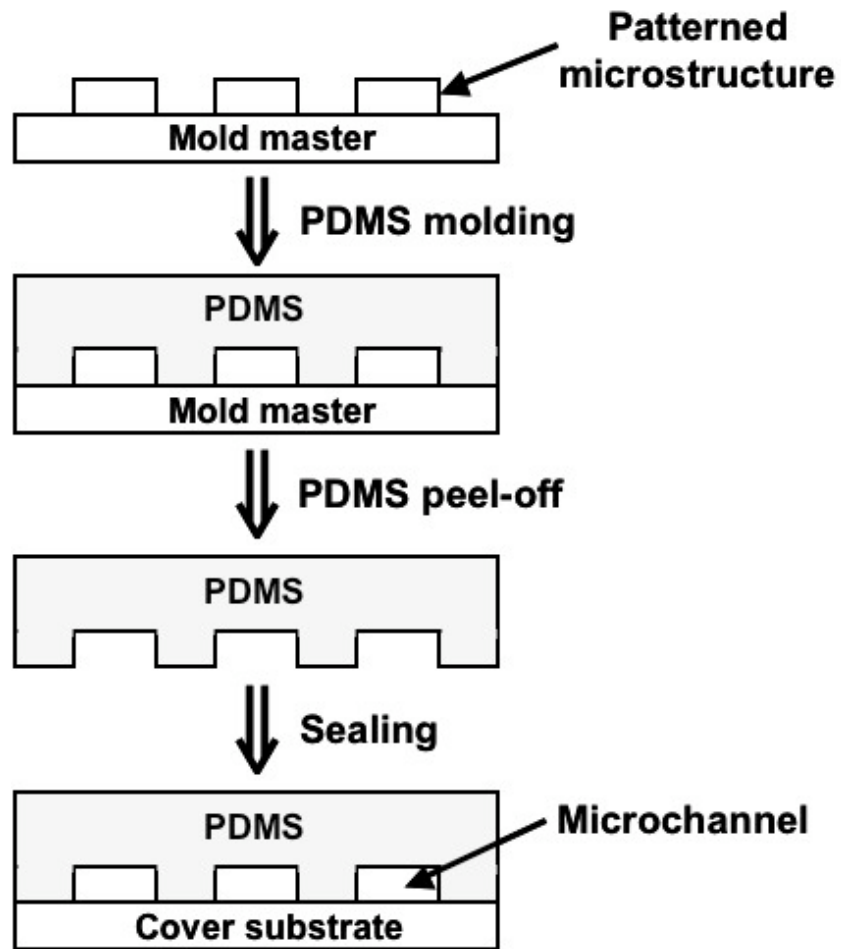
Figure 1.3. Schematic illustration of microfluidic device fabrication based on soft lithography.

faster hybridization (or other recognition processes), higher integration capability, and lower consumption of sample solution. Microfluidic devices can improve hybridization speeds because of the enhanced mass transport of targets and reduced diffusional distances by flowing target solution through a micro-scale hybridization chamber. The hybridization on 2-D array supports requires relatively long incubation times (usually several hours) to obtain probe saturation (thus, significant signals) because of slow diffusion-controlled kinetics. Target molecules in solution must diffuse to the arrayed probes on a surface and then move laterally to find their complements. For example, a DNA target molecule takes ~455 h to travel laterally across the array surface (1 cm^2), assuming the diffusion coefficient of a single-strand DNA molecule (50 bases) is 6.1 x 10^{-7} cm^2/s.[84] In addition, the local concentration of targets becomes depleted near the arrayed probes under static conditions. However, shorter incubation times can be achieved by flowing target solution in shallow microchannels. Forced flow of targets over arrayed probes on a surface provides enhanced mass transport of the targets because the transport does not depend only on diffusion. The use of shallow microfluidic channels also reduces the diffusional distances traveled by the target to reach the probes. The hybridization rate can be further improved by employing techniques such as hydrodynamic pumping,[85,86] mixer-assisting,[24,26] and electrokinetic pumping.[22,23] Other benefits offered by microfluidic devices include high integration capability and reduced sample volumes. Highly integrated microfluidic devices (so called labs-on-a-chip) enable multiple processing steps for a bioanalytical process (for example cell lysis, PCR amplification, separation, and detection) to be performed in a single microchip. Microfluidic platforms also provide reduced sample consumption even compared with conventional microarrays, especially high-density arrays, which requires relatively large amounts of samples to completely cover the array area (~1.0 cm^2) on the surface.

15

Bead-based Microfluidic Devices   Bead-based microfluidic devices have been suggested for efficient mixing and detection of target molecules in microchannels.[30,87,88] It has been demonstrated that microbeads provide a simple and efficient way to mix sample solutions in microfluidic devices where mixing normally occurs only by diffusion. The diffusion-only induced mixing is due to microfluidic channels having low Reynolds numbers and hence a very low degree of convective mixing.[87] The beads in microfluidic devices also provide a convenient platform for probe attachment.[30,88] Bead surface areas are significantly larger than the interior surface area of a typical microfluidic channel, and this results in enhanced sensitivity for assays based on immobilized probes. It is also easier to modify and characterize the surface of beads (ex-situ) than the walls of a microfluidic device. Therefore, several applications using microbeads in microfluidic devices have been reported for sensitive detection of biomolecules.[30,88-92]

Chapter 2: Experimental

2.1 CHEMICALS

All chemicals used in this work are described in the individual chapters.

2.2 TECHNIQUES

Microfabrication: Photolithography and Soft Lithography   Microfabrication in this work is based on photolithography and soft lithography. Photolithography is used to fabricate photoresist-coated molds and hydrogel microplugs, while soft lithography is for fabrication of PDMS substrates.

Photolithography has been the dominant technique for chip fabrication in the microelectronic industry. Photolithographic techniques, especially those based on projection photolithography, have enabled mass-production of microelectronic structures and ignited rapid growth of the microelectronic industry.[75] In projection photolithography, the pattern of a photomask is transferred onto a thin film of photoresist spin-coated on a wafer via exposure to light. The patterned film of photoresist protects the wafer during subsequent etching steps, which lead to microstructures on the wafer surface. After etching the wafer, the photoresist film is removed. The attainable feature sizes by this technique are, in principle, only subject to optical diffraction limitations;[74] that is, the resolution of the technique is limited by the wavelength of the light source. Even the optical limitation has been overcome by advanced lithographic techniques such as extreme ultraviolet (EUV) lithography,[93] e-beam lithography,[94] and soft X-ray lithography.[95]

In this work, chrome-coated glass or photographic films are used as a photomask. For fabrication of molds for PDMS substrates, photoresist-coated glass slides were exposed to light through the photomask using a mask aligner (Q 4000-6, Quintel Corp., San Jose, CA). The photoresist exposed to light is then removed by immersing the slides in a developer solution, which results in a patterned photoresist-coated slide. The patterned slides are used to mold PDMS substrates having microstructure features in subsequent replica molding process. The PDMS monolith having microfluidic features is then bonded to a cover glass after being treated in an O_2 plasma cleaner (PDC-32G, Harrick Scientific Ossining, NY). A photomask is also used to define the structure of the hydrogel microplugs in microchannels. The microplugs are photopolymerized inside the microfluidic devices.[31,96,97] After filling the microchannel with a hydrogel precursor solution by capillary action, UV light (365 nm, 300 mW/cm^2, EFOS Lite E3000, Ontario, Canada) is projected through a photomask attached at a side port of a microscope (Diaphot 300, Nikon) as shown in Figure 2.1.[98] Unpolymerized precursor solution is removed by pumping buffer solution through side-channels in the microfluidic device. Further experimental details for fabrication of photoresist-coated molds and hydrogel microplugs are described in Chapters 7 and 8.

Soft lithography complements photolithography in several ways. The procedure of soft lithography is rather simple; it can be carried out without expensive lithography equipment and still result in microstructure patterns as small as those provided by photolithography. Soft lithography includes a variety of techniques, including: contact printing, replica molding, microtransfer molding, injection molding, and embossing (imprinting).[64,65] The replica molding technique allows duplication of complex structures present on the surface of a mold in a single curing step. Even fabrication of microstructures from a deformed PDMS mold has been reported, which allows

18
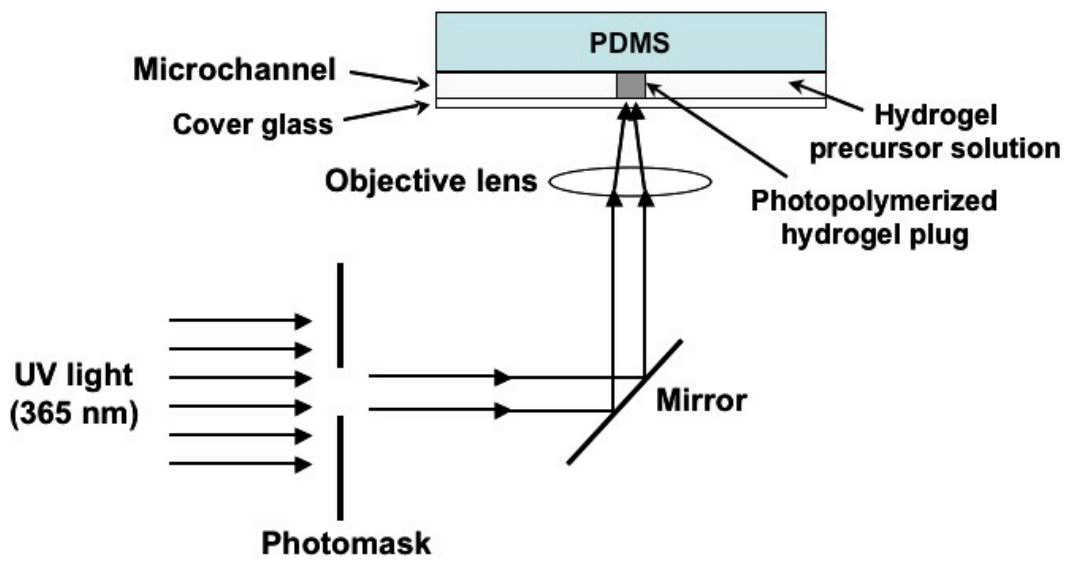
Figure 2.1. Schematic illustration of hydrogel photopolymerization. (Adapted from ref. #98)

generation of complex structures from simple structures on the PDMS mold.[64] It also allows reliable replication of the complex structures multiple times using a single mold. Importantly, this simple replication procedure has been reported to yield replicates having a resolution of <10 nm.[99] Typical procedures for replica molding are as follows. After preparing a mold having the desirable microstructures, prepolymer solution (UV or thermally curable) is poured onto the mold. The replica substrate is then peeled off after curing. The structures on the replica are complementary to those on the mold. The cured polymer replica has almost the same dimensions and topology as the mold.

In this work, glass slides patterned photoresist films are used as the molds, and PDMS is used as the thermally curable prepolymer, respectively. Glass molds having microfluidic structures or drainage patterns are fabricated using photolithography as described above. The PDMS (Sylgard 184, Dow Corning, Midland, MI) solution is cured against the photoresist mold to yield PDMS monoliths having fluidic patterns and PDMS replica array substrates containing drainage patterns. Further experimental details for the fluidic PDMS monoliths and PDMS replica array substrates are described in the Chapters 3-8.

Bioconjugation: Streptavidin-immobilized PDMS Substrates and Probe DNA-conjugated Microbeads The PDMS monolith having a specified drainage pattern is functionalized with streptavidin. The functionalization procedure involves two steps: silanization of PDMS with 3-mercaptopropyltrimethoxysilane (MPS) and immobilization of streptavidin onto the MPS-modified PDMS.[27-29] For the silanization process, the PDMS monolith is sonicated for 5.0 min each in ethanol and water, followed by drying under a stream of N_2. The surface of PDMS is then oxidized in an O_2 plasma cleaner at medium power for 2.0 min. Within 30 s after the plasma treatment, the PDMS monolith is exposed to HCl vapor by holding it over the mouth of a bottle containing concentrated

HCl for 1.0 min. The PDMS monolith is immediately transferred to a plastic desiccator and placed over the top of a Petri dish containing ~ 2.0 mL of MPS with ~1.5 cm distance between the PDMS surface and liquid MPS. The desiccator is then connected to a vacuum line for 10 s. After disconnecting from the vacuum, the PDMS monolith remains in the sealed desiccator for 30 min for the vapor-phase silanization reaction to introduce thiol groups on the surface. After the PDMS monolith is removed from the desiccator, it is baked in an oven at 80 °C for 20 min.

Streptavidin-maleimide conjugates (S9415, Sigma-Aldrich, 5.0 mg/mL in a pH 7.2 sodium phosphate buffer containing 0.15 M NaCl) are then introduced onto the MPS-modified PDMS surface allowing the reaction between the maleimide and thiol groups to proceed for > 2.0 h. The PDMS monolith is then rinsed with water and placed in an aqueous 1.5 mM 2-mercaptoethanol (M6250, Sigma-Aldrich) solution for 15 min to block any unreacted maleimide groups. After rinsing the PDMS monolith with water again, it is placed in a 3 mM N-ethylmaleimide (E3876, Sigma-Aldrich) solution in N,N-dimethylformamide (D8654, Sigma-Aldrich) for 15 min to block unreacted thiol groups. Finally, the streptavidin-coated PDMS monolith is rinsed with water and dried under N_2.

Probe DNA-conjugated microbeads are prepared using the following procedure.[30] First, streptavidin-coated microbeads (ProActive Microspheres, Bangs Laboratories Inc., Fishers, IN) are rinsed in a phosphate buffer saline (PBS) solution containing 0.05% (v/v) Tween 20 (pH 7.4, 0.15 M NaCl, 4.0 mM KCl, 8.1 mM Na_2HPO_4, and 1.5 mM KH_2PO_4) and then centrifuged at 400 rpm for 3.0 min. Second, biotinylated single-strand (ss)DNA probe solution (5.0 μM) is introduced to the rinsed bead pellet. The amount of added ssDNA probes corresponds to a five-fold excess relative to the binding capacity of the microbeads. The DNA/bead solution is then incubated with gentle mixing for 30 min at 25 ± 2 °C. After conjugation, the unbound biotinylated ssDNA probes are removed by

centrifugation. The probe-conjugated microbead pellet is rinsed with PBS buffer and centrifuged again. The probe-conjugated microbeads are re-suspended in TRIS-acetate/EDTA (TAE) buffer (pH 8.0, 40 mM tris-acetate, 1.0 mM EDTA, and 0.5 M NaCl) and kept at 2.0 °C until needed. More detailed procedures are described in Chapters 7 and 8.

Fabrication of Master DNA Microarrays Oligonucleotides are spotted and immobilized on N-hydroxysuccinimide (NHS)-coated glass slides (CodeLink slides, Amersham Bioscience) or epoxy-modified glass slides (Nexterion® Slide E, SCHOTT North America Inc.) according to the instructions provided by the vendors. Specifically, oligonucleotides are spotted using three different tools: a micropipette (Pipettor 40000-264, VWR), a manual microarrayer (Xenopore Corp., Hawthorne, NJ), and a robotic microarrayer (Omnigrid Microarrayer, San Carlos, CA, or a home-built microarrayer maintained at the Microarray Core Facility at The University of Texas at Austin). After spotting, the master slides are placed inside a sealed chamber in which the humidity is in equilibrium with a saturated NaCl solution for immobilization of the spotted oligonucleotides. Each immobilization process for different glass slides is described in detail in Chapters 3-6.

Fluorescence Imaging Fluorescence imaging involves absorption of light at specific wavelengths by an atom or molecule, followed by the emission of light at longer wavelengths. When the fluorescence molecule absorbs photon energy, electrons are excited to a higher energy level. As the electrons relax back to the ground-state, light at longer wavelengths is emitted because vibrational energy is lost during relaxation. Judiciously chosen fluorophores having well-defined excitation and emission spectra can provide useful information about molecules on a surface.

Inverted fluorescence microscopes (Eclipse TE300 and TE2000, Nikon) and a microarray scanner (GenePix 4000B, Molecular Devices Corp., Sunnyvale, CA) were used in this work. Mercury lamps (X-Cite[TM] 120, Nikon) are attached to the microscopes and are used as the excitation light source. Fluorescence is separated from the excitation light by a dichroic mirror in the microscopes. Excitation light is reflected back into the objective lens while fluorescence is transmitted. Appropriate filters exclude or transmit selected wavelengths of light, and reduce background noise. Digital cameras (SenSys 1401E for TE300 and Cascade[®] for TE2000, Photometrics Ltd., Tucson, AZ) based on a charge-coupled device (CCD) are connected to the ports of microscopes and used to image fluorescence. The microarray scanner uses dual solid-state lasers and a photomultiplier tube (PMT) as the light source and the detector, respectively.

Chapter 3: Replication of DNA Microarrays from Zip Code Masters

3.1 SYNOPSIS

This report describes a mechanical method for efficient and accurate replication of DNA microarrays from a zip code master. The zip code master is a DNA array that defines the location of oligonucleotides consisting of two parts: a code sequence, which is complementary to one or more of the zip codes, and the functional sequence, which is terminated with biotin. Following hybridization of the zip code to the code sequence, a replica surface functionalized with streptavidin is brought into conformal contact with the surface of the master. When the two surfaces are separated, the functional and code sequences are transferred to the replica and the zip code remains on the surface of the master. Using this approach it is possible to prepare replica arrays having any configuration from a single, universal master array. Here we demonstrate that this approach can be used to replicate master arrays having up to three different sequences, that feature sizes as small as 100 μm can be replicated, and that master arrays can be used to prepare multiple replicas.

3.2 INTRODUCTION

Here we report an efficient and accurate method for the replication of DNA microarrays. The general strategy is illustrated in Scheme 3.1. First, a zip code master is prepared by spotting different single-stranded oligonucleotides onto an appropriate surface. Each spot represents a different zip code that will direct the placement of a second oligonucleotide.[100,101] Second, the zip code master is exposed to a solution containing biotin-functionalized oligonucleotides that consist of two parts: a code

Scheme 3.1

ssDNA

hybridization

Master

1 2 3

Functional
sequence

Code
sequence

1 2 3

Master

contact and
surface reaction

Replica

Streptavidin

Biotin

1 2 3

Master

Replica

separation
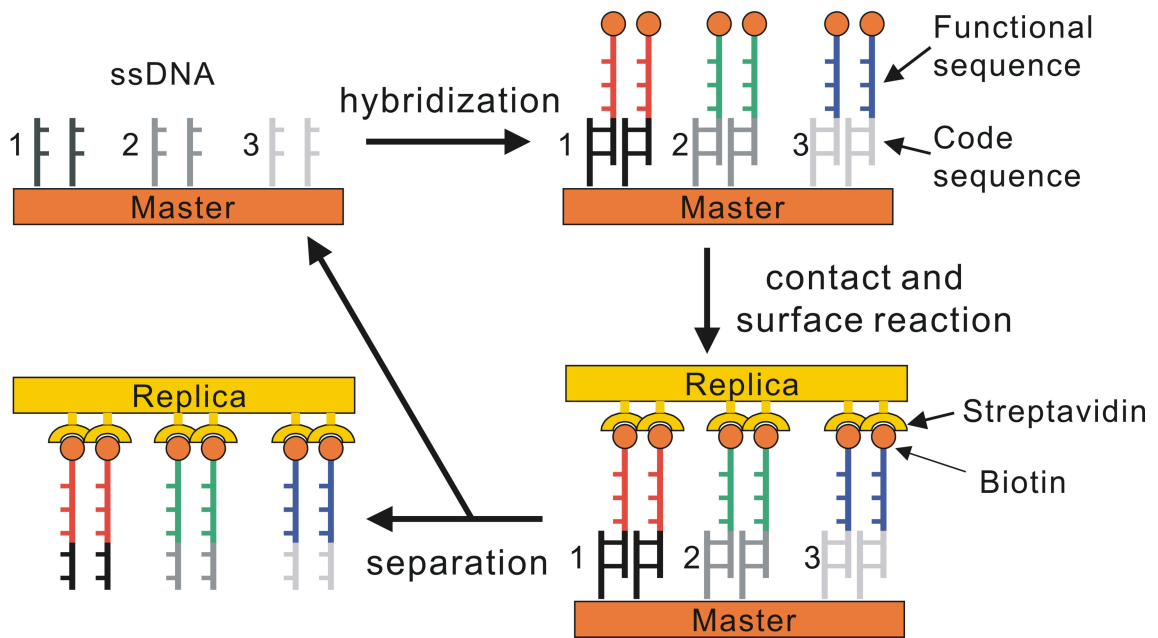
sequence and a functional sequence. Because each code sequence is designed to be complementary to just one specific zip code on the master, the biotin-functionalized oligonucleotides will be directed to their appropriate zip code locations on the master. Third, a replica surface modified with streptavidin is brought into conformal contact with the zip code master. This results in binding of the replica surface to the biotinylated DNA. Fourth, the replica is separated from the master by mechanical force. This results in transfer of the biotinylated oligonucleotide from the master to the replica. The replica is now ready to be used as a DNA array, and the zip code master can be rehybridized to generate additional replicas.

Previously, we showed that oligonucleotides spotted onto a glass surface could hybridize to their biotin-functionalized complements, and then the complement could be transferred to a streptavidin-modified replica surface.[27] A similar replication approach was recently reported by Stellacci and coworkers, who showed that dehybridization was facilitated by heating,[102] and that DNA lines as thin as 50 nm could be replicated.[103] Gaub and coworkers used a related principle to construct force sensors that could distinguish between strong and weak intermolecular interactions, but they were not concerned with pattern replication.[104,105] In contrast to these earlier studies, the zip code approach provides a means for using a single master DNA array to prepare oligonucleotide replicates having any functional sequence positioned anywhere on the array. Importantly, this new approach will also make it possible to use a master DNA array to produce replicates of any other material (for example, proteins, carbohydrates, or inorganic nanoparticles) that can be labeled with a short oligonucleotide code. Thus, the important aspect of the present work is that it represents a major expansion of the scope of our original report.

26

DNA microarrays have been increasingly used in high-throughput analysis for a wide range of applications, including monitoring gene expression,[106] drug screening based on drug-DNA interactions,[107] and fundamental studies of genetic diseases and cancers.[108,109] In-situ synthesis and ex-situ spotting are the two families of methods that have been used commercially to fabricate DNA microarrays.[49,110] The best known in-situ method integrates photolithography and solid-state synthesis.[110] Each synthesis cycle consists of protection, photo-deprotection, and addition of a nucleotide to directly grow oligonucleotides on a substrate. The growth of oligonucleotides is spatially defined by photolithographic masks, and the number of synthesis cycles required is proportional to the length of the oligonucleotides. This method has the advantages of small spot size (~8 μm spot) and design flexibility,[111] but the inefficiency of solid-state reactions limits the maximum oligonucleotide length to about 60 basepairs (bps)[49,111] and leads to increased cost. The second general method for fabricating microarrays is ex-situ spotting of pre-synthesized oligonucleotides.[112] Spotting to a DNA chip surface can be implemented by either contact printing using rigid pins[113] or by projection through microfabricated nozzles.[114] Spotting does not impose length restrictions on the patterned oligonucleotides.[115] However, the expense and time required to prepare an array is proportional to the dimensionality of the array and the size of the individual array elements, which are large (75 μm to 500 μm) compared to those prepared by in-situ methods.[49] Moreover, as for any sequential process involving multiple repetitive steps, both in-situ synthesis and ex-situ spotting are subject to an accumulation of errors.[49] Other ex-situ methods for delivering pre-synthesized oligonucleotides include patterning using microfluidic channels,[116] microcontact printing,[117] and dip-pen nanolithography;[118,119] however, all these methods involve manual loading of the

oligonucleotides and therefore, at least for now, are not well-suited for creating large-scale, complex microarrays.

3.3 EXPERIMENTAL

Chemicals and Materials. CodeLink slides (Amersham Bioscience, Piscataway, NJ), coated with a three-dimensional polymeric scaffold functionalized with N-hydroxysuccinimide (NHS), were used to fabricate masters. The poly(dimethylsiloxane) (PDMS) replicas were prepared from liquid precursors (Sylgard Silicone Elastomer-184 from Dow Corning, Midland, MI). 3-mercaptopropyltrimethoxysilane (97% from Alfa Aesar, Ward Hill, MA) and streptavidin-maleimide (from Sigma-Aldrich, St. Louis, MO) were used as received. All chemicals used to prepare buffers were purchased from Sigma-Aldrich: sodium phosphate monobasic (Sigma S0751), sodium phosphate dibasic (Sigma S0876), Trizma Base (Sigma T6791), Trizma HCl (Sigma T6666), ethanolamine (Sigma E9508), sodium dodecyl sulfate (SDS) (Sigma L4522), and 20x SSC (Sigma S6639).

All the oligonucleotides were obtained from Integrated DNA Technologies (Coralville, IA). The sequences of the oligonucleotides are provided in Table 3.1. Fluorescence micrographs were captured using an inverted microscope (Eclipse TE300, Nikon) equipped with a CCD camera (Cascade, Photometrics, Tucson, AZ). The filter set (XC102: 475 nm excitation filter, 505 nm dichroic mirror, and 510 nm long-pass emission filter) was purchased from Omega Optical, Inc. (Brattleboro, VT).

Fabrication of Master Arrays. The master slides were fabricated using CodeLink slides according to the instructions provided by the vendor (Amersham Bioscience, Piscataway, NJ). 25 μM solutions of 5'-amine-modified oligonucleotides in 50 mM pH 8.5 phosphate buffer were spotted onto a CodeLink slide using a pipette

Table 3.1 Sequences of zip codes, probes, and targets used in this study[a]

Name	Sequence
Zip code 1	5' AAC ATG CAA GGG CAA ATG 3'
Zip code 2	5' GCT GAG GTC GAT GCT GAG 3'
Zip code 3	5' GGT CCG ATT ACC GGT CCG 3'
1'A	5' GGT GAT ATG GCT TGA TGT ACC ATT TGC CCT TGC ATG TT 3'
2'B	5' GGT GAT ATC GCT TGA TGT ACC TCA GCA TCG ACC TCA GC 3'
3'C	5' TGA TTT TCA GCA GGC CTT ATC GGA CCG TAA TC GGA CC 3'
A'	5' GTA CAT CAA GC**C** ATA TCA CC 3'
B'	5' GTA CAT CAA GC**G** ATA TCA CC 3'
C'	5' ATA AGG CCT GCT GAA AAT CA 3'

[a] If a functional group, such as an amine or biotin, was attached to a DNA sequence, it was always attached at the 5' position. Fluorescein was attached at the 3' end for 1'A, 2'B, and 3'C or to the 5' end for A', B', and C'. All oligonucleotides incorporated a spacer. A C12 spacer was used for amine-functionalized DNA. A TEG spacer was used for biotin-modified DNA. The spacer used for fluorescein is known as Spacer 18. More detailed information about it, and the other spacers, can be obtained at the web site of Integrated DNA Technologies (http://www.idtdna.com/Home/Home.aspx). All oligonucleotides were purified by HPLC.

(Pipettor 40000-264, VWR) or a microarrayer (Omnigrid Microarrayer, San Carlos, CA). After spotting, the CodeLink slide was placed inside a sealed chamber above a saturated NaCl solution and incubated at 22 ± 2 °C for 15 to 20 h. Next, the slide was placed in a solution containing 50 mM ethanolamine and 0.1 M TRIS buffer (pH 9.0) at 50 °C for 30 min to block residual reactive NHS groups. After rinsing with purified water twice, the slide was placed in a buffer containing 4x SSC and 0.1% SDS, which was pre-warmed at 50 °C for 30 min. After rinsing with water again, the slide was dried under a stream of N_2.

Only about 50% of the masters prepared using the microarrayer could be replicated, but the masters spotted manually worked 100% of time. Apparently the contact spotting configuration used by the microarrayer causes some damage to the surface of CodeLink slides. Further investigation is underway to clarify this issue. Note, however, that when an array can be replicated, the replica is always 100% faithful to the master and can always be hybridized to the complement of the functional sequence. No false positive signals were ever observed.

Fabrication of Streptavidin-functionalized PDMS. Following our previously reported procedures,[27] thiol groups were first introduced onto a PDMS surface by silanization with 3-mercaptopropyltrimethoxysilane (MPS) and then streptavidin was immobilized onto MPS-modified PDMS through the reaction between maleimide and thiol groups.

Replication of DNA Microarrays. The master was exposed to a solution containing 10 μM oligonucleotide for at least 4 h, and then replication was achieved by contacting the hybridized master with a streptavidin-functionalized PDMS surface. In a typical replication process, 10 μl pH 7.2 buffer was used to wet the master surface, and then the streptavidin-functionalized PDMS was placed on top of the master with a

pressure of 1.4 N/cm^2 at 22±2 ^{o}C. Although a pH 7.2 buffer solution was used to wet the master surface in all the experiments presented here, we later found that water (no buffer) worked just as well. After 10 min of contact, the PDMS replica was manually peeled off the master, rinsed, and blown dry. This experimental approach is based on methodology reported by Gaub and coworkers.[104,105]

3.4 RESULTS AND DISCUSSION

Replication of a Zip Code Master Having One Zip Code. Figure 3.1 shows that multiple replicas can be prepared from a single zip code master. The master was prepared by applying a solution of amine-modified oligonucleotide (zip code 1, Table 3.1) onto a CodeLink slide (see Experimental Section for details). Next, the master array was exposed to oligonucleotide 1'A (Table 3.1). The first 18 bases from the 3' end of oligonucleotide 1'A are the exact complement of zip code 1, and 1'A is labeled with fluorescein at the 3' end and biotin at 5' end. Following hybridization, the master was thoroughly rinsed and the fluorescence micrograph shown in Figure 3.1a was obtained. Uniform fluorescence emission from the master surface confirms homogeneous hybridization of oligonucleotide 1'A to the zip code master.

Figures 3.1b and 3.1c are fluorescence micrographs of the master and replica, respectively, following replication. Fluorescence intensity is clearly transferred from the surface of the master to the replica after contact. The checkerboard pattern results from drainage canals (20 μm on center, 10 μm wide, and 3 μm deep) present on the replica surface that direct buffer solution away from the contact area during replication. Control experiments showed that these canals were essential for successful DNA transfer. Specifically, if both the master and the PDMS were dry, then no transfer of DNA was observed. Additionally, no transfer was observed in the absence of drainage canals

31
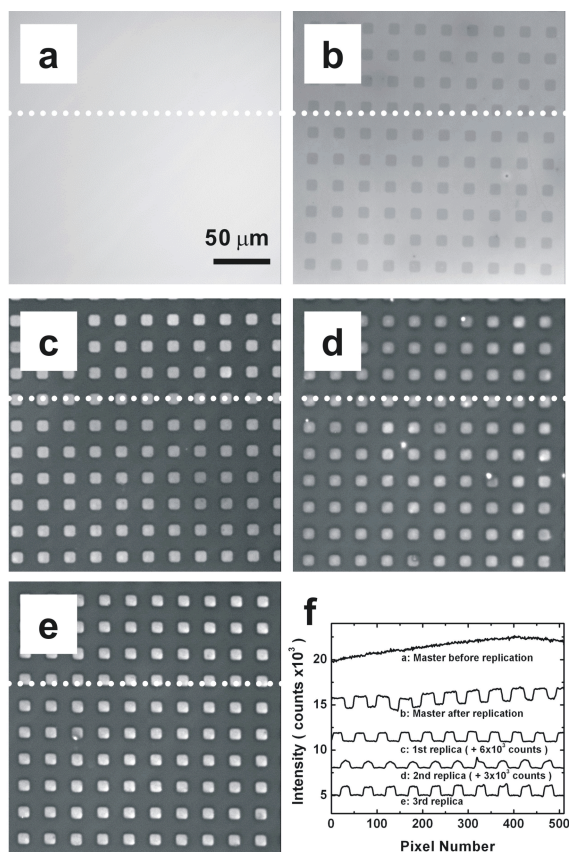
Figure 3.1. Fluorescence micrographs demonstrating transfer of fluorescein-labeled DNA from a master slide to a PDMS replica surface. (a) The master slide modified with zip code 1 (Table 3.1) and hybridized to fluorescein- and biotin-labeled oligonucleotides 1'A whose code sequence is complementary to zip code 1. (b) The master slide after transfer. (c) The PDMS replica after transfer. (d) The second replica obtained after rehybridization of the master with oligonucleotide 1'A. (e) The third replica obtained after rehybridization of the master with oligonucleotide 1'A. (f) Fluorescence intensity profiles obtained along the dashed lines shown in frames (a)-(e). For clarity, profiles (c) and (d) are offset by 6000 and 3000 counts, respectively. The image integration time was 30 s for all frames. The gray scale is 5000-25000 counts for (a) and (b), and 4500-6500 counts for (c), (d), and (e).

regardless of whether buffer was present. We suspect that, in the absence of drainage canals, solvent trapped between the two surfaces prevent molecular contact between the biotin-functionalized oligonucleotides on the master and streptavidin present on replica. Figure 3.1f provides a quantitative representation of the data shown in Figures 3.1b and 3.1c. After replication, the contrast between the light and dark areas on the master (~1300 counts, Figure 3.1b) is very close to that of the replica (~1100 counts, Figure 3.1c), indicating that only a small fraction of the DNA is lost during transfer.

Figures 3.1d and 3.1e show the second and the third replicas obtained from the same master after rehybridization with oligonucleotide 1'A labeled with fluorescein and biotin. The contrast between the light and dark areas for the three consecutive replicas is 1100, 900, and 1200 counts, respectively, indicating good reproducibility and that there is no progressive loss of DNA from the master after formation of three replicas.

The data presented thus far indicate that replication is a consequence of molecular contact and binding between the biotin groups present on the CodeLink slide and streptavidin on the PDMS replica surface. Because in the current experiment the binding force between biotin and streptavidin is stronger than between DNA base pairs,[104,105] the DNA duplexes separate and the biotin-functionalized oligonucleotides transfer to the replica surface. For very long DNA duplexes, however, it is important to separate the two surfaces slowly to avoid breaking the biotin/streptavidin bond. That is, the force required to separate a DNA duplex is independent of its length if the separation rate is appropriately controlled.[104,105]

For single-oligonucleotide replicas, the spot size is defined by the spacing of the canals on the replica surface. For example, each replica spot shown in Figures 3.1c-3.1e is 10 x 10 μm, which is comparable to the smallest feature sizes obtained by in-situ synthesis (~8 μm),[111] and much smaller than those obtained by ex-situ spotting (~75

μm).[49] However, for replicas patterned with multiple DNA oligonucleotides, the important size parameter is defined by the dimensions of the master, not the replica. Stellacci and coworkers previously demonstrated masters and replicas having feature dimensions as small as 50 nm.[103]

To demonstrate replication from a master array instead of from a homogeneous surface, a microarrayer was used to print a 3 x 3 array of nine, ~100 μm-diameter spots of zip code 1 (Table 3.1), and then the master array was copied onto a PDMS replica surface using the procedure discussed earlier for Figure 3.1. Figure 3.2a is a fluorescence micrograph obtained from the master after hybridization with fluorescein-labeled and biotin-functionalized DNA sequence 1'A (Table 3.1). The presence of fluorescence, which is absent prior to hybridization, confirms hybridization of the functional sequence. The fluorescence micrograph shown in Figure 3.2b was obtained from the PDMS replica surface after conformal contact of the two substrates. The 3 x 3 array observed on the replica (Figure 3.2b) exactly mirrors the master array (Figure 3.2a), except for the presence of the drainage canals. An optical image of the replica surface (Figure 3.2c) shows the drainage design of the replica. We have successfully replicated master arrays having up to 100 elements using this procedure, but they are not shown here because of the limited field of view of the CCD camera used in these experiments.

Replication from a Master Having Multiple Zip Codes. It is important to demonstrate that replication is successful for masters having multiple zip codes. To demonstrate this function, a 4 x 3 master array containing three different zip codes was prepared using a microarrayer. Each row is composed of four spots having a nominal diameter and edge-to-edge distance of ~100 μm. With reference to Table 3.1, the first, second, and third rows correspond to zip codes 1, 2, and 3, respectively.

34
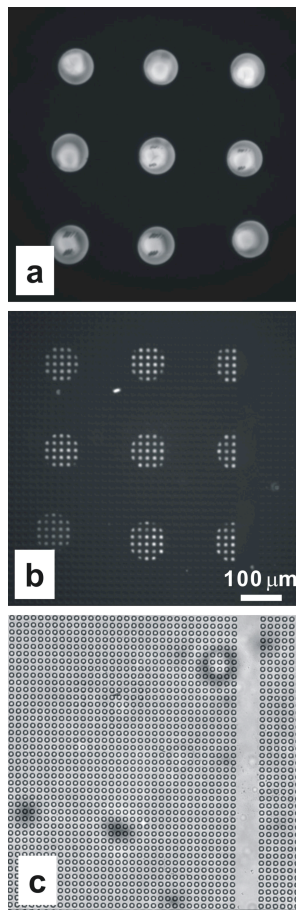
Figure 3.2. Micrographs demonstrating replication of a 3 x 3 master array having just one DNA zip code. (a) A fluorescence micrograph obtained from a master array spotted with zip code 1 (Table 3.1) and subsequently hybridized to fluorescein- and biotin-labeled oligonucleotides 1'A whose code sequence is the complement of zip code 1. (b) A fluorescence micrograph obtained from the PDMS surface after replication of the master. (c) An optical micrograph of the replica surface showing the drainage canals. The integration time for both (a) and (b) was 30 s. The gray scale is 2000-20000 counts for frame (a), and 2000-8000 counts for frame (b). In frame (b), all three spots in the right column are cut off, because they happen to intersect a major drainage canal as shown in the optical image, frame (c).

35

Hybridization was carried out for at least 4 h with 10 μM fluorescein-labeled and biotin-functionalized oligonucleotide 1'A (Table 3.1), which has a code sequence that only matches zip code 1, and afterwards fluorescence was observed only from the four spots in the first row (Figure 3.3a). This result clearly shows that the zip code master correctly directs the proper code sequence to the appropriate location on the master.[100,101] Following replication (Figure 3.3b), fluorescence is only observed from the top row of spots, corresponding to zip code 1. This confirms that only the correct functional sequence is transferred to the replica surface.

Preparation and Functionality of Replica Microarrays Having Multiple Sequences. Here, we set out to demonstrate that a master array having multiple zip codes could direct placement of multiple codes, that multiple code/functional sequences could be transferred to the replica, and that the replica functional sequences are active. The experiment demonstrating these three points was carried out as follows. First, a 4 x 3 master array having three zip codes was prepared as described for Figure 3.3. A solution containing a mixture of three non-fluorescent, biotin-functionalized oligonucleotides (1'A, 2'B, and 3'C, Table 3.1; 10 μM each) was introduced onto the master surface for at least 4 h. The code sequence of each of the three oligonucleotides is complementary to exactly one of the zip codes present on the master surface. Thus, oligonucleotides 1'A, 2'A, and 3'A are directed to zip codes 1, 2, and 3 respectively. Following replication, the replica array was exposed to a solution containing a mixture of three fluorescein-labeled targets (A', B', and C', Table 3.1; 10 μM each) for at least 4 h. Each target was chosen to match the functional sequence of one of the three oligonucleotides present on the replica surface. The fluorescence image obtained from the replica clearly shows a 4 x 3 array (Figure 3.4). This experiment demonstrated that a replica array having multiple sequences can be prepared and used for hybridization-based applications.

36
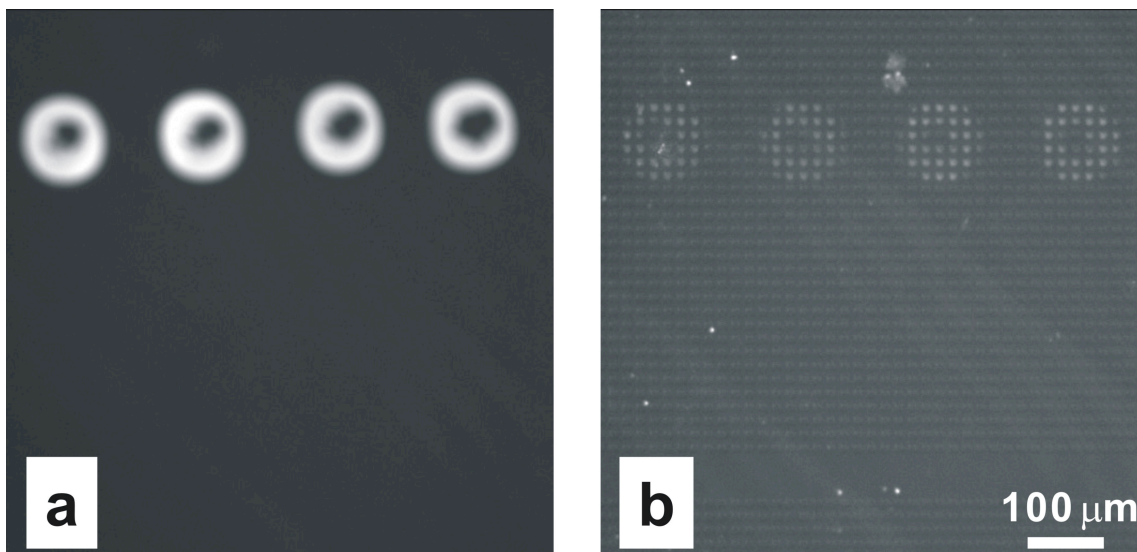
Figure 3.3. Fluorescence micrographs demonstrating accurate replication of a master having multiple zip codes. (a) A 4 x 3 master array having three zip codes (row 1, zip code 1; row 2, zip code 2; and row 3, zip code 3; Table 3.1) after hybridization with fluorescein- and biotin-labeled oligonucleotides 1'A whose code sequence is only complementary to zip code 1. (b) A PDMS replica of the master showing only one row of transferred oligonucleotides. The integration time for both (a) and (b) was 30 s. The gray scale is 5000-13000 counts for (a), and 5000-8000 counts for (b).
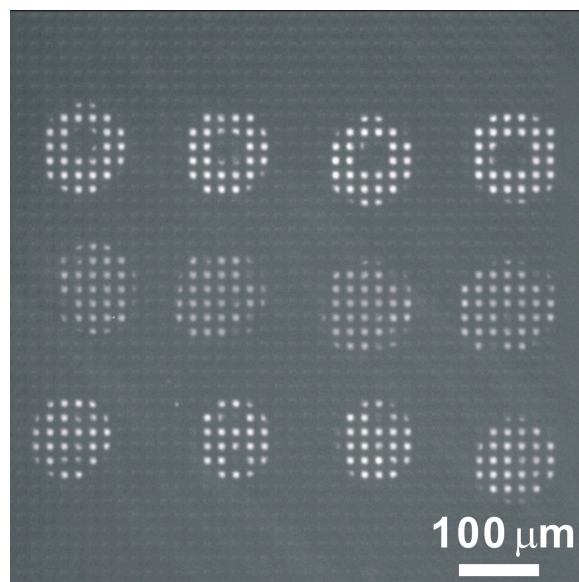
Figure 3.4. Fluorescence micrograph demonstrating the functionality of a replica. First, a 4 x 3 master array having three zip codes (row 1, zip code 1; row 2, zip code 2; and row 3, zip code 3; Table 3.1) was prepared and hybridized to a mixture of three non-fluorescent, biotin-functionalized oligonucleotides: 1'A, 2'B, and 3'C (Table 3.1) whose code sequences are complementary to zip code 1, zip code 2, and zip code 3, respectively. After replication, the resulting PDMS surfaces were exposed to a mixture of fluorescein-labeled targets A', B', and C' that are complementary to the functional sequences of 1'A, 2'B, and 3'C, respectively. The integration time was 30 s, and the gray scale is 5000-8000 counts.

3.5 CONCLUSION

In this work we demonstrated an efficient and accurate method for replication of DNA microarrays from a zip code master. For arrays containing multiple DNA sequences, the replica spots can be as small as 100 μm. Three consecutive replications from the same master were successfully achieved with no significant decrease of oligonucleotide density on the replica surface. Replication from a 4 x 3 master array having three zip codes proved to be accurate and there was no observable cross-reactivity. Future experiments will focus on larger scale arrays, smaller spot sizes, and replication of more complex biological materials (proteins and viruses) and inorganic nanomaterials.

Chapter 4: Transfer of Surface Polymerase Reaction Products to a Secondary Platform with Conservation of Spatial Registration

4.1 SYNOPSIS

Here, we describe a method for directly transferring very small amounts of reaction products from one surface to another. The approach is illustrated using a T4 DNA polymerase reaction to extend primers hybridized to a surface-confined DNA template. Following the extension reaction, the resulting oligonucleotide is transferred to a product surface. The important results are that: (1) the spatial registration of the product is preserved after transfer; (2) the same reactant surface can be used to generate and transfer multiple iterations of products; (3) the reaction products are biologically active after transfer.

4.2 INTRODUCTION

In this chapter, we describe a method for directly transferring the product of a biological surface reaction from a primary reactant surface to a secondary product surface. Our approach, which is related to an array-replication method reported previously by us,[27,28] Stellacci,[102,103,120] and others[121], is illustrated in Scheme 4.1. First, single-strand DNA (ssDNA) modified with a reactive amine group on the 5' end is spotted onto an epoxy-modified glass surface (complete experimental details are provided in the Experimental). This results in immobilization of the DNA template onto the reactant surface. Second, biotinylated primer oligonucleotides are hybridized to the ssDNA template. Third, the primers are extended via a T4 polymerase reaction.[122,123] Fourth, a streptavidin-coated PDMS monolith is brought contact with the reactant surface.[27,28] This results in binding of the reaction product (the extended DNA

Scheme 4.1

a ssDNA

Primer annealing

Extension

b Fluorescent dye

Reactant surface

Contact with product surface

d Product surface

Separation and transfer

c Streptavidin

Biotin
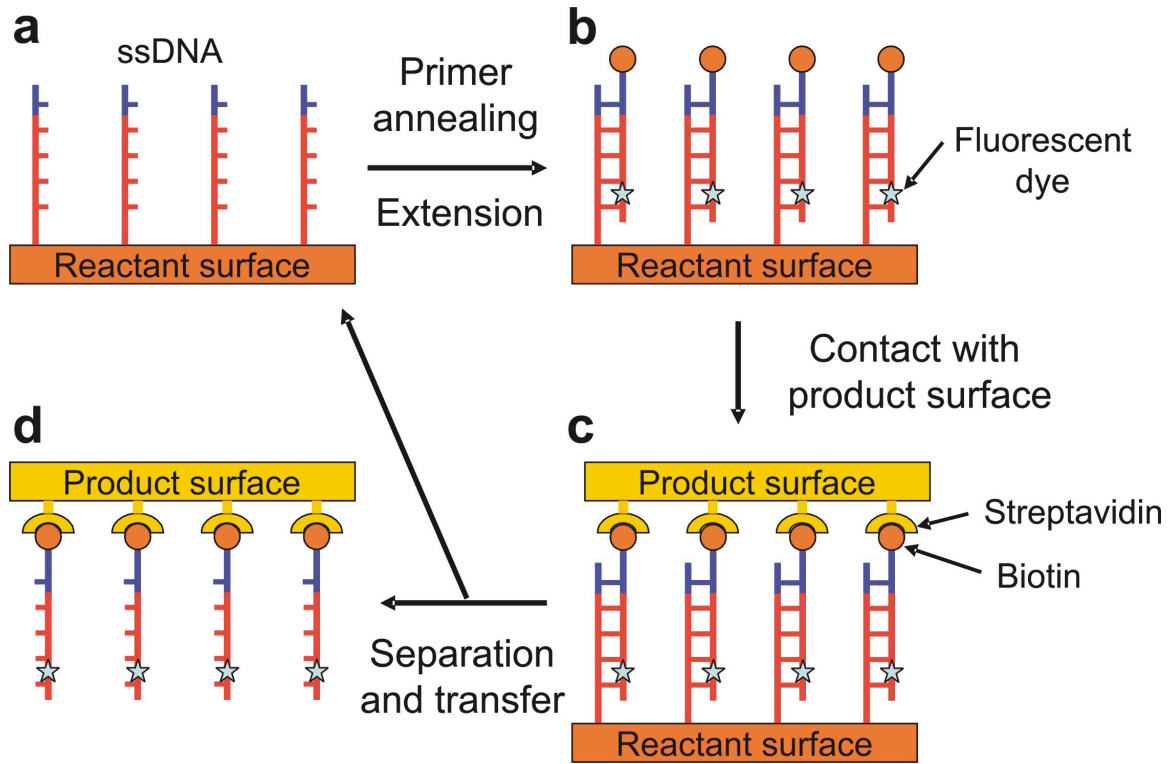
Reactant surface

complement) to the PDMS product surface via biotin/streptavidin interaction. Finally, the reactant and product surfaces are mechanically separated from one-another, resulting in transfer of the product of the polymerase reaction to the PDMS surface. We show later that product surface is able to selectively bind its complementary DNA and that a single reactant surface can be used multiple times to generate isolated product. Importantly, spatial registration is maintained between the reactant and product surfaces.

4.3 EXPERIMENTAL

Chemicals, Materials, and Characterization Glass slides coated with an epoxy monolayer (Nexterion® Slide E, SCHOTT North America, Inc., Elmsford, NY) were used to prepare the reaction surfaces. The poly(dimethylsiloxane) (PDMS) product surfaces were prepared from Sylgard 184 (Dow Corning, Midland, MI). 3-mercaptopropyltrimethoxysilane (MPS) was purchased from Alfa Aesar (Ward Hill, MA). Streptavidin-maleimide conjugates (Sigma S9415) and other chemicals for buffers or blocking solutions were obtained from Sigma-Aldrich: 20x saline-sodium citrate (SSC) buffer (Sigma S6639), 10% sodium dodecyl sulfate (SDS) solution (Sigma L4522), sodium phosphate monobasic (Sigma S0751), sodium phosphate dibasic (Sigma S0876), Triton® X-100 (Sigma T8787), Trizma base (Sigma T6791), Trizma HCl (Sigma T6666), ethanolamine (Sigma E9508), 2-mercaptoethanol (Sigma M6250), and N-ethylmaleimide (Sigma E3876). T4 DNA polymerase (EP0061), deoxyribonucleotide triphosphate (dNTP) mix (R0241), dNTP set (R0181), and nuclease-free water were used as received from Fermentas Inc. (Hanover, MD). Cy3 fluorescent dye-labeled deoxycytidine triphosphate (Cy3-dCTP) was obtained from Amersham Biosciences Corp. (Piscataway, NJ).

42

DNA oligonucleotides were obtained from Integrated DNA Technologies (Coralville, IA) and used without further purification after. The sequences and modifications are as follows: template (5'-5AmMC12-(iSp18)$_5$-TAT AAC AAG ACC TTC CTC AAT CCG GTG CAG AAT CGC AT-3'), primer (5'-5BioTEG-ATG CGA TTC TGC ACC-3'), and probe (5'-56FAM-TAT AAC AAG ACC TTC CTC AAT CC-3'). Here, 5AmMC12, (iSp18)$_5$, 5BioTEG, and 56FAM correspond, respectively, to an amino modifier having a 12-carbon spacer on the 5' end of the DNA, 18-carbon internal spacers repeated five times, a biotin modifier with a tetra-ethyleneglycol (TEG) spacer on the 5'end of the DNA, and a fluorescein dye attached to the 5' end of DNA. This is the same notation used by the DNA supplier (Integrated DNA Technologies, Coralville, IA).

A fluorescence microscope (Nikon TE2000, Nikon Co., Tokyo, Japan) equipped with filter sets (filter # 41001 for fluorescein and 31002 for Cy3, Chroma Technology Corp., Rockingham, VT), a mercury lamp (X-Cite™ 120, Nikon Co), and a CCD camera (Cascade®, Photometrics Ltd., Tucson, AZ) was used to acquire optical and fluorescence micrographs. Micrographs were processed using V++ Precision Digital Imaging software (Digital Optics, Auckland, New Zealand).

Fabrication of Reaction Master Slides Template oligonucleotides were immobilized on epoxy-modified glass slides (Nexterion® Slide E) according to the instructions provided by the vendor (SCHOTT North America, Inc.). Template solution (25 μM in 50 mM sodium phosphate buffer, pH 8.5) was pipetted onto the glass slide. Next the slide was placed into a chamber in which the humidity was controlled with saturated NaCl solution at 20 to 25 °C. After incubation, the slide was washed sequentially as follows at 20 to 25 °C to remove unbound templates and buffer substances: 1 x 5 min in 0.1% Triton® X-100 solution, 2 x 2 min in 1 mM HCl solution, 1 x 10 min in 100 mM KCl solution, and 1 x 1 min in Milli-Q water (18 MΩ•cm,

43

Millipore, Bedford, MA). Next, the slide was placed in blocking solution (50 mM ethanolamine and 0.1 % SDS in 0.1 M TRIS buffer, pH 9.0) for 15 min at 50 °C. After washing with Milli-Q water for 1 min, the slide was blown dry by N_2 stream to avoid water stains on the slide surface.

Fabrication of Streptavidin-modified PDMS Monolith The PDMS product surface was microfabricated with drainage canals and then functionalized with streptavidin as previously described.[27,28] Briefly, the PDMS surface was modified with thiol groups by silanization with 3-mercaptopropyltrimethoxysilane (MPS). Then, streptavidin-maleimide conjugate solution was introduced onto the thiol-modified PDMS surface allowing the reaction between maleimide and thiol groups. The unreacted maleimide and thiol groups were blocked by incubating the functionalized PDMS into a 1.5 mM 2-mercaptoethanol solution and a 3 mM N-ethylmaleimide solution, respectively.

Surface Polymerase Reaction The reactant surface (Scheme 4.1) immobilized with DNA templates was incubated with the primer solution (10 μM in 4x SSC buffer containing 0.1% SDS) in a sealed humidity chamber at 20 to 25 °C for 15 h to 20 h. After primer hybridization, the slide was washed sequentially as follows at 20 to 25 °C: 1 x 10 min in 2x SSC buffer containing 0.2% SDS, 1 x 10 min in 2x SSC buffer, and 1 x 10 min in 0.2x SSC buffer, and then blown dry with N_2. Next, the slide was exposed to a polymerase reaction mixture (20 μL) including T4 DNA polymerase (0.2 μL: 1 u), 5x reaction buffer (4 μL: 335 mM TRIS-HCl pH 8.8 at 25 °C, 33 mM $MgCl_2$, 5 mM DTT, 84 mM $(NH_4)_2SO_4$), a 2 mM dNTP mixture (1 μL: 0.1 mM final concentration), and nuclease-free water (14.8 μL). Polymerase solutions incorporating Cy3-dCTP were prepared with T4 DNA polymerase (0.2 μL: 1 u), 5x reaction buffer (4 μL: 335 mM TRIS-HCl pH 8.8 at 25 °C, 33 mM $MgCl_2$, 5 mM DTT, 84 mM $(NH_4)_2SO_4$), a 2 mM

dNTP mixture without dCTP (1 μL: 0.1 mM final concentration), 1 mM Cy3-dCTP (2 μL: 0.1 mM final concentration), and nuclease-free water (12.8 μL). The slide and the reaction mixture was incubated in an incubator (model # 1570, Sheldon Manufacturing Inc., Cornelius, OR) at 25 °C for 5 min. After incubation, the slide was sequentially rinsed with 2x SSC buffer containing 0.1% SDS and with 0.1x SSC buffer.

Transfer of Polymerase Reaction Products Product transfer was achieved using a slight variation of a previously reported procedure.[27,28] Briefly, 4x SSC buffer (10 μL) was dropped on the reaction master to wet the surface, and then streptavidin-functionalized PDMS was brought into contact with the reaction surface. A pressure of 1.4 N/cm^2 was applied at 20 to 25 °C for 10 min. Next, the PDMS product surface was peeled off the glass reaction surface with constant separation speed (400 μm/s) using a linear actuator (CMA-25CC, Newport Corp., Irvine, CA), and then both surfaces were washed in buffer and blown dry.

4.4 RESULTS AND DISCUSSION

Figure 4.1 demonstrates ssDNA immobilization onto the reactant surface, primer annealing and extension, and product transfer. Specifically, Figure 4.1a is a fluorescence micrograph obtained after immobilizing the 38-base, ssDNA template onto an epoxy-modified glass surface, annealing the primer to the template, and then extending the primer. In this case, the polymerase reaction mixture included dye-labeled deoxycytidine triphosphate (Cy3-dCTP), and therefore the extended primer is fluorescent (Scheme 4.1). Control experiments indicated that no fluorescence could be detected from the reactant surface after immobilization of the template and annealing of the primer, but before addition of Cy3-dCTP and primer extension (Figure 4.2a). Likewise, no fluorescence was observed when the primer-annealed reactant surface was exposed to all reactants

45
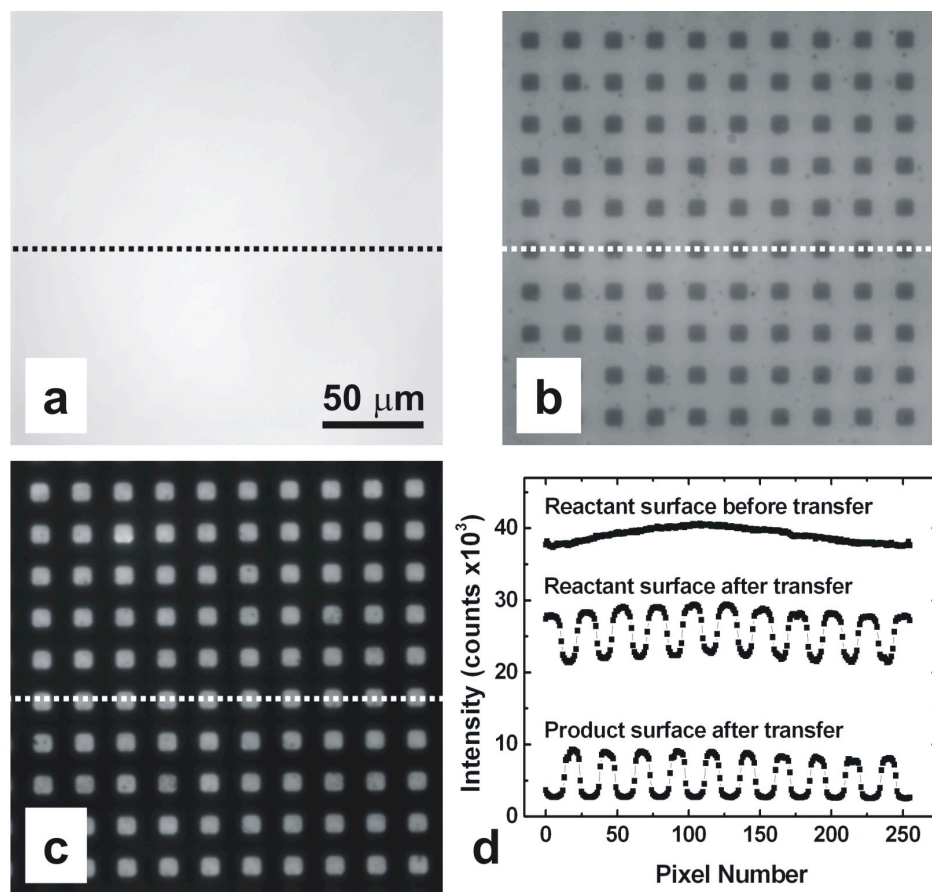
Figure 4.1. Fluorescence micrographs demonstrating extension of primers and transfer of the extended primers. (a) A fluorescence micrograph obtained from a reactant surface after a polymerase reaction incorporated Cy3-dCTP into the extended primers. (b) A fluorescence micrograph obtained from the reactant surface after transfer of the extended primers. (c) A fluorescence micrograph obtained from the product surface after transfer of the extended primers. (d) Fluorescence intensity profiles obtained along the dotted lines shown in (a)-(c). Integration time was 100 ms. Gray scales are 16000-42000 counts for (a) and (b), and 2500-15000 counts for (c).
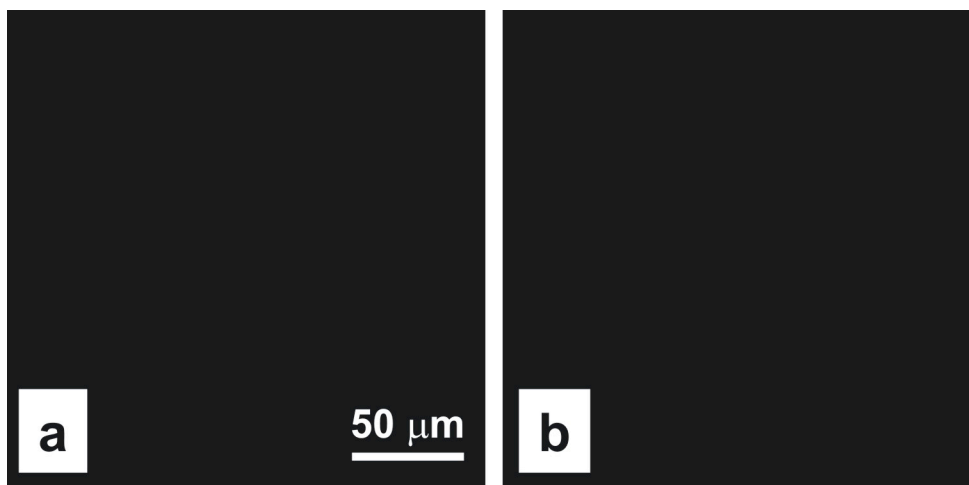
Figure 4.2. Fluorescence micrographs. (a) A reactant surface modified with template oligonucleotides and hybridized to biotinylated primer oligonucleotides, but before primer extension and incorporation of Cy3-dCTP. (b) A reactant surface treated identically to that shown in Figure 4.1a, but in the absence of the T4 DNA polymerase. The integration time was 1000 ms for (a) and 100 ms for (b). The gray scale is 16000-42000 counts for both micrographs.

(including Cy3-dCTP) except for the T4 DNA polymerase and then rinsed with buffer (Figure 4.2b). This indicates no detectable level of nonspecific adsorption of the dye. Parts b and c of Figure 4.1 are fluorescence micrographs of the reactant and product surface, respectively, after transfer of the extended primer. The dark regions on the reactant surface (Figure 4.1b) correspond to DNA incorporating Cy3-dCTP that was transferred to the product surface, and the light regions in Figure 4.1c correspond to the transferred DNA on the product surface. The checkerboard pattern results from drainage canals (20 μm on center, 10 μm wide, and 3 μm deep) on the product surface (Figure 4.3). These canals are necessary for successful DNA transfer, because they provide a means for buffer solution trapped between the reactant and product surfaces to escape.[27,28] Figure 4.1d shows fluorescence intensity profiles obtained along the dotted lines in Figures 4.1a-4.1c. The average intensity difference between the bright and dark regions on the reactant surface ((6.8 ± 0.2) x 10^3 counts, Figure 4.1b) is very close to that on the product surface ((6.0 ± 0.4) x 10^3 counts, Figure 4.1c), indicating little net loss of extended primers during transfer.

Figure 4.4 shows that multiple primer-extension reactions and transfers can be carried out using a single reactant surface. These experiments were executed using the approach shown in Figure 4.4e. After annealing the primers to the immobilized template DNA, the polymerase reaction was performed using an unlabeled mixture of deoxyribonucleotide triphosphates (dNTP). This results in a surface that is not fluorescent. Next, the extended and nonfluorescent primers were transferred to a product surface. Finally, fluorescently labeled probe DNA, complementary to only the extended sequence (not to the primer), was exposed to the product surface. This process was carried out three times using the same reactant surface, and fluorescence micrographs of the three resulting product surfaces are shown in Figures 4.4a-4.4c. Note that in the

48
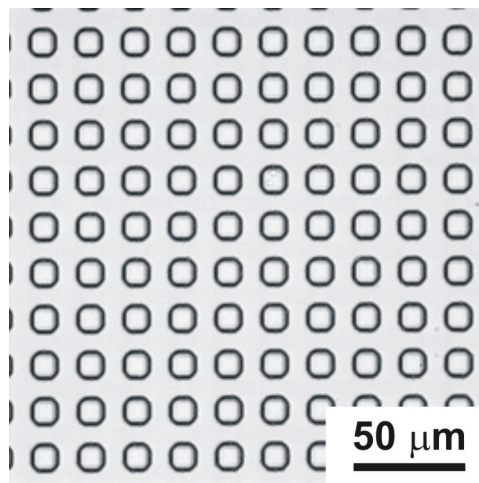
Figure 4.3. Optical micrograph showing the drainage pattern on a PDMS product surface.

Figure 4.4. Fluorescence micrographs demonstrating multiple transfers of extended primers from a single reactant surface. (a) A fluorescence micrograph obtained from a product surface after primer extension, transfer of the extended primers, and hybridization of a fluorescent probe complementary to the extended primer (but not to the primer itself). (b) Same as (a), but after a second round of primer extension, transfer, and hybridization. (c) Same as (a), but after a third round of primer extension, transfer, and hybridization. (d) Fluorescence intensity profiles obtained along the dotted white lines shown in (a)-(c). (e) Scheme showing the experimental approach used to obtain the data in Frames (a)-(d). The star symbols represent the fluorescent dye. The integration time was 1000 ms. The gray scale is 2500-5500 counts for (a)-(c). The fluorophore attached to the probe oligonucleotide was FAM (fluorescein).

50

absence of the T4 polymerase, no fluorescence was detected on the product surface (Figure 4.5). There are three important conclusions that arise from this set of experiments. First, it demonstrates that multiple product transfers can be carried out using the same reactant surface. Figure 4.4d provides line scans corresponding to the three micrographs. These show that the average modulation in fluorescence is 1040 ± 110, 920 ± 50, and 1190 ± 190 for the first, second, and third transfers, respectively. A duplicate of this experiment was carried out using a different reactant surface, and in that case there was more variation between the first (1070 ± 90), second (1090 ± 110), and third (630 ± 50) replicates (Figure 4.6). Second, when this experiment was carried out in the absence of internal spacers between the template oligonucleotide and the surface (18-carbon internal spacers repeated five time: $iSp18_5$, Integrated DNA Technologies, Coralville), no detectable hybridization of the fluorescently labeled complement was observed. This is likely a consequence of steric hindrance between the T4 polymerase and the glass surface, which results in incomplete primer extension. Third, Figure 4.4 clearly shows that the transferred reaction product is functional, because it hybridizes to its fluorescent complement.

4.5 CONCLUSION

There are two important conclusions resulting from this study. First, very small amounts of reaction products can be transferred from the reactant surface to the product surface. Here, we demonstrated transfer of ~10^{-14} moles of DNA oligonucleotides,[83,124] but there is no technological barrier for reducing this to as few as ~10^{-19} moles.[103] Second, the spatial relationship between reactant and product surfaces are preserved with micron-scale resolution after transfer, and it seems likely that this could be reduced still further.[103] This approach is demonstrated for a DNA polymerase reaction, but it should be useful for
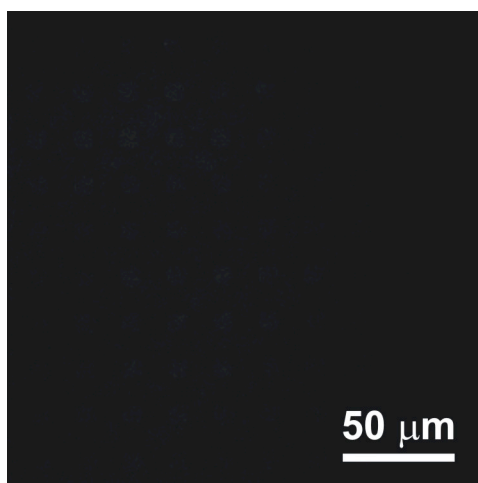
Figure 4.5. Fluorescence micrograph of a product surface obtained via transfer from a reactant surface similar to that shown in Figure 4.2b, but using an unlabeled mixture of dNTP not containing Cy3-dCTP, and subsequent exposure to the fluorescently labeled complement of the extended primer (but not to the primer itself). Note that this is a control experiment, and the experiment was carried out without exposure of the reactant surface to the T4 DNA polymerase. The integration time was 1000 ms, and the gray scale is 2500-5500 counts.
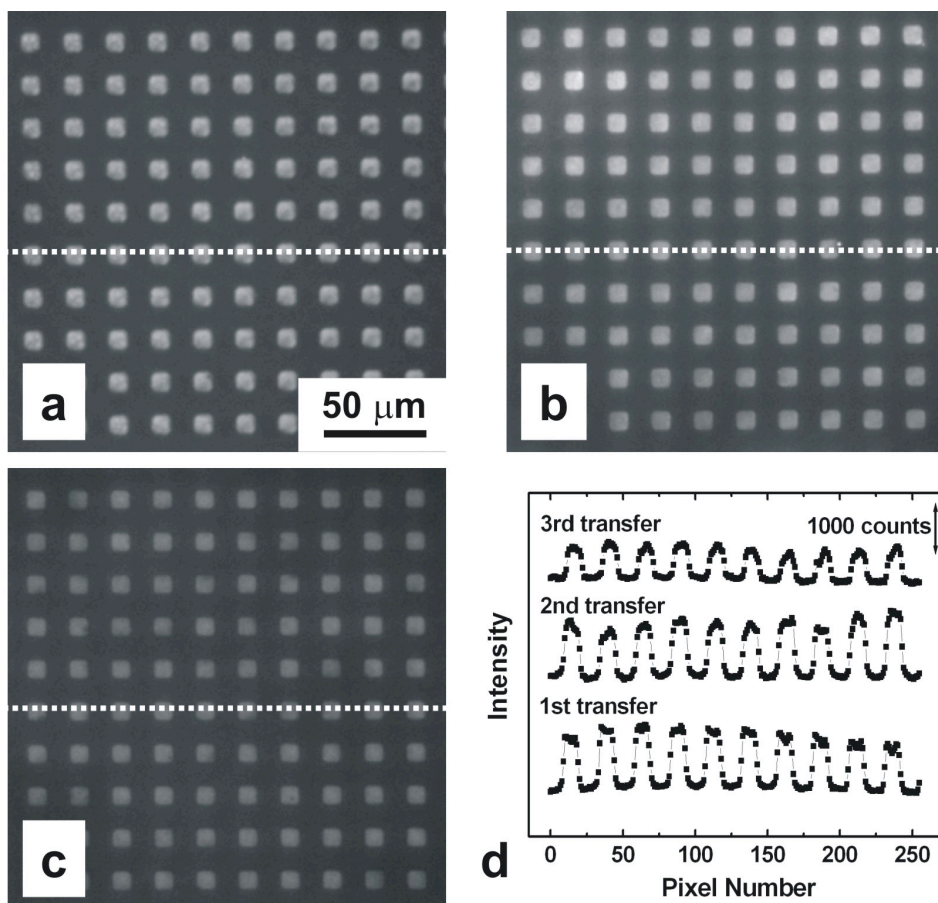
Figure 4.6. A duplicate experiment analogous to that shown in Figure 4.4. Fluorescence micrographs demonstrating multiple transfers of extended primers from a single reactant surface. (a) A fluorescence micrograph obtained from a product surface after primer extension, transfer of the extended primers, and hybridization of a fluorescent probe complementary to the extended primer (but not to the primer itself). (b) Same as (a), but after a second round of primer extension, transfer, and hybridization. (c) Same as (a), but after a third round of primer extension, transfer, and hybridization. (d) Fluorescence intensity profiles obtained along the dotted white lines shown in (a)-(c). The integration time was 1000 ms and the gray scale is 2500-5500 counts for (a)-(c).

other chemical and biological reactions too. Applications to high-throughput screening and separation of very small amounts of reaction products from a complex milieu are easily envisioned.

Chapter 5: Replication of DNA Microarrays after Enzymatic Synthesis of DNA on Masters

5.1 SYNOPSIS

In this paper we describe a method for replication of DNA microarrays. The approach involves in-situ, enzymatic synthesis of a DNA complement array on a prefabricated master array, followed of the complement array to a second substrate. The new findings reported here include the following. First, a single master array having DNA spots as small as 200 μm can be used to prepare up to three replicas without a significant degree of change in the transfer efficiency. Second, DNA master arrays containing up to at least ~2300 spots (100 μm spot size) can be replicated. Third, arrays consisting of multiple different oligonucleotide sequences can be replicated. In all cases, the replicate arrays are able to bind complementary oligonucleotide sequences.

5.2 INTRODUCTION

We recently reported a method for parallel replication of DNA microarrays (Scheme 5.1).[27-29] The approach consists of 5 steps. First, a master DNA array is prepared by covalent immobilization of amine-functionalized DNA templates on an epoxy-modified glass substrate. Second, biotinylated primer oligonucleotides, consisting of a single sequence, are hybridized to the distal end of the template DNA. Third, the primers are extended using a T4 DNA polymerase enzyme. Fourth, a streptavidin-coated poly(dimethylsiloxane) (PDMS) monolith is brought into contact with the master. This results in binding of the extended, biotinylated primers to the PDMS surface. Fifth, the PDMS substrate is mechanically separated from the glass master array. This results in

Scheme 5.1

a ssDNA → Primer annealing / Extension → b

Master

b → Contact and surface reaction → c

Master

c Replica / Master — Streptavidin / Biotin

c → Separation → d
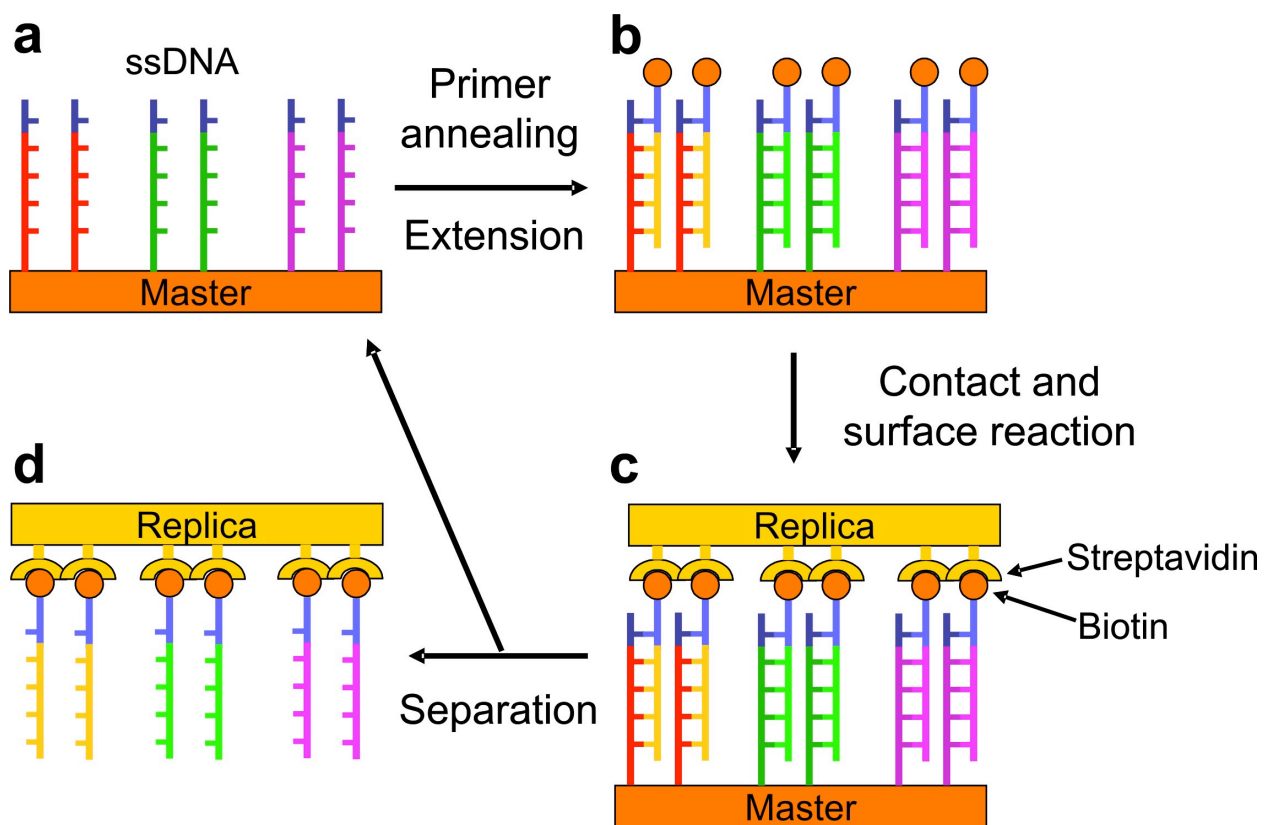
d Replica

transfer of the extended primers to the PDMS surface, and it leaves the original master array ready to prepare a second replicate array.

In our first report of this method,[29] we demonstrated that a single, large DNA spot could be replicated up to three times. Here, we expand upon the scope of this approach in three ways. First, we show that master DNA microarrays consisting of three unique DNA sequences (200 μm spot size) can be faithfully replicated. Second, master arrays containing up to ~2300 individual 100 μm DNA spots are replicated. Third, a single master having DNA spots as small as 200 μm is used to prepare three replicate arrays without a significant decrease in transfer efficiency. Importantly, these findings indicate that mechanical replication of DNA microarrays is robust and scaleable.

Most existing methods for the fabrication of DNA microarrays fall into one of two categories: parallel light-directed synthesis and serial mechanical spotting of pre-synthesized DNA oligonucleotides.[49,51,125-127] The light-directed method combines either photolithography or micromirror[128] technology with stepwise, in-situ solid-phase oligonucleotide synthesis. Light-directed synthesis can yield spot sizes as small as 25 μm, but the length of the resulting oligonucleotides is usually limited to 25 bases.[127,129] DNA microarrays can be also produced by delivery of pre-synthesized oligonucleotides. Spotting is carried out using either a rigid pin to transfer solution to the array substrate or by projecting a liquid drop from a jet nozzle. This delivery method does not exert limitations on the length of the oligonucleotides, but it does require the use of presynthesized oligonucleotides and results in larger spot sizes (75~500 μm) compared to light-directed methods.[49] Additionally, the serial spotting approach could be subject to an accumulation of errors such as contamination of spots, particularly for large-scale arrays. A few other microarray fabrication methods have been reported, but like ours, they are still in the development stage. These include scanning probe methods[130-132] (dip-pen

57

nanolithography, nanografting, and meniscus force nanografting), and approaches based on microcontact printing.[133]

In addition to the method shown in Scheme 5.1,[29] our group[27,28] and the Stellacci group[102,103,120] have reported related methods for microarray replication. For example, we showed that presynthesized oligonucleotides could be used in place of in-situ, enzymatic synthesis.[27] At about the same time, Stellacci and coworkers reported a similar replication approach, but they used heating rather than mechanical unzipping[104,105] to separate the master and replicate oligonucleotides. They also showed that DNA features as small as 50 nm could be transferred using this approach.[103] Finally, we recently demonstrated the use of 'zip code' master arrays, which provide a means for replicating microarrays having different spot patterns using a single master array.[28]

5.3 EXPERIMENTAL

Chemicals and Materials. Glass slides coated with an epoxy monolayer (Nexterion® Slide E, SCHOTT North America, Inc., Elmsford, NY) were used to fabricate master DNA microarrays. The poly(dimethylsiloxane) (PDMS) monoliths were prepared from Sylgard 184 (Dow Corning, Midland, MI). Streptavidin-maleimide conjugates (Sigma S9415), 3-mercaptopropyltrimethoxysilane (MPS) (Fluka 63800), and other chemicals for buffers or blocking solutions were obtained from Sigma-Aldrich: 20x saline-sodium citrate (SSC) buffer (Sigma S6639), 10% sodium dodecyl sulfate (SDS) solution (Sigma L4522), sodium phosphate monobasic (Sigma S0751), sodium phosphate dibasic (Sigma S0876), Triton® X-100 (Sigma T8787), Trizma base (Sigma T6791), Trizma HCl (Sigma T6666), ethanolamine (Sigma E9508), 2-mercaptoethanol (Sigma M6250), and N-ethylmaleimide (Sigma E3876). T4 DNA polymerase (EP0061) supplied with 5x reaction buffer (335 mM TRIS-HCl pH 8.8 at 25 °C, 33 mM $MgCl_2$, 5 mM DTT,

84 mM $(NH_4)_2SO_4$), deoxyribonucleotide triphosphate (dNTP) mix (R0241), dNTP set (R0181), and nuclease-free water were used as received from Fermentas Inc. (Hanover, MD). Cy3 fluorescent dye-labeled deoxycytidine triphosphate (Cy3-dCTP) was obtained from Amersham Biosciences Corp. (Piscataway, NJ). DNA oligonucleotides were obtained from Integrated DNA Technologies (Coralville, IA). The sequences and modifications are provided in Table 5.1.

Characterization. A fluorescence microscope (Nikon TE2000, Nikon Co., Tokyo, Japan) equipped with appropriate filter sets (filter #: 41001 for fluorescein, 31002 for Cy3, and 41008 for Cy5, Chroma Technology Corp., Rockingham, VT), a mercury lamp (X-Cite™ 120, Nikon Co), and a CCD camera (Cascade®, Photometrics Ltd., Tucson, AZ) was used to acquire optical and fluorescence micrographs. Micrographs were processed using V++ Precision Digital Imaging software (Digital Optics, Auckland, New Zealand). Large density master arrays were scanned using a microarray scanner (GenePix 4000B, Molecular Devices Corp., Sunnyvale, CA).

Fabrication of Master Arrays. The master arrays were fabricated using epoxy-modified glass slides (Nexterion® Slide E) as previously described,[27-29] but with some modifications. Briefly, template oligonucleotide solutions (25 μM in 50 mM sodium phosphate buffer, pH 8.5) were spotted onto the glass slides using either a manual microarrayer (Xenopore Corp., Hawthorne, NJ) in a home-built humidity chamber, or a home-built robotic microarrayer. Next, the spotted slide was placed in a chamber in which the humidity was in equilibrium with a saturated NaCl solution at 20 to 25 °C. After incubation, the slide was washed to remove unbound templates and buffer substances using the following protocol (at 20 to 25 °C): 1 x 5 min in 0.1% Triton® X-100 solution, 2 x 2 min in 1 mM HCl solution, 1 x 10 min in 100 mM KCl solution, and 1 x 1 min in Milli-Q water (18 MΩ•cm, Millipore, Bedford, MA). Next, the slide was

59

Table 5.1 Sequences of templates, targets, and a primer in this study[a].

Name	Sequence
Template I	5'-5AmMC12-(iSp18)₅-TAT AAC AAG ACC TTC CTC AAT CCG GTG CAG AAT CGC AT-3'
Template II	5'-5AmMC12-(iSp18)₅-CGC GGT GGA GTT CCT TCT GGC TTG GTG CAG AAT CGC AT-3'
Template III	5'-5AmMC12-(iSp18)₅-GCC ATA CTA TCA CAA TTA CTC ATG GTG CAG AAT CGC AT-3'
Target I	5'-56FAM-TAT AAC AAG ACC TTC CTC AAT CC-3'
Target II	5'-5Cy3-CGC GGT GGA GTT CCT TCT GGC TT-3'
Target III	5'-5Cy5-GCC ATA CTA TCA CAA TTA CTC AT-3'
Primer	5'-5BioTEG-ATG CGA TTC TGC ACC-3'

[a]Here, 5AmMC12, (iSp18)₅, 5BioTEG, 56FAM, 5Cy3, and 5Cy5 correspond, respectively, to an amino modifier having a 12-carbon spacer on the 5' end of the DNA, 18-atom hexaethyleneglycol spacers repeated five times, a biotin modifier with a tetraethyleneglycol (TEG) spacer on the 5' end of the DNA, a fluorescein dye attached to the 5' end of the DNA, a Cy3 dye attached to the 5' end of the DNA, and a Cy5 dye attached to the 5' end of the DNA. This is the same notation used by the DNA supplier (Integrated DNA Technologies, Coralville, IA).

placed in a blocking solution (50 mM ethanolamine and 0.1 % SDS in 0.1 M TRIS buffer, pH 9.0) for 15 min at 50 °C. After washing with Milli-Q water for 1 min, the slide was blown dry by a N_2 stream to avoid water stains on the slide surface.

Fabrication of Streptavidin-modified PDMS Monoliths. Nanoscale, conformal contact between the master and replica surfaces is required for transfer of the replicate DNA array (Scheme 5.1, step c). This requires the use of micron-scale canals to direct buffer solution away from the interface during contact. As previously described,[27-29] these canals were introduced into the PDMS surface using a micromolding process,[134] and then the entire PDMS surface was functionalized with streptavidin. The latter functionalization was carried out as follows. First, the microstructured PDMS surface was silanized with 3-mercaptopropyltrimethoxysilane (MPS). Second, a streptavidin-maleimide conjugate was covalently linked to the PDMS surface via the resulting thiol groups. The unreacted maleimide and thiol groups were blocked by incubating the functionalized PDMS into a 1.5 mM 2-mercaptoethanol solution and a 3 mM N-ethylmaleimide solution, respectively.

Replication of Master Arrays. The replication procedure used here was similar to that we reported earlier, but there were a few modifications.[27-29] First, the master slide was exposed to a primer solution, which was then extended for 5 min in a polymerase solution at 25 °C. The polymerase reaction mixture contained T4 DNA polymerase (0.05 u/μL) and a dNTP mixture (0.1 mM) in a polymerase reaction buffer (1x: 67 mM TRIS-HCl (pH 8.8), 6.6 mM $MgCl_2$, 1 mM DTT, 16.8 mM $(NH_4)_2SO_4$). Polymerase solutions incorporating Cy3-dCTP were prepared the same way, except using a dNTP mixture with Cy3-dCTP (0.1 mM) unless specifically mentioned otherwise. For polymerase reactions on high-density master arrays, incubation chambers (CoverWell™, Grace Bio-Labs, Inc., OR) were used for uniform spreading of the reaction mixture on the surface. Following

primer extension, 4x SSC buffer (10 μL) was dropped on the master to wet the surface, and then the streptavidin-functionalized PDMS monolith was brought into contact with the surface. A pressure of 1.4 N/cm² was applied at 20 to 25 °C for 10 min. Next, the PDMS monolith was peeled off the master surface at constant separation speed (400 μm/s) using a linear motion actuator (CMA-25CC, Newport Corp., Irvine, CA), and then both surfaces were washed in buffer and blown dry.

5.4 RESULTS AND DISCUSSION

Surface Polymerization and DNA Transfer. Figure 5.1 demonstrates template-driven DNA polymerization on a master and subsequent transfer onto PDMS surfaces. The experiment was conducted following the approach shown in Scheme 5.2a. Template I solution (Table 5.1) was spotted onto a glass master using a manual microarrayer. This resulted in formation of a ~200 μm-diameter Template I spot. After annealing, the biotinylated primers were extended using the polymerase reaction mixture including dye-labeled deoxycytidine triphosphate (Cy3-dCTP). The extended primers were then transferred to a PDMS replica surface as previously reported.[27-29] Figure 5.1a shows a fluorescence micrograph obtained from a single ~200 μm spot on the glass master after primer extension of Template I and subsequent washing. The extended primer is fluorescent, because Cy3-dCTP is incorporated into the extended primer. There was no detectable level of fluorescence when the primer-annealed glass surface was exposed to the reaction mixture in the absence of the T4 DNA polymerase and washed using the same protocol used for the surface shown in Figure 5.1a.[29] Figures 5.1b and 5.1c are fluorescence micrographs of the glass master and PDMS replica, respectively, after transfer of the extended primers. The grid pattern visible on the PDMS surface (Figure 5.1c) corresponds to microfabricated drainage canals (20 μm on center, 10 μm wide, and
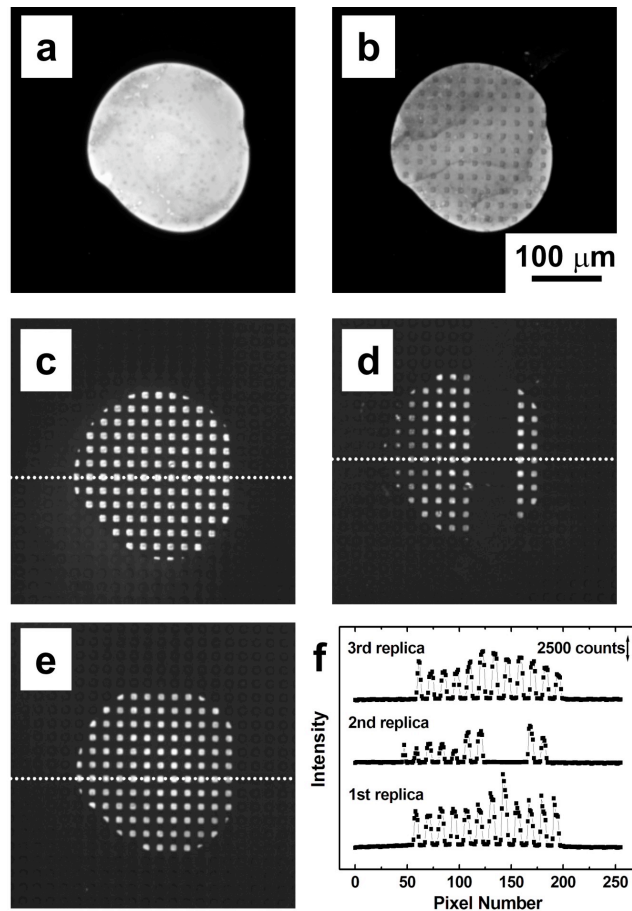
Figure 5.1. Fluorescence micrographs demonstrating polymerization of DNA on a master and transfer of the polymerized DNA. (a) A fluorescence micrograph obtained from a master after a surface T4 DNA polymerase reaction incorporating Cy3-dCTP into the polymerized DNA. (b) A fluorescence micrograph obtained from the master after transfer of the polymerized DNA. (c) A fluorescence micrograph obtained from a replica after transfer of the polymerized DNA. (d) Same as (c), but after a second round of polymerization and transfer. (e) Same as (c), but after a third round of polymerization and transfer. (f) Fluorescence intensity profiles obtained along the dotted white lines shown in (c)-(e). Integration time was 500 ms. Gray scales are 2000-60000 counts for (a) and (b), and 1500-10000 counts for (c)-(e).

63

Scheme 5.2
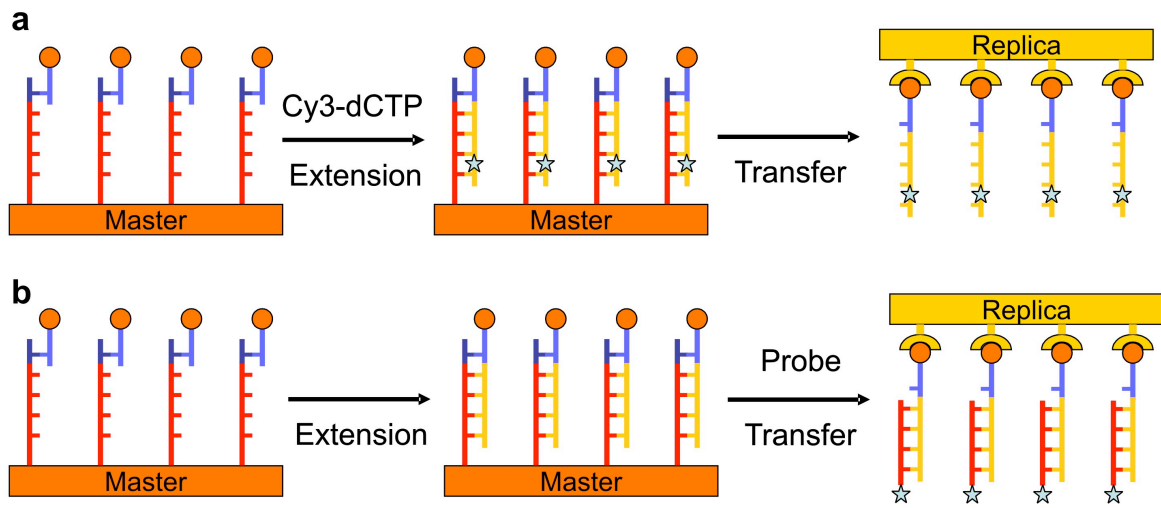
3 μm deep), which are necessary to direct buffer solution away from the glass/PDMS interface during conformal contact.[28,29] Optical micrographs of the images shown in Figures 5.1c–5.1e are provided in Figure 5.2. The drainage canals restrict contact between the glass and PDMS surfaces to multiple square areas (10 x 10 μm^2) that reside between the canals. The dark areas within the spot on the master surface (Figure 5.1b) correspond to primer-extended DNA that incorporated Cy3-dCTP but was subsequently transferred to the PDMS surface.

Figures 5.1d and 5.1e show additional PDMS replicas obtained after a second and a third round of primer annealing, extension, and mechanical transfer from the same master. The prominent dark area bisecting the second replica spot (Figure 5.1d) results from a wider canal that intersects the smaller ones and facilitates drainage during contact. Figure 5.1f shows fluorescence intensity profiles obtained along the white dotted lines in Figures 5.1c-5.1e. The average peak intensities on the profiles are 4200 ± 1100, 2200 ± 800, and 3400 ± 700 for the first, second, and third replicas, respectively. We observed relatively low intensity especially on the left area of the second replica spot, which caused the rather large variation between the first and second replicas. An optical micrograph of the second replica shows some abnormal surface residue on the left part of the replica spot, which could cause the lower intensity (Figure 5.2b). However, the reasonable consistency in the intensities indicates the replication cycle can be repeated at least three times using a single master without significant degradation. In addition, the fluorescence intensity profile obtained from the glass master after transfer shows that ~25% of the extended primers were transferred from the master to a replica surface (Figure 5.3).

Replication of a Small Master Array Having One Template Sequence. Thus far, our enzyme-based replication studies have resulted in transfer of a single spot. Here
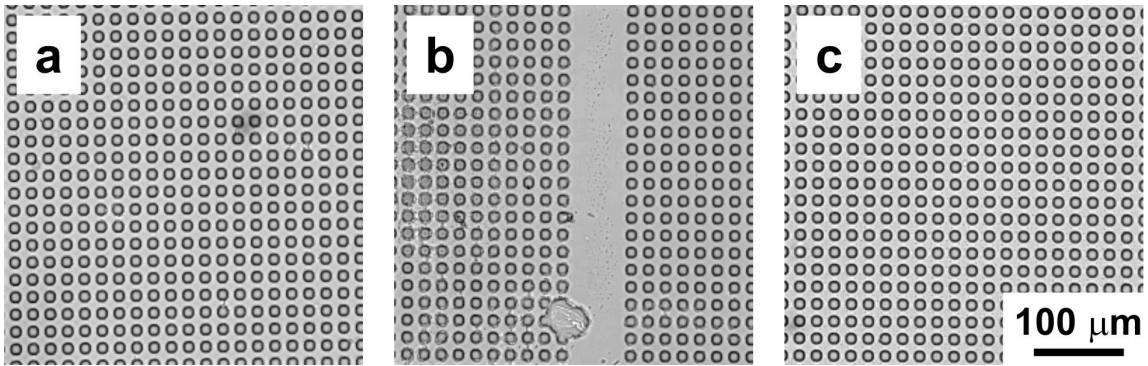
Figure 5.2. Optical micrographs of PDMS replicas shown in Figures 5.1c-5.1e. (a) An optical micrograph of the replica shown in Figure 5.1c. (b) An optical micrograph of the replica shown in Figure 5.1d. (c) An optical micrograph of the replica shown in Figure 5.1e.
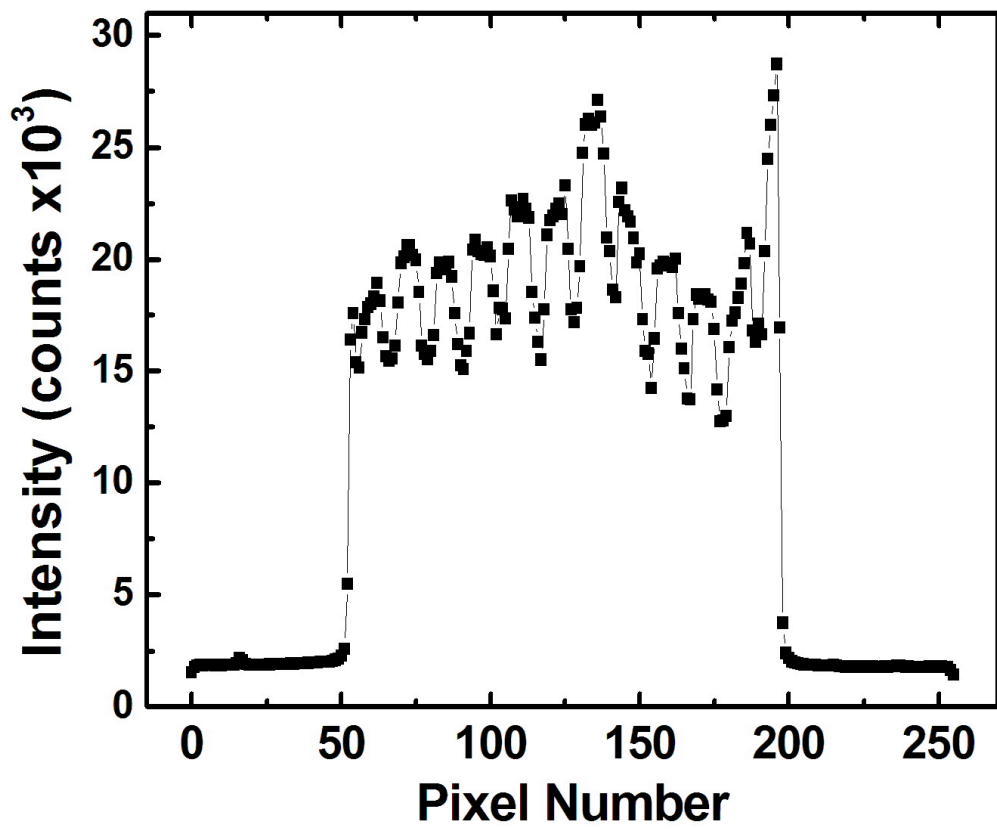
Figure 5.3. Fluorescence intensity profile obtained from a master spot (Figure 5.1b) after transfer of extended primers.

we show that a small array consisting of a single oligonucleotide sequence can also be transferred, and in the next section we include three different oligonucleotide sequences in a single array.

In contrast to the approach used to obtain the results shown in Figure 5.1 (Scheme 5.2a), the experiments corresponding to Figure 5.4 were performed as shown in Scheme 5.2b. Specifically, the primer extension reaction was carried out using Template I in the absence of a labeled nucleotide (Cy3-dCTP), and consequently the resulting master surface is not fluorescent. However, after primer extension and transfer to the PDMS surface, the replica was exposed to fluorescently labeled DNA Target I (10 μM, Table 5.1), which is complementary to the extended DNA sequence but not the primer. Figure 5.4a is a fluorescence micrograph obtained from a replica surface obtained after the three steps outlined in Scheme 5.2b. The result clearly shows that six functional spots are transferred from the 3 x 2 master array to the replica. Control experiments showed that there is no detectable fluorescence on the replica surface if the T4 polymerase is omitted during the primer-extension step.[29]

In addition to the fluorescently labeled spots, the wide drainage canals shown in Figure 5.4a also appear bright. Indeed, the canals also appear bright in the optical micrograph of the replica surface (Figure 5.4b). However, a series of control experiments confirmed that this is an optical effect unrelated to fluorescence (Figure 5.5). Figures 5.4c-5.4h are higher magnification fluorescence micrographs of the six spots shown in Figure 5.4a. The replica spot shown in Figure 5.4d was cut off because of the wide drainage canal apparent in Figures 5.4a and 5.4b. The characteristic grid pattern, arising from the smaller canals, is also apparent at this magnification.

Replication of a Master Array Having Multiple Template Sequences. Replication of a 3x2 master array having three unique templates was also carried out

Figure 5.4. Micrographs demonstrating replication of a 3x2 master array having one DNA template (Template I, Table 5.1). (a) A fluorescence micrograph obtained from a replica after polymerization of DNA, transfer of the polymerized DNA, and hybridization of a fluorescent Target I (Table 5.1) complementary to the extended sequence (but not to the primer itself). Integration time was 1000 ms. Gray scale is 2100-3200 counts. (b) An optical micrograph obtained from the replica showing a drainage canal pattern. (c)-(h) Fluorescence micrographs representing closer look of each replica spot shown in (a): (c) Top left replica spot. (d) Top middle replica spot. (e) Top right replica spot. (f) Bottom left replica spot. (g) Bottom middle replica spot. (h) Bottom right replica spot. Integration time was 1000 ms. Gray scale is 3000-13000 counts.

69
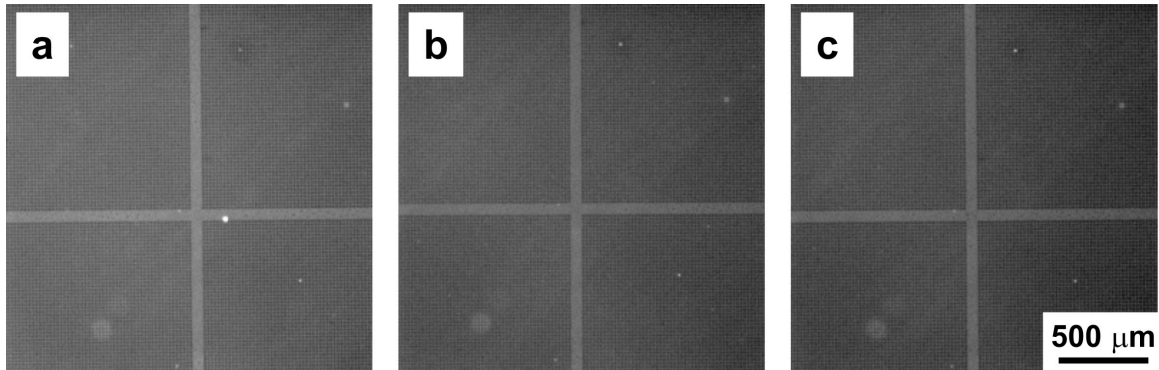
Figure 5.5. Fluorescence micrographs showing bright wide drainage canals. (a) A fluorescence micrograph obtained from a streptavidin-coated PDMS surface. (b) A fluorescence micrograph obtained from the streptavidin-coated PDMS after incubation with hybridization buffer (No fluorescently labeled Target I) and post-hybridization washing. (c) A fluorescence micrograph obtained from the streptavidin-coated PDMS after incubation with Target I in hybridization buffer and post-hybridization washing. Integration time was 1000 ms. Gray scale is 2100-3200 counts.

(Figure 5.6) using the approach shown in Scheme 5.2b. First, a 3x2 master array having three DNA templates (left column, Template I; middle column, Template II; right column, Template III) was fabricated. After polymerization of DNA and transfer of the polymerized DNA, the replica PDMS surface was exposed to a mixture of fluorescent targets (Target I, II, and III; 10 μM each, Table 5.1) complementary to each extended sequence (but not to the primer itself). Three fluorescence micrographs were obtained from the replica using different filter sets for each fluorescent target. Figure 5.6 shows the fluorescence micrographs. Each fluorescence micrograph shows only one type of synthesized DNA hybridized with each fluorescent target. This result clearly indicates that the DNA polymerization is performed correctly depending on the template sequences. The closer look at each replica spot shown in Figure 5.6 is also presented in Figure 5.7.

Replication of a Large Density Master Array. Replication of a large density master array was demonstrated using the approach shown in Scheme 5.2a. A master array having 2304 DNA spots (Template I, Table 5.1) was fabricated using a robotic microarrayer. After annealing of primers, a polymerase reaction mixture including dye-labeled deoxycytidine triphosphate (Cy3-dCTP) was introduced onto the master slide. The polymerized DNA incorporating Cy3-dCTP was transferred onto a replica surface. Figure 5.8a shows a fluorescence micrograph obtained by scanning the entire master after the polymerase reaction and washing. All polymerized DNA spots incorporating Cy3-dCTP showed homogeneous fluorescence, indicating a uniform polymerase reaction on the large density master. Figure 5.8b shows fluorescence micrographs of the entire master (left micrograph) and its part (right micrograph) after transfer of the polymerized DNA. The right micrograph shows a typical dark checkerboard pattern on each DNA spot,
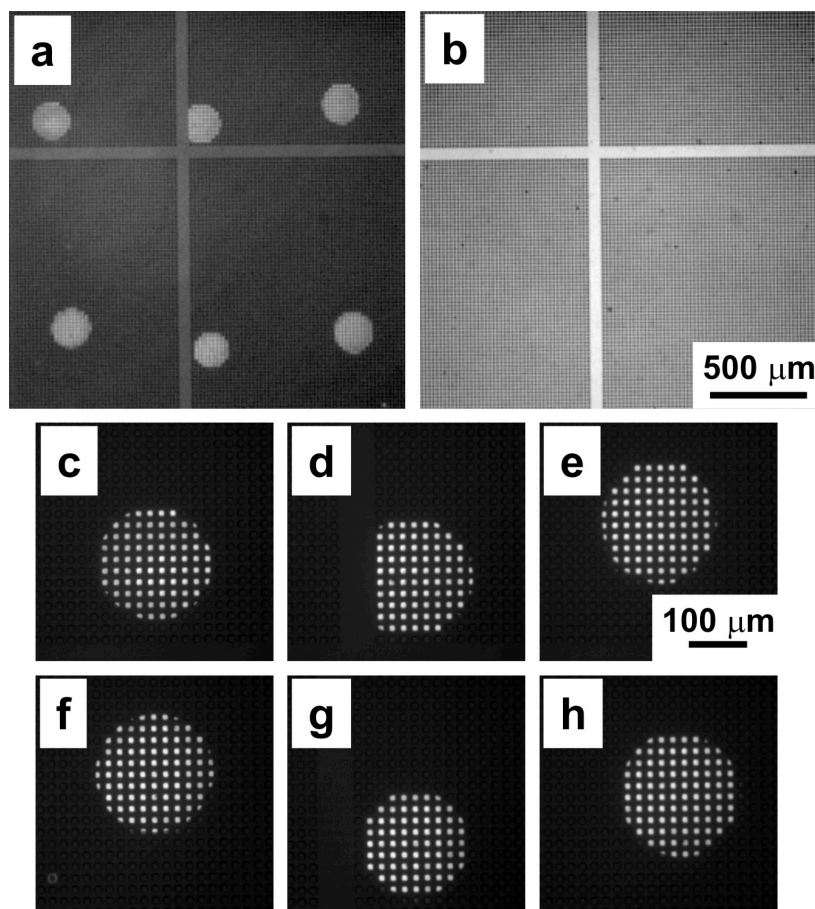
71
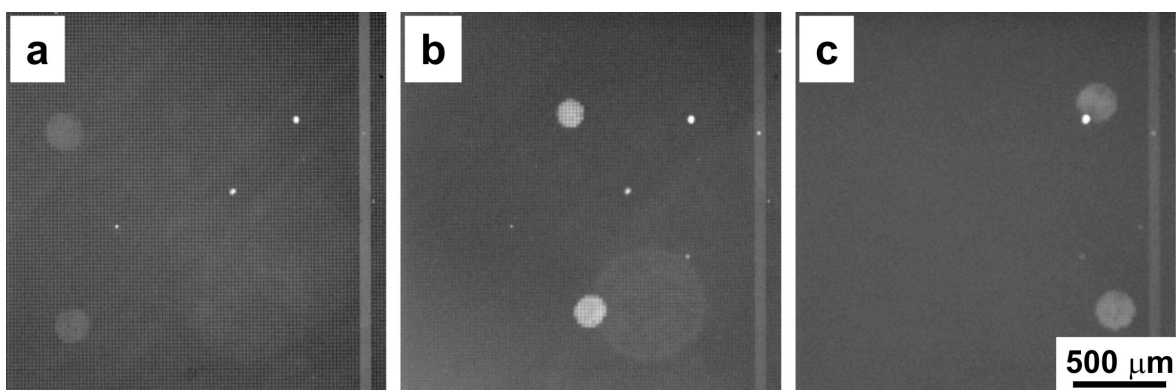
Figure 5.6. Fluorescence micrographs demonstrating replication of a 3x2 master array having multiple DNA templates (Template I, II, and III; Table 5.1). (a) A fluorescence micrograph obtained from a replica using a filter for Target I labeled with FAM. (b) Same as (a), but using a filter for Target II labeled with Cy3. (c) Same as (a), but using a filter for Target III labeled with Cy5. Integration time was 1000 ms. Gray scales are 2400-3800 counts for (a) and (b), and 1800-3200 counts for (c).
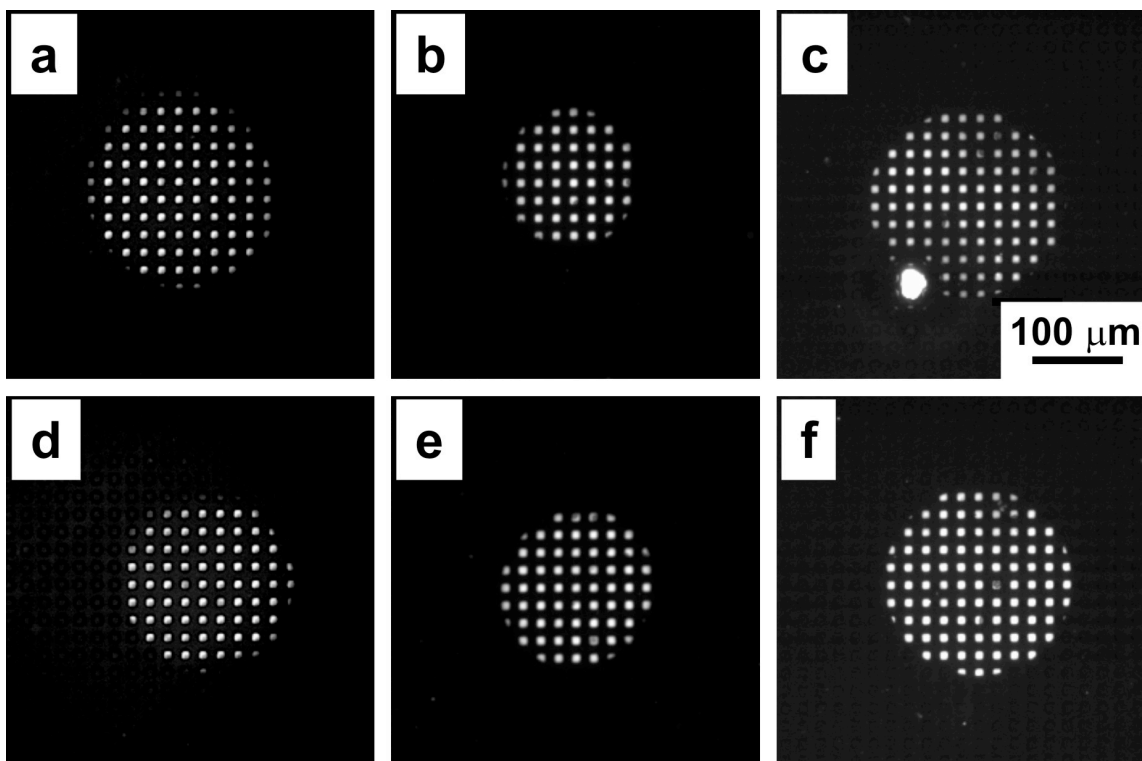
Figure 5.7. Fluorescence micrographs representing closer look of each replica spot shown in Figure 5.6. (a) Top left replica spot in Figure 5.6a. (b) Top middle replica spot in Figure 5.6b. (c) Top right replica spot in Figure 5.6c. (d) Bottom left replica spot in Figure 5.6a. (e) Bottom middle replica spot in Figure 5.6b. (f) Bottom right replica spot in Figure 5.6c. Integration time was 10000 ms. Gray scales are 3700-6000 counts for (a) and (d), 3000-30000 counts for (b) and (e), and 2000-8000 counts for (c) and (f).
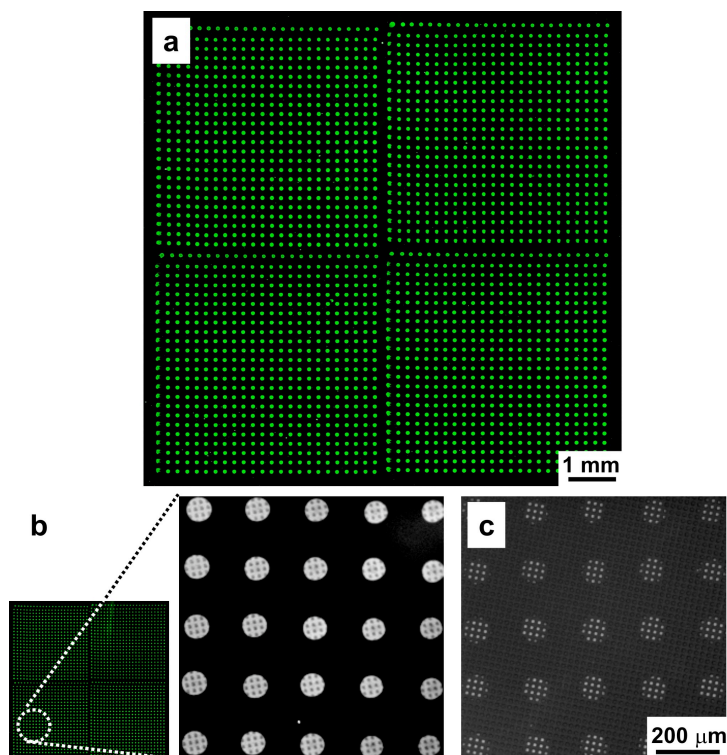
Figure 5.8. Fluorescence micrographs demonstrating replication of a large density DNA microarray. Polymerase reaction mixture included T4 DNA polymerase (0.05 u/μL), a dNTP mixture without dCTP (0.1 mM), and a dCTP mixture (Cy3-dCTP: 10 μM, unlabeled dCTP: 90 μM) in a polymerase reaction buffer (1x: 67 mM Tris-HCl (pH 8.8), 6.6 mM MgCl$_2$, 1 mM DTT, 16.8 mM (NH$_4$)$_2$SO$_4$). Micrographs of the entire master slide were obtained using a microarray scanner. (a) A fluorescence micrograph obtained by scanning the entire master after a surface T4 DNA polymerase reaction incorporating Cy3-dCTP into the polymerized DNA. (b) Fluorescence micrographs obtained from the master after transfer of the polymerized DNA. The right micrograph shows the closer look on a part of the entire master surface; Integration time was 1000 ms. Gray scale is 2600-4000 counts. (c) A fluorescence micrograph obtained from a replica after transfer of the polymerized DNA. Integration time was 1000 ms. Gray scale is 2000-4500 counts.

74

indicating transfer of the polymerized DNA. Figure 5.8c is a fluorescence micrograph obtained from the replica corresponding to the right micrograph shown in Figure 5.8b.

5.5 CONCLUSION

      In this work, we demonstrated a method for replication of DNA microarrays utilizing a surface polymerase reaction and mechanical transfer. Multiple replications (at least three times) from a single master array having DNA spots as small as 200 μm were successfully achieved with no significant degree of change in the transfer efficiency. Replication from a master array having three different sequences was performed accurately and there was no observable cross-hybridization on the replica. DNA master arrays consisting of ~2300 spots were also replicated. Further experiments will focus on improvement of transfer efficiency and replication of arrays having other biological materials (proteins, RNA oligonucleotides, and cells).

Chapter 6: Mechanical Transfer of Ligated RNA Strands for Fabrication of RNA Microarrays

6.1 SYNOPSIS

Here, a method for fabrication of RNA microarrays is described. The fabrication involves enzymatic formation of RNA array components on a prefabricated master DNA array, followed by mechanical transfer of the RNA array components to another substrate. The RNA array components are formed by a T4 DNA ligase reaction joining unmodified single strand (ss)RNA to short ssDNA oligonucleotides on the master surface. Importantly, the fabricate cycle can be repeated multiple times using a single master array. Consecutive fabrication of RNA microarrays (18 times) from a single master is achieved without significant degradation of functionality of the resulting RNA arrays. RNA microarrays having three different RNA sequences are fabricated and show no observable cross-hybridization of DNA complements.

6.2 INTRODUCTION

In this paper we describe a simple means for parallel conversion of DNA master arrays into RNA replicate arrays. The approach is based on a surface enzymatic reaction followed by mechanical transfer. The RNA replicate microarrays consist of single-strand RNA (ssRNA) oligonucleotides (probe RNA) ligated to short ssDNA oligonucleotides (anchor DNA). The details of the approach are shown in Scheme 6.1. First, amine-modified ssDNA templates are immobilized on an epoxy-modified glass slide. The distal ends of all the DNA templates are configured to be identical. Second, this master slide is exposed to single-sequence biotinylated anchor ssDNA, which hybridizes to the distal ends of the templates (the blue sequence in Scheme 6.1), and to the unmodified probe

Scheme 6.1

a

b

Hybridization

DNA & RNA

Master

Master

Nick

Ligation &
Surface contact

d

c

PDMS

PDMS

Master

Separation

Biotin-Streptavidin
binding

77
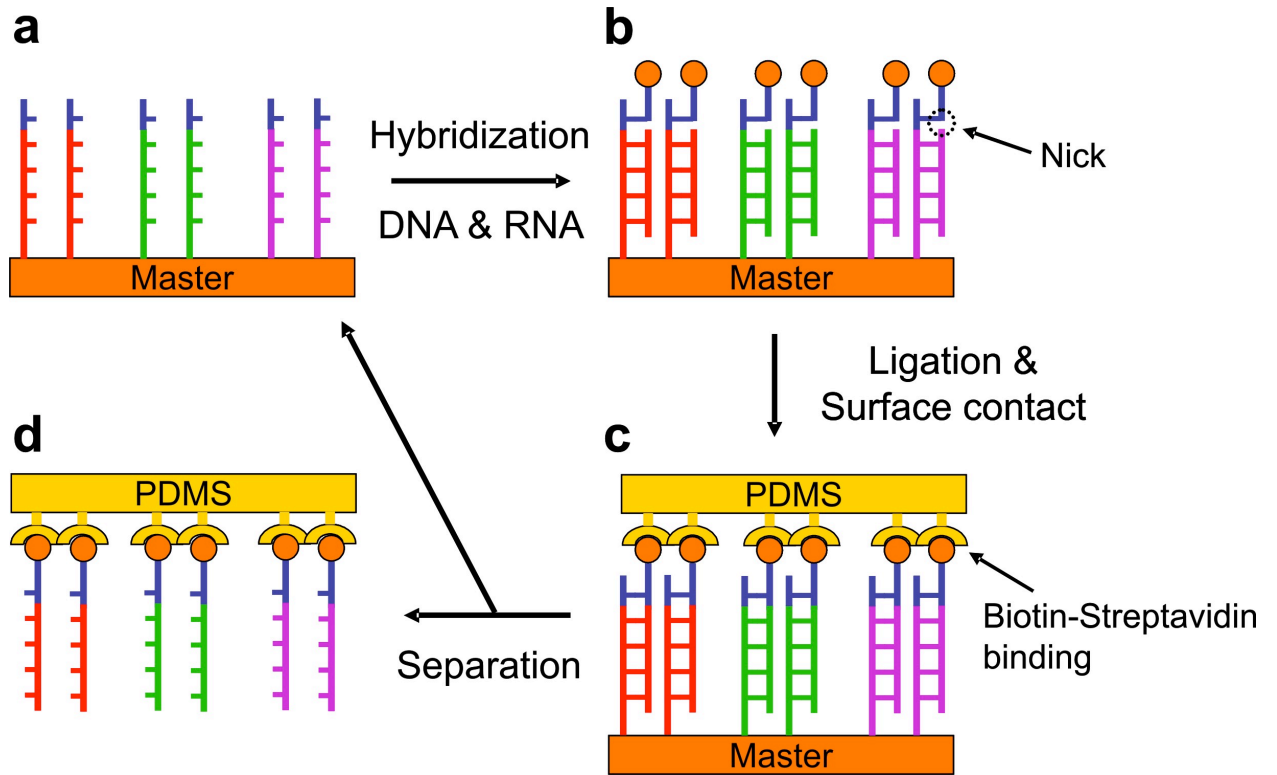
ssRNA, which is complementary to each ssDNA sequence comprising the master array. Third, the nick between the anchor ssDNA and the probe ssRNA is ligated using a T4 DNA ligase.[135-137] Next, a streptavidin-coated poly(dimethylsiloxane) (PDMS) monolith is brought into conformal contact with the master. This results in binding of the biotin anchor (now linked to the RNA probe) to the streptavidin-modified PDMS surface. When the PDMS monolith is mechanically separated from the master, the RNA array is transferred to the PDMS surface while the DNA templates remain on the master surface. This series of steps can be repeated many times without loss of fidelity, resulting in multiple RNA replicate arrays from a single master.

Previously, we showed that an approach similar to that illustrated in Scheme 6.1 could be used to replicate DNA microarrays.[27,28] In one case, the replicate oligonucleotides were formed in-situ using a surface polymerase reaction.[29] A related method, which relies on dehybridization by heating rather than by mechanical transfer, has been reported by Stellacci and coworkers.[102,103,120] They have shown that DNA lines as thin as 50 nm could be replicated.[103] Park and coworkers have recently used this method to replicate DNA arrays fabricated on nylon membranes.[121] RNA microarrays are a powerful tool for the analysis of nucleic acids and proteins. For example, ultrasensitive detection of DNA oligonucleotides was reported using RNA microarrays in conjunction with the enzyme RNase H.[138,139] The use of RNA aptamer microarrays also allowed simultaneous detection of multiple proteins[140] and demonstrated the potential for diagnosis of cancers.[141,142] RNA microarrays are normally fabricated by tethering modified RNA oligonucleotides on functionalized surfaces; for example, biotinylated RNA oligonucleotides on streptavidin-functionalized glass slides[140,143,144] or thiol-modified RNA oligonucleotides on maleimide-terminated gold surfaces.[138,139] Recently, Corn and coworkers showed that it was possible to prepare RNA microarrays using

surface ligation chemistry.[137,145,146] This approach made it possible to attach unmodified ssRNA to a DNA array, to convert the DNA array to an RNA array. They also showed the DNA array can be used for at least three ligation-hydrolysis cycles.[137]

In this paper, we expand the scope of our mechanical-transfer approach for replicating DNA arrays by showing that a related series of steps can be used to prepare many RNA replica arrays from a single DNA master using unmodified RNA oligonucleotides. The key step is a surface ligase reaction, first reported by Corn and coworkers,[137] required to link the anchor DNA to the RNA oligonucleotides. This step is carried out using a T4 DNA ligase. We show that the series of steps illustrated in Scheme 6.1, which proceed under mild conditions, can be executed at least 18 times using a single DNA master array without loss of fidelity of the replicate RNA array. RNA microarrays consisting of 2500 spots and consisting of up to three different RNA sequences were prepared, and no evidence of cross-hybridization was detected.

6.3 EXPERIMENTAL

Chemicals. Streptavidin-maleimide conjugates (Sigma S9415), 3-mercaptopropyltrimethoxysilane (MPS) (Fluka 63800), and other chemicals for buffers or blocking solutions were obtained from Sigma-Aldrich: 20x saline-sodium citrate (SSC) buffer (Sigma S6639), 10% sodium dodecyl sulfate (SDS) solution (Sigma L4522), sodium phosphate monobasic (Sigma S0751), sodium phosphate dibasic (Sigma S0876), Triton® X-100 (Sigma T8787), Trizma base (Sigma T6791), Trizma HCl (Sigma T6666), ethanolamine (Sigma E9508), 2-mercaptoethanol (Sigma M6250), and N-ethylmaleimide (Sigma E3876). The poly(dimethylsiloxane) (PDMS) precursor solution (Sylgard 184) was ordered from Dow Corning Inc. (Midland, MI). T4 DNA ligase (M0202S) provided with 10x reaction buffer (500 mM TRIS-HCl, 100 mM MgCl$_2$, 100 mM DTT, and 10

mM ATP; pH 7.5 at 25 °C) was used as received from New England BioLabs Inc. (Ipswich, MA). Nuclease-free water was obtained from Fermentas Inc. (Hanover, MD). DNA and RNA oligonucleotides were obtained from Integrated DNA Technologies Inc. (Coralville, IA) and Dharmacon Corp. (Lafayette, CO), respectively. The sequences and modifications are provided in Table 6.1.

Instrumentation. A fluorescence microscope (Nikon TE2000, Nikon Co., Tokyo, Japan) equipped with appropriate filter sets (filter #: 31002 for DY547 and Cy3, and 41008 for Cy5, Chroma Technology Corp., Rockingham, VT), a mercury lamp (X-Cite™ 120, Nikon Co), and a CCD camera (Cascade®, Photometrics Ltd., Tucson, AZ) was used to acquire optical and fluorescence micrographs. Micrographs were processed using V++ Precision Digital Imaging software (Digital Optics, Auckland, New Zealand). High-density arrays were scanned using a microarray scanner (GenePix 4000B, Molecular Devices Corp., Sunnyvale, CA).

Fabrication of Master DNA Arrays. The master DNA arrays were fabricated using epoxy-modified glass slides (Nexterion® Slide E, SCHOTT North America Inc., Elmsford, NY) as previously described.[27,28] Briefly, template DNA solutions (25 μM in 50 mM sodium phosphate buffer, pH 8.5) were spotted onto the glass slides using either a micropipette or a home-built robotic microarrayer. Next, the spotted slide was incubated in a chamber in which the humidity was in equilibrium with a saturated NaCl solution at 20 to 25 °C. After incubation, the slide was washed as following (at 20 to 25 °C): 1 x 5 min in 0.1% Triton® X-100 solution, 2 x 2 min in 1 mM HCl solution, 1 x 10 min in 100 mM KCl solution, and 1 x 1 min in Milli-Q water (18 MΩ•cm, Millipore, Bedford, MA). The slide was then placed in a blocking solution (50 mM ethanolamine and 0.1 % SDS in 0.1 M TRIS buffer, pH 9.0) for 15 min at 50 °C. After washing with Milli-Q water for 1 min, the slide was blown dry by a N_2 stream and stored under dark and dry condition.

Table 6.1 Sequences of the nucleic acids used in this study[a].

Name	Sequence
Template DNA I (D_T I)	5'-TTT TTT TTT TTT TTT TTT TTG CAA GCC CCA CCT AGA CCG CAG AG-3AmM-3'
Template DNA II (D_T II)	5'-TTT TTT TTT TTT TTT TTT TTT AGC ATT AGG TAC GTC ATT ACA GT-3AmM-3'
Template DNA III (D_T III)	5'-TTT TTT TTT TTT TTT TTT TTC GTA AGT TCA GCA CAG TAT GAC CC-3AmM-3'
Probe RNA I (R_P I)	5'-CUC UGC GGU CUA GGU GGG GCU UGC-3'
Probe RNA II (R_P II)	5'-ACU GUA AUG ACG UAC CUA AUG CUA-3'
Probe RNA III (R_P III)	5'-GGG UCA UAC UGU GCU GAA CUU ACG-3'
Probe RNA I with dye (R_P I with dye)	5'-DY547-CUC UGC GGU CUA GGU GGG GCU UGC-3'
Probe RNA II with dye (R_P II with dye)	5'-DY547-ACU GUA AUG ACG UAC CUA AUG CUA-3'
Anchor DNA (D_A)	5'-5Phos-AAA AAA AAA AAA AAA AAA AA-3BioTEG-3'
Anchor DNA without PO_4	5'-AAA AAA AAA AAA AAA AAA AA-3BioTEG-3'
Target DNA I	5'-GCA AGC CCC ACC TAG ACC GCA GAG-3Cy3Sp-3'
Target DNA II	5'-TAG CAT TAG GTA CGT CAT TAC AGT-3Cy5Sp-3'

[a]Here, 3AmM, DY547, 5Phos, 3BioTEG, 3Cy3Sp, and 3Cy5Sp correspond, respectively, to an amino modifier on the 3' end of the DNA, a Cy3 alternate dye attached to the 5' end of the RNA, phosphorylation on the 5' end of the DNA, a biotin modifier with a tetraethyleneglycol (TEG) spacer on the 3' end of the DNA, a Cy3 dye attached to the 3' end of the DNA, and a Cy5 dye attached to the 3' end of the DNA. This is the same notation used by the DNA supplier (Integrated DNA Technologies, Coralville, IA) and the RNA supplier (Dharmacon Inc., Lafayette, CO).

Fabrication of RNA Replica Arrays. The RNA arrays were fabricated by simultaneously exposing the DNA master array to the anchor DNA oligonucleotide, the RNA probe, and the T4 DNA ligase for 1 h at 25 °C. Specifically, the ligase reaction mixture contained the anchor DNA strands (0.5 μM), the probe RNA strands (0.5 μM), and T4 DNA ligase (20 u/μL) in a ligase reaction buffer (1x: 50 mM TRIS-HCl, 10 mM MgCl$_2$, 10 mM DTT, and 1 mM ATP; pH 7.5 at 25 °C). Incubation chambers (CoverWell™, Grace Bio-Labs Inc., OR) were used to ensure uniform spreading of the reaction mixture on the surface. Following ligation, the master slide was rinsed with buffer solutions (at 20 to 25 °C): 2x SSC buffer containing 0.2 % SDS and 2x SSC buffer. The master slide was washed again as follows (at 20 to 25 °C): 10 min in 2x SSC buffer containing 0.2 % SDS, 10 min in 2x SSC buffer, and 10 min in 0.2x SSC buffer. Next, 4x SSC buffer (10 μL) was dropped on the master to wet the surface, and then a streptavidin-functionalized PDMS monolith was brought into contact with the surface. A pressure of 1.4 N/cm^2 was applied at 20 to 25 °C for 10 min. Note that the streptavidin-functionalized PDMS monolith was prepared as reported previously.[27-29] Finally, the PDMS monolith was peeled off the master surface at a constant separation speed (400 μm/s) using a linear motion actuator (CMA-25CC, Newport Corp., Irvine, CA), and then both surfaces were washed in buffer and blown dry.

6.4 RESULTS AND DISCUSSION

Surface Ligation and Transfer of Ligated RNA Strands. The fluorescence micrographs shown in Figure 6.1 demonstrate the viability of the replication procedure shown in Scheme 6.1. The specific approach for this experiment is illustrated in Figure 6.1e. Template DNA (D$_T$ I; Table 6.1) immobilized on the master slide was exposed to a ligase reaction mixture composed of biotinylated anchor DNA (D$_A$; Table 6.1),

82
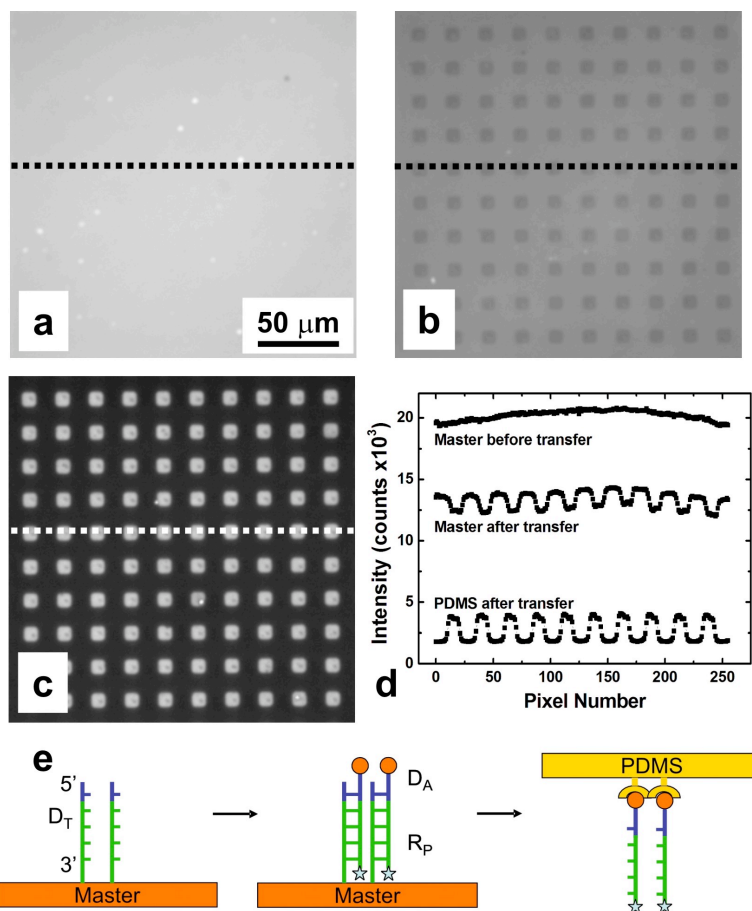
Figure 6.1. Fluorescence micrographs demonstrating ligation of RNA on a master and transfer of the ligated RNA. (a) A fluorescence micrograph obtained from a master after a surface T4 DNA ligase reaction joining fluorescently labeled probe RNA I (R_P I with dye; Table 6.1) to the biotinylated anchor DNA (D_A; Table 6.1). (b) A fluorescence micrograph obtained from the master after transfer of the ligated RNA (joined D_A and R_P). (c) A fluorescence micrograph obtained from a PDMS surface after transfer of the ligated RNA. (d) Fluorescence intensity profiles obtained along the dotted lines shown in (a)-(c). (e) Scheme showing the experimental approach used to obtain the data in (a)-(d). The star symbols represent the fluorescent dye. Integration time was 100 ms. Gray scales are 5000-25000 counts for (a) and (b), and 1500-5000 counts for (c).

83

fluorescently labeled probe RNA (dye-labeled R_P I; Table 6.1), and T4 DNA ligase. This resulted in hybridization and ligation of the anchor DNA and probe RNA on the master surface. The ligated RNA/DNA conjugates were then transferred to a PDMS surface.[27-29]

Figure 6.1a is a fluorescence micrograph obtained from the glass master after exposure to the ligase reaction mixture and subsequent washing. The fluorescence intensity in this micrograph indicates that the labeled probe RNA hybridized with the template DNA. There was no detectable level of fluorescence when the master DNA template was treated identically to the surface shown in Figure 6.1a, but using probe RNA II (dye-labeled R_P II, Table 6.1) which is not complementary to template DNA I. Figure 6.1b and 6.1c are fluorescence micrographs obtained from the glass master and PDMS surface, respectively, after transfer of the ligated RNA strands. Drainage canals (20 μm on center, 10 μm wide, and 3 μm deep) were microfabricated on the PDMS surface as reported previously[27-29] to direct buffer solution away from the glass/PDMS interface during conformal contact (Figure 6.2). The drainage canals restrict contact between the glass and PDMS surfaces to multiple square areas (10 x 10 μm^2), which results in the grid pattern present on both surfaces. The light areas on the PDMS surface in Figure 6.1c correspond to transfer of fluorescently labeled probe RNA from the darker regions apparent in Figure 6.1b. Figure 6.1d shows fluorescence intensity profiles obtained along the dotted lines in Figures 6.1a-6.1c. Importantly, the average intensity difference between the bright and dark regions on the master surface (1540 ± 140 counts, Figure 6.1b) is close to the intensity difference measured from the PDMS surface (2010 ± 60 counts, Figure 6.1c), suggesting no significant loss of ligated RNA strands during the transfer.

It is important to demonstrate that the fluorescence shown in Figure 6.1c results from transfer of probe RNA strands ligated to the biotinylated anchor DNA rather than
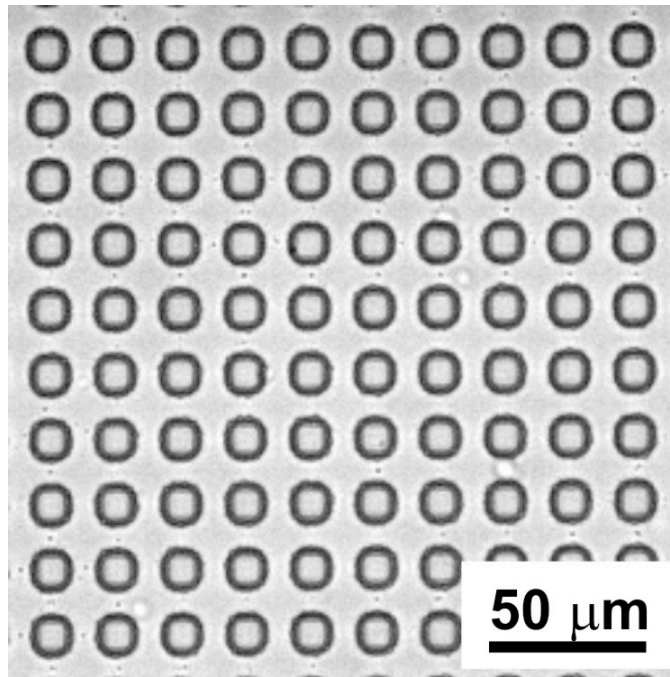
Figure 6.2. An optical micrograph of the PDMS surface shown in Figure 6.1c.

from nonspecific adsorption of unligated RNA on the PDMS surface. Accordingly, we carried out the two key control experiments illustrated in Figures 6.3a and 6.3b. Specifically, fluorescence micrographs were obtained from PDMS surfaces treated identically to that shown in Figure 6.1c, but in the absence of 5'-phosphoryl group of the anchor DNA (Figure 6.3a, anchor DNA without PO_4; Table 6.1) and the T4 DNA ligase (Figure 6.3b), respectively. In the absence of 5'-phosphoryl group of the anchor DNA or the T4 DNA ligase, the ligation of the anchor DNA to the probe RNA is not expected to proceed. Indeed, fluorescence micrographs obtained from the PDMS surfaces after these two control experiments were carried out indicated no detectable fluorescence from the PDMS surface after contact with the master. In Figure 6.3c, fluorescence intensity profiles from these two control experiments are compared to the profile of the replica surface shown in Figure 6.1c. On the basis of these results, we conclude that both the 5'-phosphoryl group of the anchor DNA and the T4 DNA ligase are required to transfer RNA to the PDMS surface and that there is no detectable level of nonspecific adsorption of RNA on the PDMS.

Multiple Transfers of Ligated RNA Strands from a Single Master. Multiple transfers of ligated RNA strands from a single master to different replica surface were demonstrated using the approach shown in Figure 6.4g. In contrast to the experiments used to obtain the results shown in Figures 6.1 and 6.3, the surface ligase reaction here was carried out using unlabeled probe RNA (R_P I; Table 6.1), and consequently the resulting master surface is not fluorescent. However, after transfer of the nonfluorescent and ligated RNA strands, the PDMS surface was exposed to fluorescently labeled target DNA (Target DNA I; Table 6.1) complementary to the probe RNA sequence but not to the anchor DNA. Figure 6.4a is a fluorescence micrograph obtained from a PDMS surface after the ligation, transfer, and hybridization steps. The presence of the bright

86

Figure 6.3. Control experiments confirming ligation of probe RNA on a master and transfer to a PDMS surface. (a) Scheme of a control experiment: A fluorescence micrograph was obtained from a PDMS surface treated identically to that shown in Figure 6.1c, but in the absence of 5'-phosphoryl group of anchor DNA (Table 6.1). Integration time was 100 ms. (b) Scheme of a control experiment: A fluorescence micrograph was obtained from a PDMS surface treated identically to that shown in Figure 6.1c, but in the absence of the T4 DNA ligase. Integration time was 100 ms. (c) Fluorescence intensity profiles obtained along lines on the fluorescence micrographs described in (a) and (b). Fluorescence intensity profile along the dotted white line shown in Figure 6.1c is included for comparison (Top intensity profile).

87
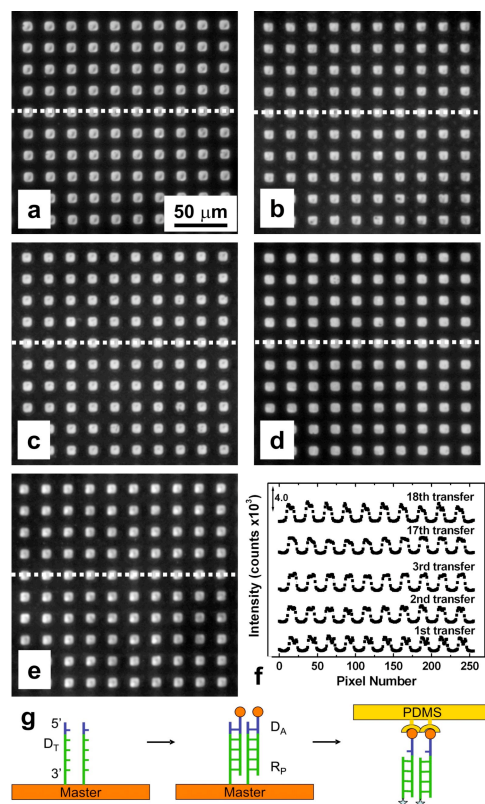
Figure 6.4. Fluorescence micrographs demonstrating multiple fabrication of RNA arrays from a single master slide. (a) A fluorescence micrograph obtained from a PDMS surface after ligation, transfer of ligated RNA single strands (R_P I; Table 6.1), and hybridization of a fluorescently labeled target DNA I (Table 6.1) complementary to the RNA sequence (but not to the sequence of anchor DNA). (b) Same as (a), but after a 2nd round of ligation, transfer, and hybridization. (c) Same as (a), but after a 3rd round of ligation, transfer, and hybridization. (d) Same as (a), but after a 17th round of ligation, transfer, and hybridization. (e) Same as (a), but after a 18th round of ligation, transfer, and hybridization. (f) Fluorescence intensity profiles obtained along the dotted white lines shown in (a)-(e). (g) Scheme showing the experimental approach used to obtain the data in (a)-(f). The star symbols represent the fluorescent dye. Integration time was 100 ms. Gray scale is 1800-5000 counts for (a)-(e).

spots indicates that the unlabeled RNA sequence transferred to the replica surface, and that the RNA is functional; that is, it is able to bind fluorescently labeled complementary DNA.

Control experiments analogous to those described earlier indicate no detectable level of fluorescence on the PDMS surfaces in the absence of 5'-phosphoryl group of the anchor DNA or the T4 DNA ligase during the ligation step (Figure 6.5).

This fabrication cycle, consisting of ligation, transfer, and hybridization with labeled, complementary DNA was repeated a total 18 times using the same master. Micrographs corresponding to the first, second, third, seventeenth, and eighteenth cycles are presented in Figures 6.4a-6.4e, respectively. As shown in the fluorescence line scans in Figure 6.4f, the contrasts in fluorescence between the light and dark areas on the surfaces of these replicas were 1860 ± 130, 2070 ± 180, 2310 ± 90, 2120 ± 180, and 2460 ± 530 counts, respectively. These data indicate that there is no significant or progressive degradation of the master up to the eighteenth round of replication. Note that the master slide was stable, and produced replicas indistinguishable from those shown in Figure 6.4, for more than 1 month when stored in dark and dry conditions.

Fabrication of an RNA Microarray. Here, we show that it is possible to prepare large-scale RNA microarrays consisting of a single probe RNA sequence (R_P I; Table 6.1) using the hybridization, ligation, and transfer steps discussed in the context of Figure 6.4. This was accomplished as follows. First, a master DNA array having 2500 spots (~70 μm-diameter) of template DNA I (Table 6.1) was fabricated using a robotic microarrayer. The T4 DNA ligase reaction was performed on the master surface using unlabeled probe RNA (R_P I; Table 6.1) as shown in Figure 6.4g. Finally, the ligated RNA strands were transferred to a PDMS surface. Figure 6.6 is a fluorescence micrograph obtained by scanning a part of the PDMS surface using a microarray scanner after hybridization of
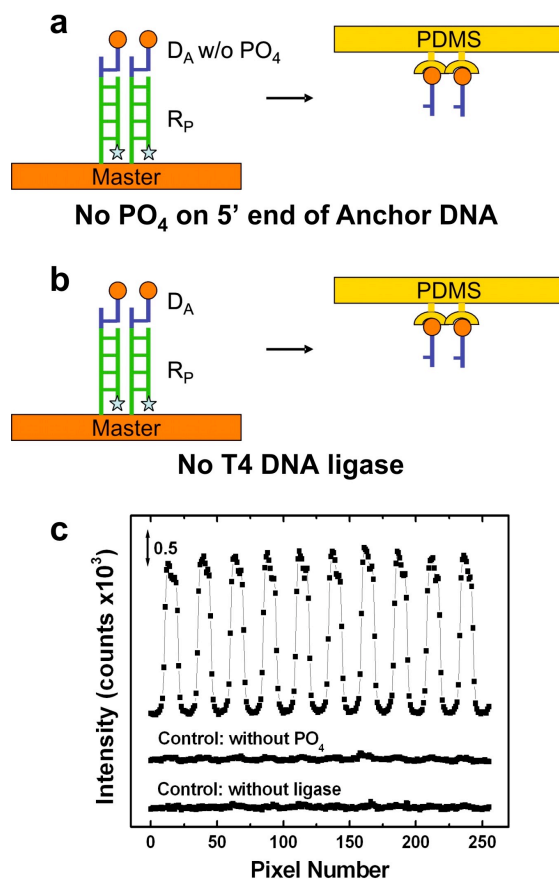
89
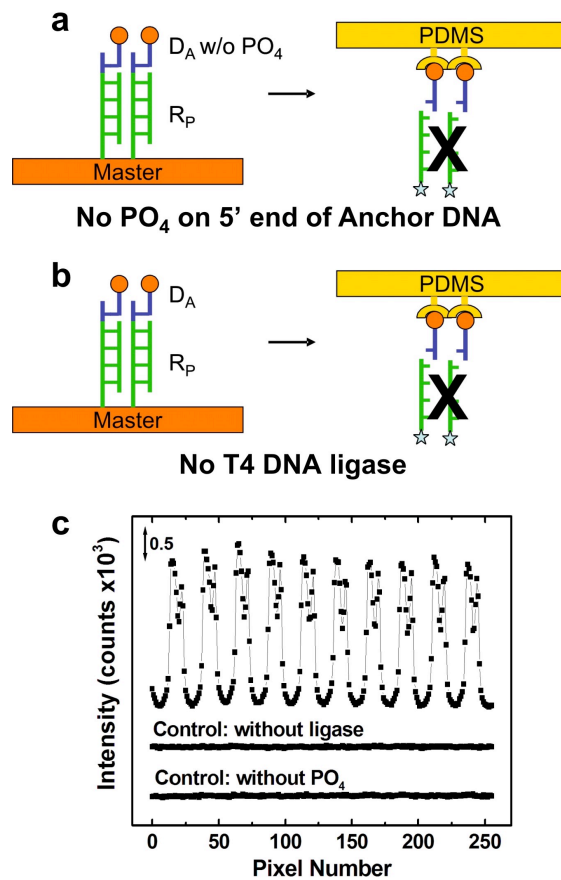
Figure 6.5. Control experiments confirming ligation of probe RNA on a master and transfer to a PDMS surface. (a) Scheme of a control experiment: A fluorescence micrograph was obtained from a PDMS surface treated identically to that shown in Figure 6.4a, but in the absence of 5'-phosphoryl group of anchor DNA. Integration time was 100 ms. (b) Scheme of a control experiment: A fluorescence micrograph was obtained from a PDMS surface treated identically to that shown in Figure 6.4a, but in the absence of the T4 DNA ligase. Integration time was 100 ms. (c) Fluorescence intensity profiles obtained along lines on the fluorescence micrographs described in (a) and (b). Fluorescence intensity profile along the dotted white line shown in Figure 6.4a is included for comparison (Top intensity profile).

90
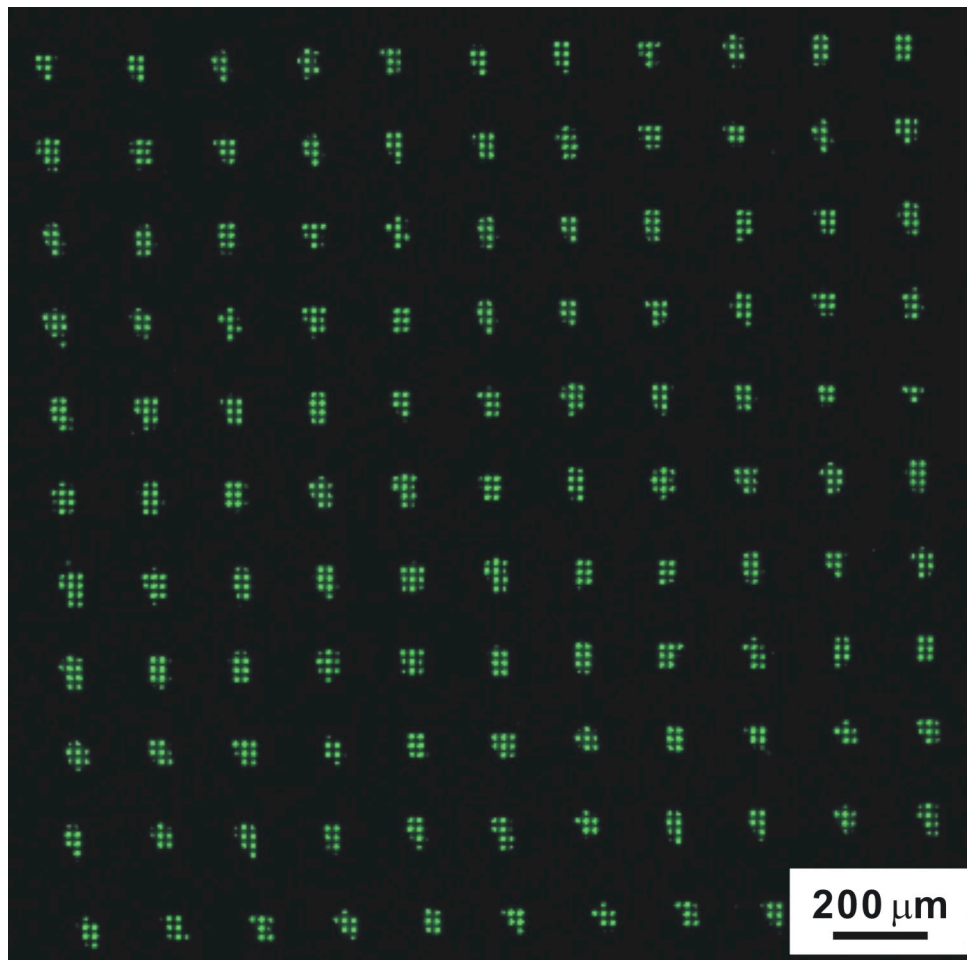
Figure 6.6. Fluorescence micrograph obtained from a RNA array (PDMS surface) which was fabricated using a master DNA array having multiple micro-scale spots, not a spot in macro-scale (one template sequence, D_T I; Table 6.1). The micrograph was obtained from the PDMS surface after ligation, transfer of ligated RNA strands (R_P I; Table 6.1), and hybridization of a fluorescently labeled target DNA I (Table 6.1) complementary to the RNA sequence (but not to the sequence of anchor DNA).

target DNA I (Table 6.1) and washing. The micrograph shows that all 121 RNA spots on the PDMS surface are active toward hybridization of labeled target DNA I. The pixelated appearance of the individual spots is a consequence of the drainage canals present on the PDMS surface.

Fabrication of an RNA Microarray Comprised of Multiple Probe Sequences. RNA microarrays having multiple probe sequences were fabricated using the approach illustrated in Figure 6.4g. A master DNA array having three different template sequences (D_T I, D_T II, and D_T III; Table 6.1) and a total of 1500 spots was fabricated using a robotic microarrayer. The three different DNA templates were spotted in consecutive rows as shown in Figure 6.7. After hybridization and ligation of a mixture of unlabeled RNA probes (R_P I, R_P II, and R_P III; Table 6.1) on the master, the probe RNA strands were transferred to a PDMS replica surface. Finally, the PDMS surface was exposed to a mixture of fluorescently labeled DNA targets (Target DNA I and target DNA II; Table 6.1) which are complementary to probe RNA I (R_P I) and probe RNA II (R_P II), respectively. Note that only two different target sequences were introduced on the PDMS surface. Figure 6.7 is a fluorescence micrograph obtained by scanning a part of the PDMS surface. It shows that the correct, labeled DNA complements hybridized to the appropriate probe RNA sequences. That is, Cy3-labeled DNA I hybridized with R_p I, Cy5-labeled DNA II hybridized with R_p II, and neither of the labeled DNA targets hybridized with R_p III. No cross-hybridization was observed.

6.5 CONCLUSION

In this report, we described a method for fabrication of RNA microarrays utilizing a surface ligase reaction and mechanical transfer. Eighteen replicas were prepared from a single master array with no detectable degradation of activity of the resulting replica
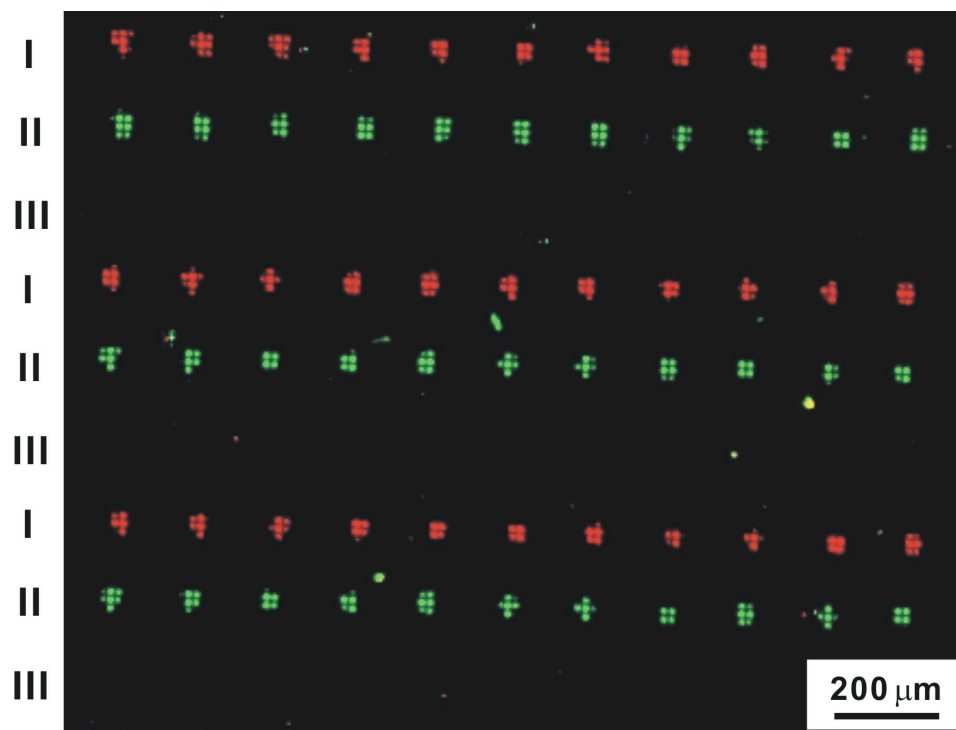
Figure 6.7. Fluorescence micrograph obtained by scanning a part of the PDMS surface after ligation, transfer, and hybridization, which demonstrates fabrication of RNA microarrays having multiple different probe sequences. First, a master array having three different template sequences (D_T I, D_T II, and D_T III; Table 6.1) in consecutive rows was fabricated. After ligation and transfer, the PDMS surface was exposed to a mixture of fluorescently labeled DNA targets (Target DNA I and target II; Table 6.1) complementary to the sequence of each probe RNA (R_P I and R_P II; Table 6.1), respectively.

RNA array or the master DNA array. Finally, a master DNA array consisting of three different sequences was prepared and faithfully replicated as a functional RNA microarray with no observable cross-hybridization. This approach provides a robust means for fabricating RNA microarrays in parallel and with no requirement for RNA modification (for example, with biotin). Finally, this report expands the scope of this general approach for microarray fabrication from DNA to RNA. At present we are examining the possibility of using the same general strategy for preparing replicas of protein arrays.

Chapter 7: Hybridization of DNA to Bead-immobilized Probes Confined within a Microfluidic Channel

7.1 SYNOPSIS

We report the factors influencing the capture of DNA by DNA-modified microbeads confined within a microfluidic channel. Quantitative correlation of target capture efficiency to probe surface concentration, solution flow rate, and target concentration are discussed. The results indicate that the microfluidic system exhibits a limit of detection of ~10^{-10} M (~10^{-16} mol) DNA and a selectivity factor of ~8×10^3. Typical hybridization times are on the order of minutes.

7.2 INTRODUCTION

Here, we report an investigation of parameters influencing the hybridization of DNA onto probe-conjugated microbeads confined within a microfluidic channel. The use of beads as supports for capture probes in microfluidic systems is advantageous for a number of reasons. First, the bead surface area is significantly larger than the interior surface area of a typical microfluidic channel, and this results in enhanced sensitivity and limit of detection for assays based on immobilized capture probes.[87,147,148] Second, in addition to providing a platform for probe attachment, beads also effectively mix solutions in microfluidic systems.[87] Third, it is easier to modify and characterize the surface of beads than the walls of a microfluidic device.[149,150] Because of the importance of these three points, it makes sense to develop a better understanding of the conditions that lead to target capture on bead surfaces. Accordingly, we have studied capture efficiency in terms of target concentration, probe surface concentration, and flow rate within the microfluidic channel.

We previously reported on fluorescence-based methods for studying bio/chemical reactions on functionalized beads immobilized within microfluidic channels.[87,88] For example, we demonstrated that multiple, sequential catalytic reactions could be carried out in this format by immobilizing catalytic enzymes on microbeads, placing the beads into microreactors, and then passing reactants through one or more of these reactors to yield products. The enzyme-modified beads mixed reactants and increased the effective surface area of the channel interior, both of which improved reaction velocities compared to open channels.[87] We also demonstrated efficient DNA hybridization on DNA-functionalized microbeads packed in a serial microchamber array. Hybridization, which was 90% complete within 1 min, was carried out by moving multiple DNA targets across the microbead array by electrophoresis.[88] These types of experiments demonstrate the viability of this general approach for bead-based microfluidic assays, but until now we have not provided quantitative insight into the factors that control the efficiency of such devices.

In addition to our own reports, a number of other groups have also been actively studying bead-based microanalytical systems. For example, DNA hybridization using paramagnetic beads modified with targets was demonstrated in a microfluidic array format.[89] A capillary platform for DNA analysis was prepared by lining up individual beads, each modified with a different probe sequence, within a capillary having approximately the same inside diameter as the bead outer diameter.[91,151] A chip-based sensor array composed of individually addressable microbeads and having point mutation selectivity has also been demonstrated.[90] There are a number of other interesting studies of bead-based microfluidic biosensors.[152-155]

In the present study, experimental factors controlling the hybridization of DNA onto probe-conjugated microbeads under microfluidic flow conditions is reported.

Specifically, streptavidin-coated microbeads were conjugated with biotinylated single-strand (ss) DNA probes. The density of probe ssDNA on the microbeads (1.9×10^{12} probes/cm^2) was controlled to be within the range that leads to rapid hybridization.[124,156,157] The probe-conjugated microbeads are sufficiently closely packed in the microfluidic channel that mass transfer from solution to the bead surface is significantly enhanced compared to the corresponding open channel. A limit of detection (LOD) of ~10^{-10} M ssDNA (~10^{-16} mol) was obtained. The hybridization time was on the order of a few minutes and the selectivity factor was greater than 8×10^3. Typically, ~2 μL volume of solution was required for an analysis. We expect this simple microfluidic system to complement the use of planar DNA arrays,[158-160] and to be particularly useful for applications requiring fast response and simplicity.

7.3 EXPERIMENTAL

Materials. DNA oligonucleotides modified with biotin or fluorescein (probes or targets) were used as received from Integrated DNA Technologies (Coralville, IA). Tris-acetate/EDTA (TAE) buffer (pH 8.0, 40 mM tris-acetate, 1.0 mM EDTA, and 0.5 M NaCl) and hybridization buffer (Perfecthyb Plus) solutions were obtained from the Sigma-Aldrich Co. (St. Louis, MO). The hybridization buffer solution was diluted by a factor of two with water prior to use. TAE buffer was used for rinsing bead beds after hybridization. Milli-Q water (18 MΩ·cm, Millipore, Bedford, MA) was used throughout. The sequences of 5'-biotin-modified probe and 5'-fluorescein-labeled targets are as follows:[161] ssDNA probe, 5' (Biotin-TEG) AGT TGA GGG GAC TTT CCC AGG C 3'; ssDNA complementary target, 5' (6-FAM) GCC TGG GAA AGT CCC CTC AAC T 3'; ssDNA noncomplementary target, 5' (6-FAM) CTA GAA TCG CTG ATT ACA GCT T 3'.

Fabrication of Microfluidic Devices. Microfluidic devices were fabricated under clean room conditions, as previously described, but with some modification.[88] Briefly, positive photoresist (AZP4620, Clariant Co., Somervile, NJ) was spin-coated twice onto a glass substrate (Fisher Scientific, Pittsburgh, PA) at 1500 rpm for 2 min, followed by soft baking at 92 °C for 5 min on a hot plate. The photoresist-coated glass substrate was exposed to UV light for 2 min using a mask aligner (Q 4000-6, Quintel Corp., San Jose, CA) and a photographic film mask. The resulting image was then developed with 100% AZ421K solution (Clariant Co.) to yield a photoresist master. Next, the master was exposed to UV light again for 1 min through a slit-type, chrome-coated soda lime glass mask (Nanofilm, Westlake Village, CA) having a slit width of 100 μm. The master was developed again in a 75% AZ421K/25% water (v/v) solution for 1 min, which resulted in formation of a weir structure on the master. The depth and width of the resulting microstructures were measured using a profilometer (Veeco Dektak 3, Veeco Instruments, Plainview, NY).

PDMS (Sylgard 184, Dow Corning, Midland, MI) was molded against the photoresist master to yield the microfluidic device. The PDMS replica and a cover glass were then oxidized in a plasma cleaner/sterilizer (PDC-32G, Harrick Scientific Ossining, NY) at medium power for 25 s. Immediately after the plasma treatment, they were brought into conformal contact and permanently sealed together.[79,81]

Preparation and Characterization of Probe-conjugated Microbeads. Biotinylated ssDNA probe oligonucleotides were conjugated to SuperAvidin-coated microbeads (ProActive Microspheres, dia. 9.95 μm, Bangs Laboratories Inc., Fishers, IN) using the following procedure. First, 15 μL of stock microbeads (1.8×10^4 beads/μL) were rinsed in phosphate buffer saline (PBS) solution containing 0.05% (v/v) Tween 20 (pH 7.4, 0.15 M NaCl, 4.0 mM KCl, 8.1 mM Na_2HPO_4, and 1.5 mM KH_2PO_4) and then

centrifuged at 4000 rpm for 3 min. Second, 4.0 μL of the biotinylated ssDNA probe solution (5.0 μM), which corresponds to a five-fold excess relative to the binding capacity of the microbeads, was added to the rinsed microbead pellet. This solution was gently mixed for 30 min at 25 ± 2°C. After conjugation, the mixture was centrifuged to remove unbound biotinylated ssDNA probes. The probe-conjugated microbead pellet was rinsed with PBS buffer solution and centrifuged again. The probe-conjugated microbeads were re-suspended in TAE buffer (5.4×10^2 beads/μL) and refrigerated (2 °C) until needed.

To estimate the probe density on the microbeads, ssDNA probes, which were modified with fluorescein and biotin, at the 3' and 5' ends, respectively, were immobilized on microbeads by the previously described method except all rinsing solutions were collected during the conjugation process. An additional filtering step (0.22 μm syringe filter, Millex-GV13, Sigma-Aldrich Co., St. Louis, MO) was performed with the rinsed microbeads to ensure collection of all unbound, ssDNA probes. The amount of unbound probe DNA was estimated by comparing the fluorescence from the retrieved probe solution to standards. The amount of immobilized probe DNA was calculated from the difference between the initially added DNA and the free DNA in solution. A fluorescence spectrometer (SLM-Aminco Spectrofluorometer, Jobin Yvon Inc., Edison, NJ) with excitation and emission wavelength of 494 nm and 518 nm, respectively, was used to measure the fluorescence intensity of solutions.

DNA Hybridization. Probe-conjugated microbeads were packed in the microfluidic chambers with a syringe pump (PHD 2000, Harvard Apparatus, Hollistion, MA), and then the microchambers were extensively rinsed with hybridization buffer for 10 min. Hybridization experiments were performed by flowing fluorescein-labeled ssDNA over the beads at 25 ± 2°C, rinsing with TAE buffer, and then measuring the

resulting fluorescence. A fluorescence microscope (Nikon Eclipse TE 300, Nikon Co., Tokyo, Japan) equipped with band-pass filters, a 100 W mercury lamp and a CCD camera (Photometrics Ltd., Tucson, AZ) was used to acquire optical and fluorescence micrographs of the microchambers. Micrographs were obtained with a 4× or 10× objective lens (numerical apertures: 0.10 and 0.30, respectively). The integration times for the CCD camera were 1 or 700 ms for optical and fluorescence micrographs, respectively. Micrographs were processed using V++ Precision Digital Imaging software (Digital Optics, Auckland, New Zealand). Fluorescence intensities were measured in the center regions of the bead-packed microchambers (40 × 205 pixels). Background fluorescence intensities were acquired before flowing the target solution and subtracted from micrographs obtained after flowing the targets and rinsing the beads with buffer. For hybridization efficiency experiments, the subtracted intensity was normalized to the maximum hybridization intensity obtained after flowing a relatively concentrated target solution (1.0 μM) over the bead bed for 10 min at a flow rate of 1.00 μL/min and then rinsing for 10 min at a flow rate of 1.00 μL/min. The average and standard deviation were obtained using three independently prepared microfluidic devices.

7.4 RESULTS AND DISCUSSION

Microfluidic Devices. As discussed in the Experimental Section, the microfluidic devices used in this study were fabricated using standard photolithographic techniques.[79,81] Microbeads were introduced into the microchambers using pressure-driven flow and retained there by the presence of weirs. Figure 7.1a is a schematic illustration of the cross section of a microchip and Figure 7.1b is a top-view optical micrograph of a microchamber packed with beads. The height of the microchannels was 21 ± 2 μm. The height of weirs ranged from 5-8 μm, and depended on the UV exposure
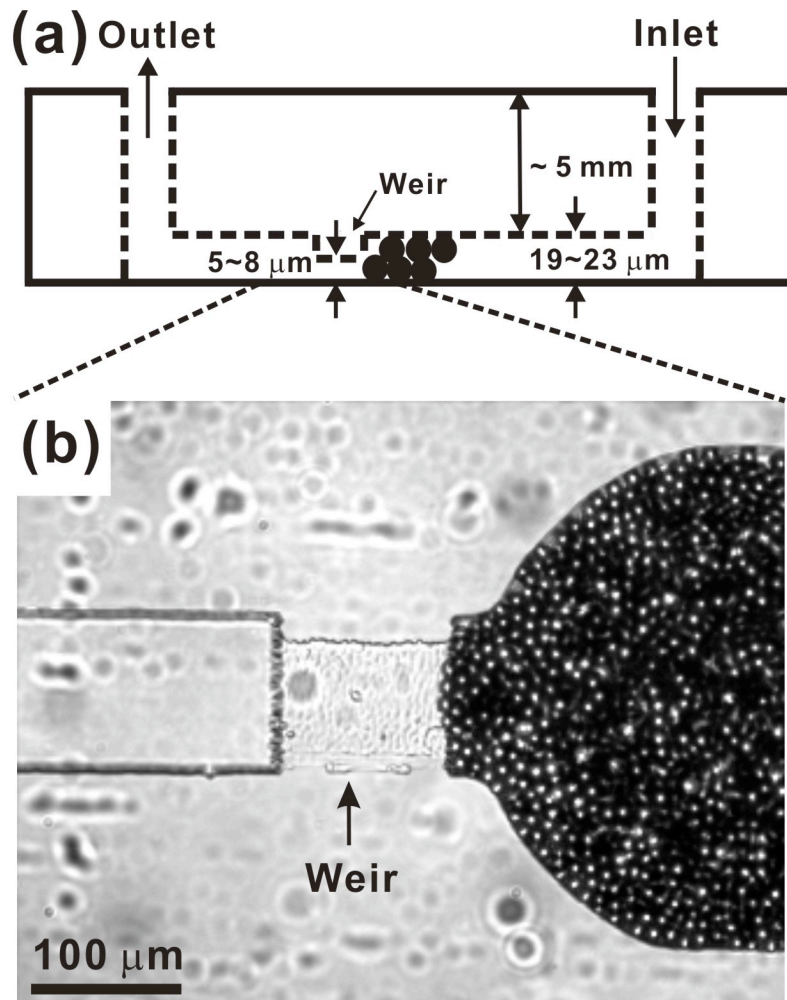
Figure 7.1. (a) Schematic cross-section of the microchip design used for all experiments (not to scale). (b) Optical micrograph of a weir and the corresponding microchamber packed with 9.95 μm-diameter microbeads.

time, the concentration of resist developer, and the resist development time. To ensure reproducible packing of the microbeads, a fixed concentration of beads (5.4×10^2 beads/μL) and solution flow rate (10.00 μL/min) were used. Microbead packing was completed in <30 s. Each microchamber typically contained about 2×10^3 microbeads,[162] which corresponds to a packing efficiency, defined as the total bead volume/microchamber volume, of about 0.8. This unusually high value probably arises because of a slight pressure-induced expansion of the PDMS microchamber.[163] Consistent with this view, we observed microbeads (dia. 9.95 μm) packed up to 3 layers thick near the center region of the microchambers, even though the measured height (at zero pressure) was only sufficient to accommodate two beads.

Probe Density. To determine the density of DNA on the microbead surface, the beads were exposed to an excess of biotinylated DNA labeled with fluorescein (see Experimental Section). After immobilization of a fraction of this excess, the remaining free DNA was retrieved and quantified by measuring the fluorescence of the resulting solution (Figure 7.2). The measured probe density was $(1.0 \pm 0.4) \times 10^{-17}$ moles/microbead or 1.9×10^{12} probes/cm^2 of bead surface area. Considering the total number of streptavidin binding sites on the surface of the beads, this value corresponds to a DNA binding efficiency of 73%.[164]

There is an optimal surface-probe density for maximum DNA hybridization efficiency.[124,156,157] At surface densities higher than this optimal value, repulsive electrostatic interactions and steric hindrance between oligonucleotides reduce hybridization efficiency. The calculated maximum density of 22-mer duplex DNA lying flat on the surface of a microbead is 6.7×10^{12} molecules/cm^2.[156,165,166] This value is about three times larger than the measured probe DNA density of 1.9×10^{12} probes/cm^2, suggesting that electrostatic and steric barriers to hybridization should be minimal on the
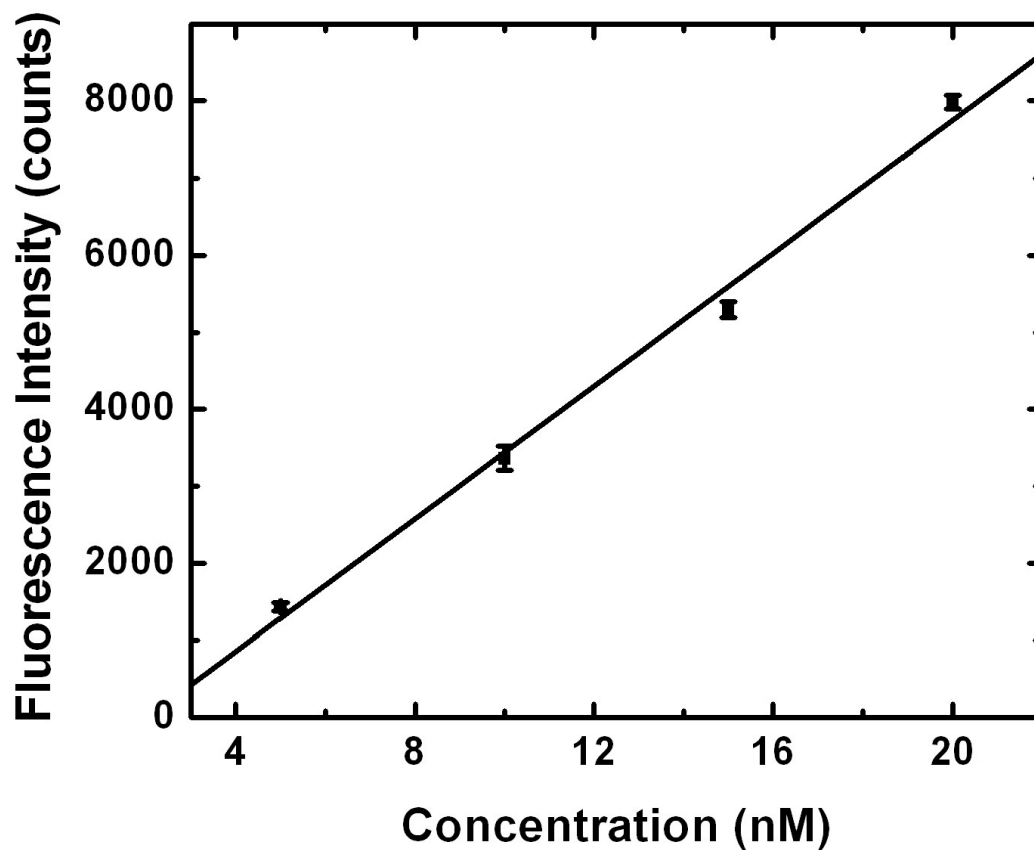
Figure 7.2. Calibration curve obtained using solution-phase (no microbeads) ssDNA probes modified with fluorescein and biotin. The excitation and emission wavelengths were 494 and 518 nm, respectively. Data were obtained using a fluorescence spectrometer (SLM-Aminco Spectrofluorometer, Jobin Yvon Inc., Edison, NJ).

microbead surface. This conclusion is consistent with previous reports;[156,157] for example, it has been reported that rapid hybridization occurs on surfaces for probe densities $< \sim 3 \times 10^{12}$ molecules/cm^2.[157]

DNA Hybridization. To confirm hybridization of DNA onto the probe-conjugated microbeads, and to evaluate the extent of nonspecific adsorption, a microfluidic device having two independent microchambers was prepared. Probe-free microbeads were packed in one chamber and probe-conjugated microbeads were packed in the other (Figure 7.3a), and then a 1.0 μM solution of the fluorescein-labeled complement of the probe was simultaneously pumped into both microchambers. After rinsing with TAE buffer, significant fluorescence was only observed from the microchamber packed with the probe-conjugated microbeads (Figure 7.3b). Fluorescence intensity profiles for the region contained within the dashed white box in Figure 7.3b are shown in Figure 7.3c. The data indicate that after rinsing the extent of nonspecific binding of the target to the probe-free beads is below the detection limit of the measurement system. Similar experiments were carried out to ensure the absence of nonspecific adsorption on the PDMS and glass surfaces of the microfluidic device (Figure 7.4). The stability of the probe/target hybrid was investigated by measuring target fluorescence after rinsing the microbeads with buffer for 10-30 min. The results (Figure 7.5) indicate no detectable change in the extent of hybridization within this time interval.

Hybridization experiments were carried out in the bead-based microfluidic system using concentrations of fluorescently labeled targets ranging from 0.5 - 100.0 nM. Fluorescence intensities as a function of target concentration, obtained from the center region of the microchambers, are plotted in Figure 7.6a. The target solutions were flowed at 0.50 μL/min for 4 min and fluorescence intensities were measured after rinsing for 10 min. Figure 7.6b is an optical micrograph showing the region of the microchamber used

104
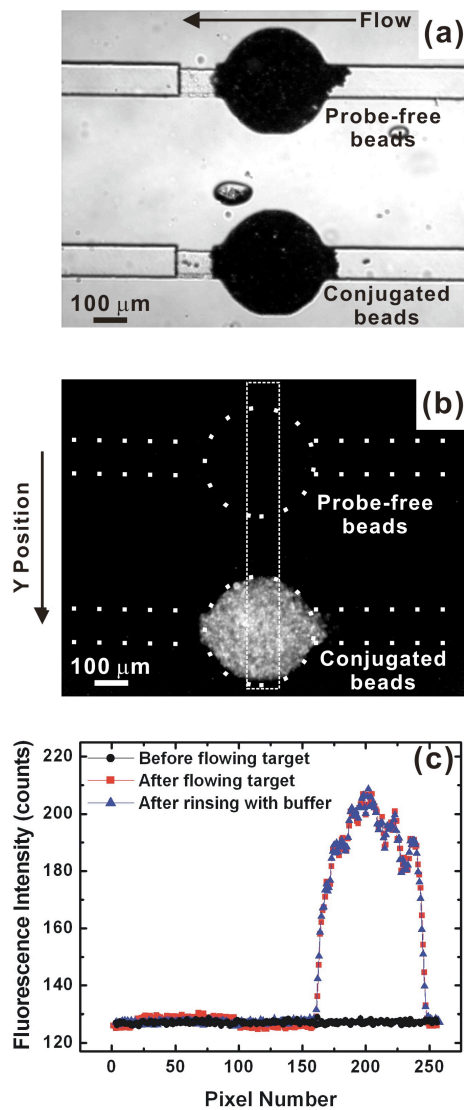
Figure 7.3. (a) Optical micrograph of a two-chamber microfluidic device packed with probe-free microbeads (top chamber) and probe-conjugated microbeads (bottom chamber). (b) Fluorescence micrograph of the two microchambers after exposure to a fluorescently labeled DNA target. Experimental conditions: a 1.0 μM target solution was flowed for 10 min at a rate of 1.00 μL/min and then the microchannels were rinsed with buffer for 10 min at a flow rate of 1.00 μL/min. (c) Fluorescence intensity profiles obtained in the regions defined by the dashed white box in (b).
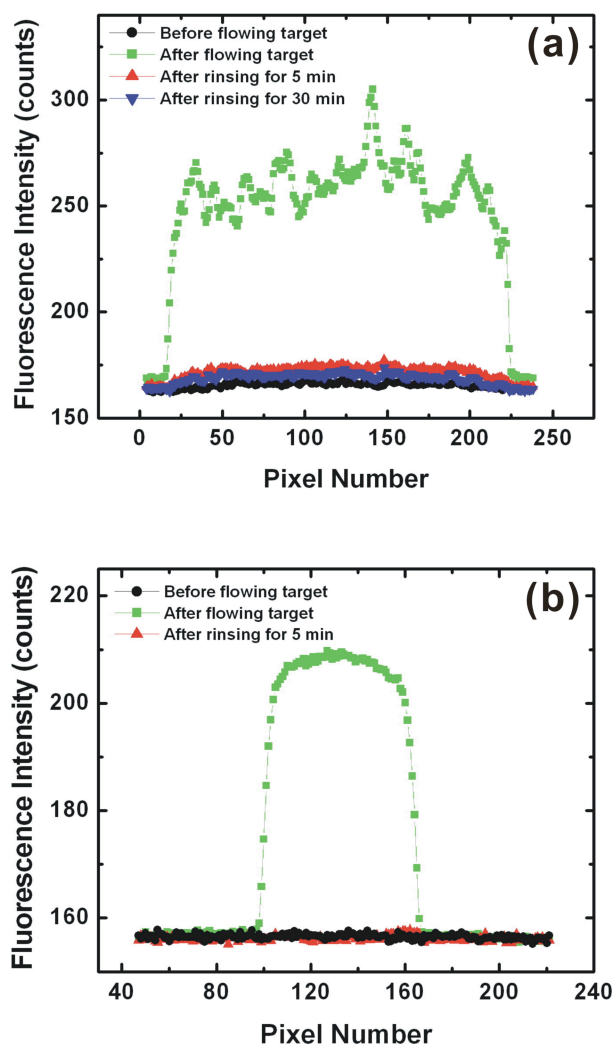
Figure 7.4. Fluorescence intensities of rectangular regions perpendicular to (a) a microchamber packed with the probe-free microbeads and (b) the long axis of an open (bead-free) microchannel. The 1.0 μM target DNA solution was flowed for 30 min. These intensities were compared to those obtained following rinsing with TAE buffer for 5 or 30 min. After rinsing the fluorescence intensities were below the detection limit of the microscope, indicating no significant level of nonspecific adsorption on the probe-free microbeads or the open channel surface.

106
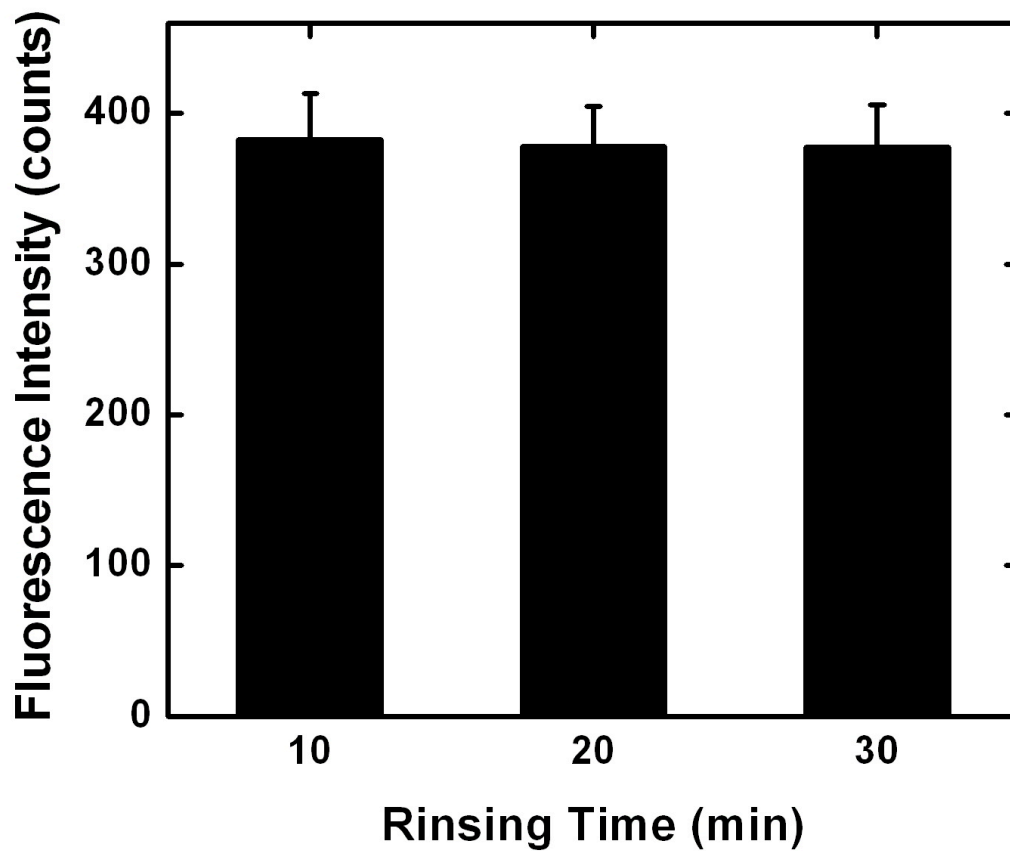
Figure 7.5. Fluorescence intensities of hybridized dsDNA on probe-conjugated microbeads as a function of rinsing time. A 1.0 μM DNA target solution was flowed for 10 min at 1.00 μL/min, and then the microchambers were rinsed with buffer at 1.00 μL/min for the indicated times.
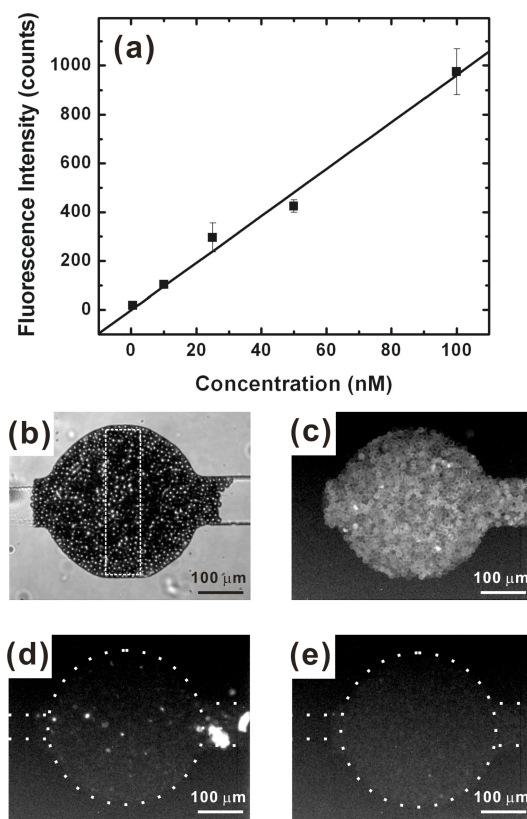
Figure 7.6. Hybridization of DNA onto probe-conjugated microbeads as a function of target-solution concentration. (a) Fluorescence intensities obtained in the center region of the microchambers (indicated by the dashed white box in (b)) as a function of target-solution concentration. (b) Optical micrograph of a microchamber. (c) Fluorescence micrograph after flowing complementary DNA target solution (0.5 nM) and rinsing. (d) Fluorescence micrograph after flowing noncomplementary target solution (100.0 nM) and rinsing. The bright spots near the inlet were impurities observed in a corresponding optical micrograph. (e) Fluorescence micrograph after flowing only buffer solution. Experimental conditions: target solution was flowed from right to left for 4 min at a flow rate of 0.50 μL/min and then the microchannels were rinsed for 10 min at a flow rate of 1.00 μL/min.

to obtain the fluorescence results. The data in Figure 7.6a were corrected by subtracting the fluorescence intensity from the center region of the microchamber prior to filling with the target solution. The limit of detection (LOD), defined as the concentration corresponding to a signal 3 standard deviations above the zero-concentration blank solution, was found to be $\sim 10^{-10}$ M or $\sim 10^{-16}$ mol of target based on the sample volume of ~ 2.0 μL. Figures 7.6c and 7.6d demonstrate the selectivity of the assay. Figure 7.6c was obtained using a 0.5 nM complementary target DNA solution, and Figure 7.6d was obtained under identical conditions but using a 100.0 nM noncomplementary DNA target solution. Figure 7.6e represents a control experiment obtained using only buffer solution (zero concentration of DNA). The selectivity ratio, defined as the ratio of fluorescence intensities obtained using complementary and noncomplementary targets present at the same concentration (and with all other conditions identical), is $> 7.9 \times 10^3$ at 100.0 nM. Despite the simplicity of the microfluidic architecture used for these experiments, the resulting performance specifications (LOD, analysis time, and specificity) are comparable to more complex methods such as electric field-assisted DNA hybridization,[167] other bead-based DNA methods,[89-91,151] and mixing-assisted DNA hybridization.[168,169]

In addition to determining fluorescence intensities as a function of DNA concentration, we also examined hybridization efficiency as a function of the total moles of target exposed to the microbeads relative to the number of surface-immobilized probes (Figure 7.7). In this experiment, the target concentration and flow rate were fixed at 50.0 nM and 0.25 μL/min, respectively, and the moles of target solution passed through the microchamber were controlled by varying the exposure time between 110 and 1100 s. As discussed in the Experimental Section, hybridization efficiency (Figure 7.7) is defined as the normalized fluorescence intensity for a particular experiment to the limiting

109
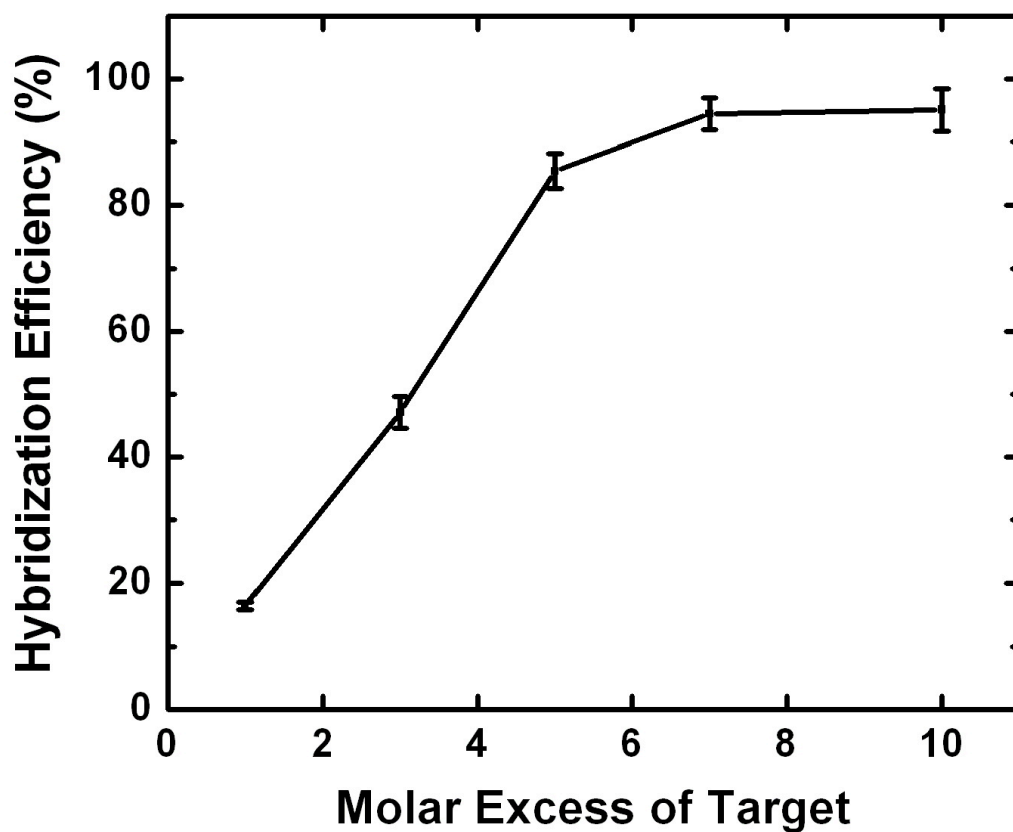
Figure 7.7. Hybridization efficiency as a function of the molar excess of target flowed over the bead bed at a fixed flow rate (0.25 μL/min). The molar excess is given in terms of the ratio of total moles of target DNA flowed per total moles of immobilized probe. The concentration of the target solution was 50.0 nM, and the amount of target DNA was controlled by varying the duration of the exposure. After exposure to the target, the microchannels were rinsed for 10 min at a flow rate of 1.00 μL/min.

fluorescence intensity obtained upon exposure of the probe-modified beads to a high concentration (1.0 μM) of target DNA for an extended period of time (10 min). The results indicate that hybridization efficiency reaches a maximum value of ~90% after exposure of the beads to a seven-fold molar excess of target. Another way of viewing this is that ~15% of the DNA in this sample is captured in ~13 min. This hybridization response can be understood in terms of the good mass transfer characteristics of the microfluidic channel, the high surface-area-to-volume ratio of the microbeads, and the capture-probe surface density. For example, the microbeads are packed very close together, thus decreasing the diffusive transport time of targets from the bulk to the probe surface.[92] This is because the solution volume in the bead bed (0.45 nL) is about 3 times smaller than that of the open microchamber (1.5 nL).[170] In addition, the high surface-area-to-volume ratio of microbeads provides a higher probe surface area ($6.2 \times 10^5 \ \mu m^2$) compared to the open microchamber ($0.71 \times 10^5 \ \mu m^2$).[171]

Figure 7.8 is a plot of hybridization efficiency as a function of flow rate for a fixed amount of target DNA passed through the probe-labeled bead bed. In these experiments the number of moles of target presented to the beads was three times that of the immobilized probes. The flow rate was varied from 0.10 to 1.00 μL/min, which corresponds to times ranging from 830 s to 83 s, respectively. After flowing the target solution at a specific rate, the microchamber was rinsed with TAE buffer for 20 min at the same flow rate. Even at the lowest flow rate (0.10 μL/min), rinsing for 20 min with buffer was sufficient to displace the solution of target DNA from the channel (Figure 7.9). Figure 7.8 shows that hybridization efficiency increases as the flow rate decreases. This observation can be understood in terms of the increase in the flux of target onto the probe-conjugated microbeads at lower flow rates. This observation is consistent with others showing that the flux of analyte to an active surface is inversely proportional to
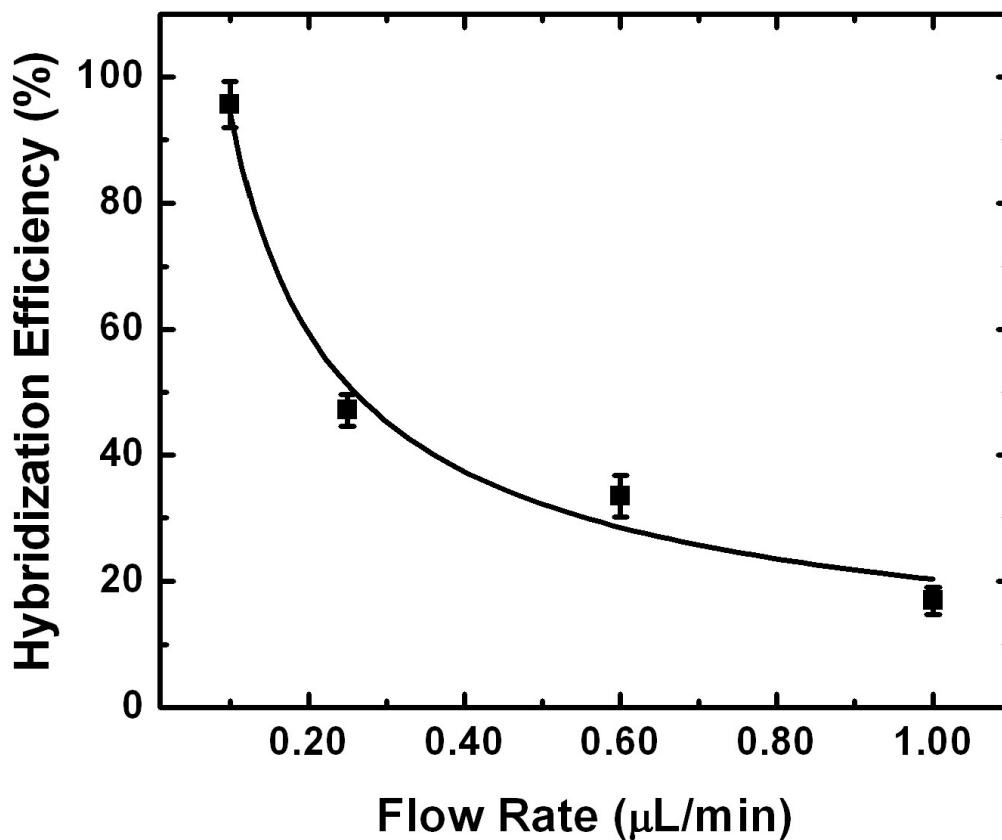
Figure 7.8. Hybridization efficiency as a function of flow rate for a fixed amount of target DNA. For all flow rates, the amount of target DNA represented a three-fold molar excess relative to the amount of immobilized probe DNA. The number of moles of target DNA was controlled by varying the flow time. After flowing the target solution (50.0 nM), the microchannels were rinsed for 20 min with buffer. The solid line is the best nonlinear fit to the data using Origin software.
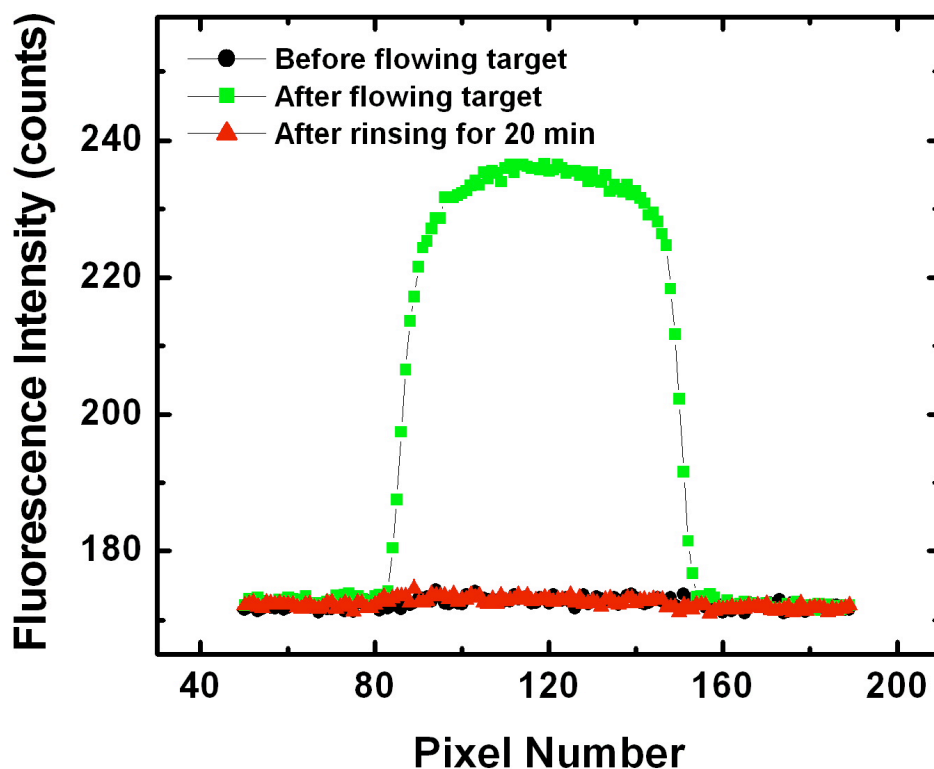
Figure 7.9. Fluorescence intensities of a rectangular region perpendicular to the long axis of an open (bead-free) microchannel before and after exposure to a DNA target solution (1.0 μM, flow rate = 0.10 μL/min, exposure time = 830 s), and after rinsing with buffer at 0.10 μL/min for 20 min. After rinsing the fluorescence intensities were below the detection limit of the microscope, indicating complete removal of the bulk target solution without significant level of nonspecific adsorption on the open channel surface.

flow rate in fluidic channels.[172,173] For example, theory and experiments indicate that flux is proportional to $q^{-2/3}$ (q is the flow rate in units of m/s) under mass-transfer-limited reaction conditions and to q^{-1} under kinetically limited conditions.[173] Consistent with these earlier findings, the best fit to the data in Figure 7.8 (solid line) is proportional to $q^{-2/3}$.

7.5 CONCLUSION

We have described a simple microfluidic device packed with microbeads conjugated to DNA capture probes and the parameters that affect its performance. These include target concentration, probe surface concentration, and flow rate. The inherently high surface-area-to-volume ratio of microbeads, coupled with their close proximity, leads to efficient target capture. Specifically, the microfluidic device has an LOD of $\sim10^{-10}$ M ($\sim10^{-16}$ mol) and a selectivity factor greater than 7.9 x 10^3. Analysis times are typically on the order of a few minutes.

We recently reported a simple means for enhancing the local concentration of DNA in microfluidic systems by a factor of up to ~500 within 150 s.[31] At present, we are integrating this preconcentrator into a bead-based capture chip similar to that described here. Through this and other improvements, we expect that bead-based microfluidic devices of this sort will ultimately have significantly lower LODs, faster analysis times, and parallel detection capabilities that may make them viable tools for gene expression studies, clinical diagnostics, and high-throughput drug screening.

Chapter 8: Sensitive DNA Detection Based on Concentration of Target Strands and Subsequent Bead-based Capture in a Simple Microfluidic Device

8.1 SYNOPSIS

We report a novel approach for simple and sensitive DNA detection, which relies on the concentration of fluorescein-labeled target DNA strands and their subsequent capture in a microfluidic device. The device consists of probe-conjugated microbeads packed in front of a hydrogel microplug photopolymerized in a microchamber. The microbeads are conjugated with a probe that is complementary to a desired target. The target DNA strands are electrokinetically transported and concentrated at an interface between the highly cross-linked hydrogel microplug and buffer solution, and are captured by the probe-conjugated microbeads through DNA hybridization. The hydrogel microplug provides an analyte enrichment factor of ~20-fold within 120 s, resulting in ~10-fold enhancement in the sensitivity of the microbead-based DNA detection. In addition, the microbead-based assay with hydrogels provides a rapid and simple target analysis in terms of short analysis time (as little as 3 min including a washing step) and a simple washing step, as well as easy regeneration of probe-conjugated microbeads for subsequent assays. This work is important because it enables sensitive detection of trace amounts of DNA as well as a rapid and simple DNA detection methodology within a simple microfluidic architecture.

8.2 INTRODUCTION

Here, we report a novel approach for simple and sensitive DNA detection, which relies on the concentration of fluorescein-labeled target DNA strands and their

subsequent capture in a microfluidic device. The device consists of probe-conjugated microbeads packed in front of a photopolymerized hydrogel. The microbeads are conjugated with a probe DNA that is complementary to a target DNA. The target DNA strands are electrokinetically transported and concentrated at an interface between the highly cross-linked hydrogel microplug and buffer solution, and are captured by the probe-conjugated microbeads through DNA hybridization (Scheme 8.1). The probe-conjugated microbeads allow fast and sequence-specific capture of the targets.

The study described here is an extension of our previous work in which we showed efficient DNA hybridization on probe-conjugated microbeads,[30,174] and electrokinetic concentration of charged molecules using a hydrogel microplug within a microfluidic device.[31] Previously, we introduced a microfluidic system with probe-conjugated microbeads packed within microchannels for DNA hybridization applications. The microbeads were closely packed in a microchamber and narrow fluid paths between the packed microbeads were obtained. This resulted in decreasing the diffusion distance, thereby increasing the hybridization reaction rate. We also reported a novel strategy for the concentration of single-stranded DNA (ssDNA) in microfluidic systems using highly cross-linked nanoporous hydrogel microplugs. When applying an appropriately biased voltage across the hydrogel microplug, charged analyte molecules (ssDNA or fluorescein) move and concentrate at the hydrogel/solution interface. This is because the nanoporous hydrogel plug works as a physical barrier to the eletrophoretic transport of charged analytes resulting in size-based concentration.[31,175]

With the ever-increasing interest in DNA analysis techniques for food safety,[176] clinical diagnosis,[177,178] and detection of pathogens in the environment,[179] there is a need for DNA assays which enable rapid and sensitive DNA detection. Usually, ultra-high sensitivity is required to directly detect the specific genomic sequences of infectious

Scheme 8.1

Power supply

−

Source
reservoir

Probe-conjugated
microbeads

Polymerized
hydrogel plug

+

Waste
reservoir

⬭ : Target DNA   ➡ : Electrokinetic mobility
in a hydrogel plug   ➡ : Electrokinetic mobility
in a microchannel

117
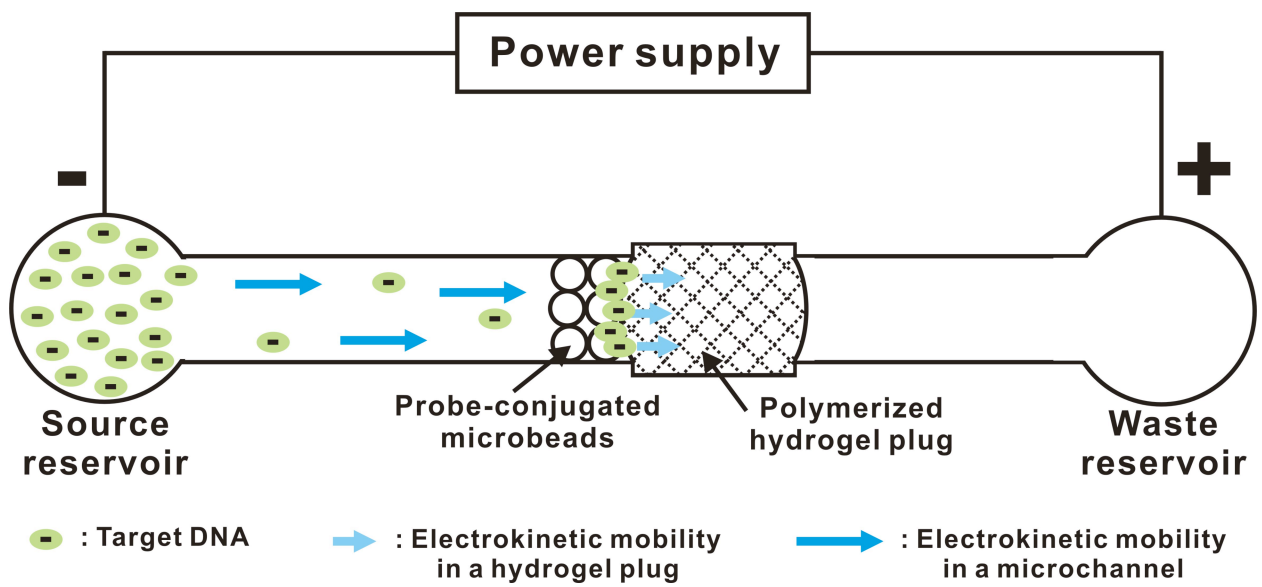
agents. A fairly useful assay may be required to detect ssDNA targets to the order of 10^4~10^5 molecules.[180] Traditional methods for the detection of trace amounts of ssDNA require a pre-enrichment step (culture) and an in-vitro amplification step (polymerase chain reaction, PCR) before detection. The disadvantage of these methods is that they are laborious and time-consuming because of the complicated assay procedures. A practical, simple and sensitive amplification approach, which does not involve PCR steps on a chip, would be more desirable.

The demand for more useful DNA assays has encouraged many researchers to enhance the sensitivity of DNA detection in several ways: the use of highly fluorescent bioconjugated nanoparticles,[181] bio-bar-code-based DNA detection,[182] signal amplification via engineered allosteric enzymes,[183] and dendritic amplification of DNA analysis based on enzyme dendritic architectures or oligonucleotide-functionalized Au-nanoparticles.[184,185] Although PCR-like sensitivity was demonstrated, these approaches still require non-trivial synthetic manipulation and complicated assay procedures. Several researchers have also investigated chip-based DNA detection. Microfluidics-based chips enable processing of very small volumes of reagents in a rapid and controlled manner, which is especially useful for analyses in the life sciences. Various designs such as microbead-based devices,[90,186] electrokinetically controlled DNA hybridization chips,[22] and PCR chips for simultaneous DNA amplification and detection[20,21] have been used for rapid and sensitive detection of DNA hybridization. However, amplification approaches without PCR steps on a chip, which would provide rapid and sensitive DNA detection with simpler chip design, have not been exploited.

Here, we compare microbead-based DNA detection assays with and without hydrogel microplugs. We demonstrate the enhancement of sensitivity of the microbead-based assay with hydrogels (Scheme 8.1). The hydrogel microplug provides ~20-fold

enrichment of the ssDNA concentration within 120 s, resulting in ~10-fold enhancement in the sensitivity of the microbead-based DNA detection with hydrogels. In addition, we show that the assay provides rapid and simple target analysis in terms of short analysis time (as little as 3 min including a washing step) and a simple washing step, as well as easy regeneration of the probe-conjugated microbeads for subsequent assays. A DNA sequence unique to the pathogen *Bacillus anthracis* is used to demonstrate the clinical usefulness of the technique.[187]

8.3 EXPERIMENTAL

Materials. DNA oligonucleotides modified with biotin or fluorescein were used as received from Integrated DNA Technologies (Coralville, IA). The hydrogel precursor solutions - 2-hydroxyethyl methacrylate (HEMA), ethylene glycol dimethacrylate (EGDM), and Irgacure 651 -, and buffer solutions - phosphate buffer saline (PBS) buffer (pH 7.4, 1.5 x 10^{-1} M NaCl, 4.0 mM KCl, 8.1 mM Na_2HPO_4, and 1.5 mM KH_2PO_4) and tris-acetate/EDTA (TAE) buffer (pH 8.3, 4.0 x 10 mM tris-acetate, 1.0 mM EDTA, 0.5 M NaCl) - were obtained from Sigma-Aldrich Co. (St. Louis, MO). 18 MΩ·cm Millipore Milli-Q (Bedford, MA) water was used throughout. The sequences of 5'-biotin-modified probe and 5'-fluorescein-labeled targets are as follows.

Probe: 5' (Biotin-TEG) TCA GGT TTA GTA CCA GAA CAT GCA G 3'

Complementary target: 5' (6-FAM) CTG CAT GTT CTG GTA CTA AAC CTG A 3'

Noncomplementary target: 5' (6-FAM) ACA TCG ACG TGT AGC TCG GCA TGA C 3'

Fabrication of Microfluidic Chips. Microfluidic chips were fabricated under clean room conditions as described below. Briefly, positive photoresist (AZP4620, Clariant Co., Somervile, NJ) was spin-coated onto a glass substrate (Fisher Scientific,

Pittsburgh, PA), followed by baking on hot plates. The design of the microchannels and weirs (Figure 8.1) was patterned onto the photoresist-coated glass master by exposing it to UV light (365 nm Hg I-line, 350 mW: current @ 5.4 A and voltage @ 67 V) through film photomasks followed by developing (AZ421K, Clariant Co.). The depth and width of the microstructures were measured using a profilometer (Veeeco Dektak 3, Veeco Instruments, Plainview, NY). The poly(dimethylsiloxane) (PDMS) precursor mixture (Sylgard 184, Dow Corning, Midland, MI) was molded on the fabricated photoresist-coated master. The PDMS replica was bonded to a cover glass (24 mm x 24 mm, 0.13~0.17 mm thick, VWR Scientific) after both were treated with an O_2 plasma (PDC-32G, Harrick Scientific, Ossining, NY) for 25 s.

Preparation of Probe-conjugated Microbeads. The conjugation of SuperAvidin™ coated microbeads (ProActive® Microspheres, diameter 9.95 μm, Bangs Lab., Fishers, IN) with the biotinylated ssDNA probes was performed as follows. 15.0 μL of stock microbeads (1.8×10^7 beads/mL) were washed in a PBS buffer solution with 0.05% (v/v) Tween 20 and then centrifuged. 4.0 μL of the biotinylated ssDNA probes (5.0 μM), corresponding to a five times excess of the binding capacity of the microbeads, was added to the washed microbead pellets and the resulting suspension was mixed slowly for 30 min at 20 to 25 °C. After conjugation, the mixture was centrifuged to remove unbound biotinylated ssDNA probes. The probe-conjugated microbead pellets were rinsed with the PBS buffer, centrifuged, re-suspended in TAE buffer and finally stored in a refrigerator until use.

Fabrication of Hydrogel Microplugs. The hydrogel microplugs were fabricated using the following procedure. The main microchannel was filled with a hydrogel precursor solution (92 wt% HEMA, 5 wt% EGDM, and 3 wt% photoinitiator Irgacure 651) by capillary action (Figure 8.1). A UV light (365 nm, 200 s, 300 mW/cm^2, EFOS

Lite E3000, Ontario, Canada) was projected onto the microchamber region of the microchannel from the side port of a microscope (DIAPHOT 300, Nikon, Japan) through a 10x objective lens. Any unpolymerized precursor solution was removed by pumping the TAE buffer (pH 8.3) through the side-microchannels at a flow rate of 10.0 μL/min for >10 min using a syringe pump (Harvard Apparatus, Hollistion, MA). Before carrying out the experiments, the hydrogel microplug was conditioned by applying 100~200 V voltages for 8~10 min. This conditioning step allowed removal of any unpolymerized precursor solution within the microplug.

Instrumentation. A fluorescence microscope (Nikon Eclipse TE 300, Nikon Co., Tokyo, Japan) equipped with band-pass filters, a 100 W mercury lamp and a CCD camera (Photometrics Ltd., Tucson, AZ) was used to acquire optical and fluorescence images. The acquired images were processed using an image process software (V++ Precision Digital Imaging, Digital Optics, Auckland, New Zealand).

Electric voltages were applied between two coil electrodes (90% Pt/10% Ir, 2.5 x 10^{-1} mm in diameter and 5.0 x 10 mm in length) immersed in the source and waste reservoirs (Figure 8.1). The bias voltage (range 0~1067 V, Ultra Volt, Ronkonkoma, NY) was controlled with a time resolution of 100 ms using a computer equipped with custom software.

8.4 RESULTS AND DISCUSSION

Microfluidic Chips. Two types of microfluidic chips – one with and one without a hydrogel microplug - were designed to compare the sensitivities of the microbead-based assays. The chips were fabricated with PDMS using standard photolithographic techniques, and sealed to glass substrates.[81,188] Figure 8.1 shows the schematic layouts (not drawn to scale) and optical images of the chips; microchip A consists of a weir
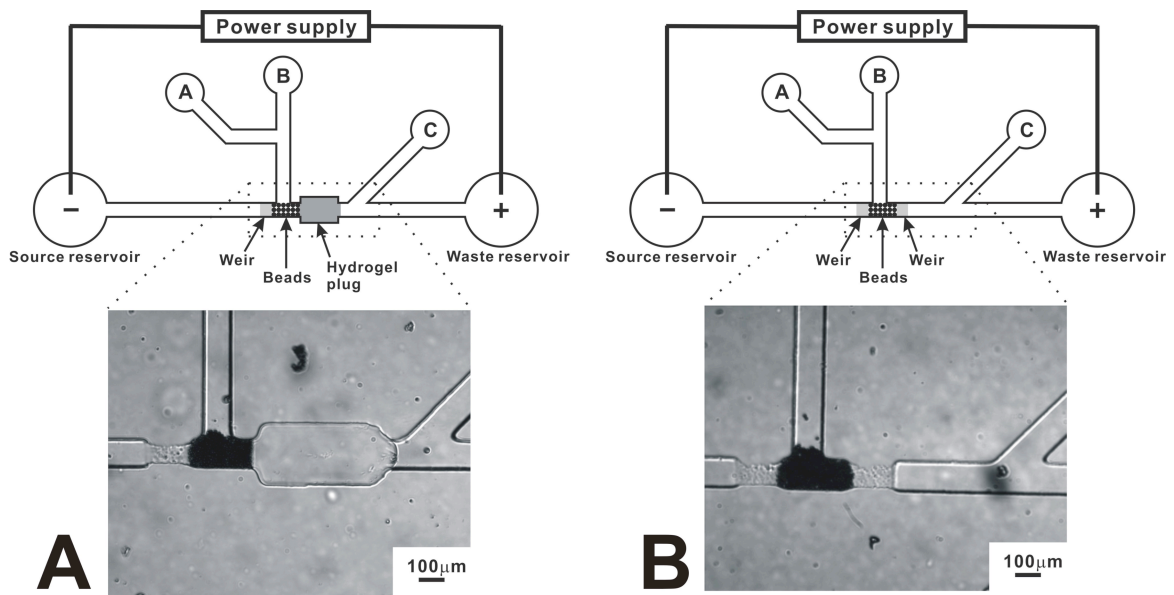
Figure 8.1. Schematic layouts and optical micrographs of microchips. (A) Microchip A with a weir and a microchamber. (B) Microchip B with two weirs.

(70~80 μm wide and 100 μm long) to hold the microbeads in place, and a microchamber (190~200 μm wide and 400 μm long) to house the hydrogel microplug (Figure 8.1A). Microchip B has an additional weir to hold the microbeads inside the microchannel in place of the microchamber (Figure 8.1B). The depth of the weirs ranged from 4 to 6 μm, which enabled the microbeads (diameter 9.95 μm) to be held in place. The main microchannel is 90~100 μm wide and ends in two 3 mm diameter reservoirs (source and waster reservoirs). The three side-microchannels (SMCh) were used to introduce microbeads (SMCh B) or to wash out the hydrogel precursor solution (SMCh A and C). The optical micrographs in Figure 8.1A and 1B show probe-conjugated microbeads packed with and without the hydrogel microplug, respectively.

Detection of Targets Using Bead-based Capture. With probe-conjugated microbeads packed in microchip B, the complementary target solution (20 μL) was loaded in the source reservoir, while the waste reservoir was filled with the TAE buffer solution (pH 8.3). A voltage of 100 V (100 V, waste reservoir positive) was then applied along the main microchannel for 2 min (10~130 s) after an initial 10 s (0~10 s) at 0 V. This results in continuous electrokinetic transport of the target solution over the probe-conjugated microbeads. Next, a reverse voltage of 40 V (-40 V, source reservoir positive) was applied for 30 s (130~160 s) to wash away bulk target solution and nonspecifically adsorbed targets that may be present. The reverse voltage is called the washing voltage. The experiment was repeated with noncomplementary target solution.

Figure 8.2 shows the fluorescence intensity profiles observed from the probe-conjugated microbeads (dotted box area in Figure 8.2D, ROI 40x65 pixels) next to the right-hand weir during the electrokinetically-controlled flow of targets. Background fluorescence signals were measured before loading the target solution and were subsequently subtracted from the overall fluorescence. Figure 8.2A shows that the

123
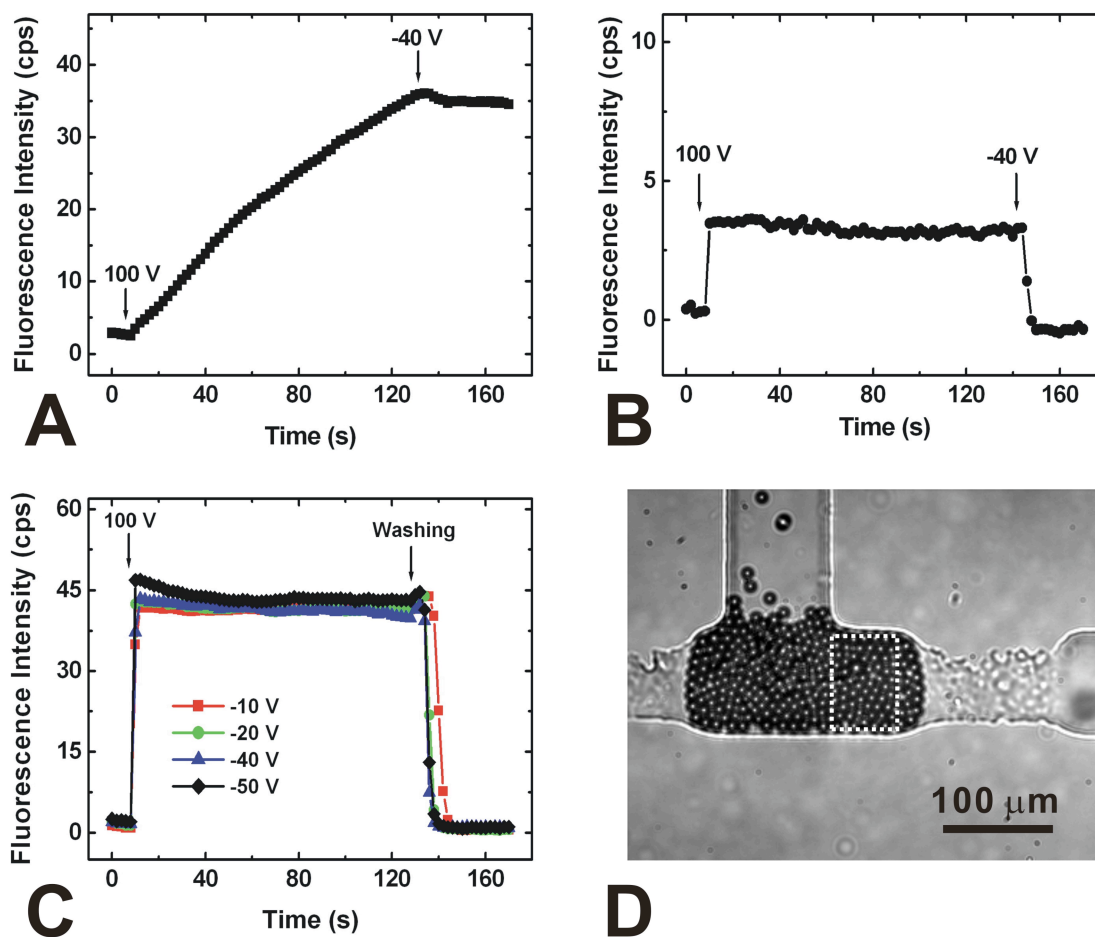
Figure 8.2. Hybridization of targets onto probe-conjugated microbeads during electrokinetically-controlled flow of targets. (A) and (B) Fluorescence intensity profiles of probe-conjugated microbeads (ROI 40x65 pixels): 100 nM complementary and noncomplementary target solution, respectively. (C) Fluorescence intensity profiles on the probe-conjugated microbeads (ROI 40x65 pixels) with different washing voltages: 1 μM noncomplementary target solution. (D) Optical micrograph showing Microchip B packed with probe-conjugated microbeads.

fluorescence signal increased during the application of 100 V when using complementary targets, while no increase in the intensity was observed with noncomplementary targets (Figure 8.2B). Only the bulk solution was found to give a fluorescence signal (3.2 ± 0.2 cps) when the noncomplementary target solution was used (Figure 8.2B). This indicates that the probe-conjugated microbeads only captured the complementary targets. Note that the small fluorescence signal (2.7 ± 0.1 cps) observed in Figure 8.2A before applying 100 V arises from targets reaching the bead bed during loading the target solution using a pipette. Figure 8.2A also shows only a small decrease (1.3 ± 0.2 cps) in intensity when applying the washing voltage (-40 V) to the hybridized beads, while noncomplementary targets were washed away completely under the same conditions. This result indicates that the captured complementary targets were retained on the probe-conjugated microbeads even after applying a washing voltage (-40 V), which was enough to remove all nonspecifically adsorbed noncomplementary targets. Even applying up to -150 V for 200 s did not significantly remove the captured complementary targets (data not shown). This result suggests that the complementary targets were hybridized onto the probe-conjugated microbeads and not just nonspecifically adsorbed. In addition, there is no detectable nonspecific binding of the noncomplementary targets on the probe-conjugated microbeads after washing at -40 V (signal-to-background ratio: ~1.0). Even at high concentration (1 μM), the nonspecific binding of noncomplementary targets was negligible (Figure 8.3B) compared to a much lower concentration (50 nM) of complementary targets (Figure 8.3A). To investigate the effect of the magnitude of washing voltages, different voltages were applied following the application of 100 V for 2 min with the noncomplementary target solution at high concentration (1 μM). Figure 8.2C shows that the noncomplementary targets were completely washed away at all washing voltages. Even -10 V was enough to remove the bulk target solution and the
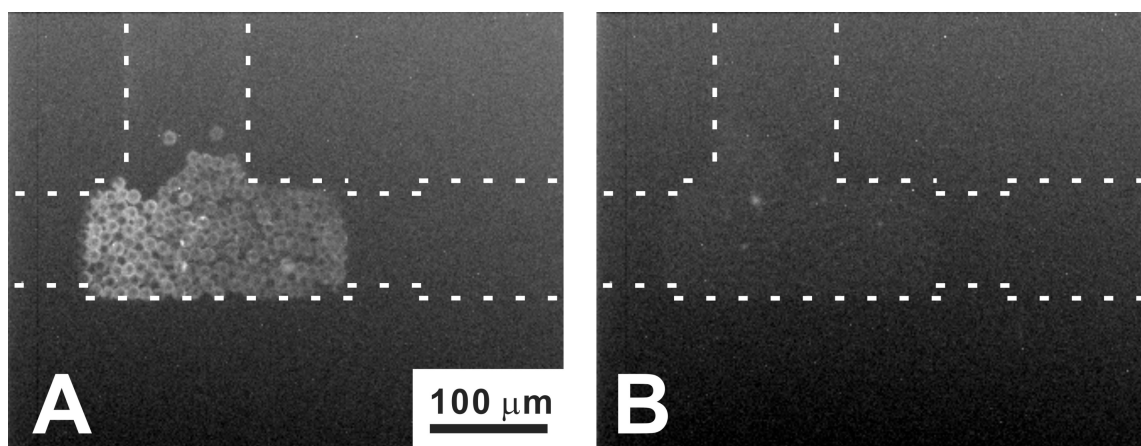
Figure 8.3. Fluorescence micrographs of microchip B packed with probe-conjugated microbeads after the assay. (A) 50 nM complementary target solution. (B) 1 μM noncomplementary target solution. Applied voltage: 100 V for 2 min. Washing voltage: -20 V for 30 s. Gray scale: 125~215.

nonspecifically adsorbed targets within 10 s. -20 V was chosen and used as a washing voltage in later experiments.

Concentration Enrichment Using a Hydrogel Microplug. The concentration of targets using a HEMA-based uncharged hydrogel microplug was demonstrated without probe-conjugated microbeads. A complementary target solution was loaded in the source reservoir and a voltage of 100 V was applied between the source reservoir (left, negative) and the waste reservoir (right, positive) for 2 min (10~130 s) after an initial 10 s at 0 V (0~10 s). This causes the target DNA strands to be electrokinetically transported from left to right and concentrated at the interface between the highly cross-linked hydrogel microplug and buffer solution. After applying 100 V for 2 min, the voltage was turned off (130~160 s), resulting in the slow diffusion of the concentrated targets back toward the source reservoir or SMCh B.

A series of fluorescence micrographs obtained during the concentration of targets is shown in Figure 8.4. Figure 8.4A shows no concentration of the targets in front of the microplug initially (0~10 s). By applying 100 V for 2 min (10~130 s), targets were transported from left (source reservoir) to right (waste reservoir) along the main microchannel, and a growing fluorescence band originating from concentrated targets (concentration band in Figure 8.4B) was observed next to the hydrogel microplug. Figure 8.4B also shows that some ssDNA moves into the hydrogel microplug. When the voltage was turned off (130~160 s), the concentrated target diffused back (diffusion band in Figure 8.4C) and slowly dissipated (Figure 8.4D). Some of the ssDNA trapped inside the microplug also went out from its right end (Figure 8.4C and 8.4D). We understand the observed concentration phenomenon in terms of an abrupt mobility change of the target at the boundary between the hydrogel and the buffer.[31,175] The high cross-linking density and tortuous nature of the inhomogeneous nanoporous hydrogel decrease the effective

Figure 8.4. A series of fluorescence micrographs obtained during concentration of targets using a HEMA-based hydrogel microplug. Target solution: 1 μM. The concentration band represents a fluorescent band next to the hydrogel microplug. The diffusion band represents a fluorescent band next to the concentration band. Gray scale: 120~200.

diffusivity and hence the electrophoretic mobility of ssDNA within the hydrogel. Subsequent velocity difference between the electrophoretic migration in the microchannel and within the hydrogel results in concentration of ssDNA at the boundary between the hydrogel and the buffer.

A similar experiment was designed to calculate an enrichment factor using the HEMA-based hydrogel microplug. The fluorescence intensity was measured in the diffusion-band region (Figure 8.5 inset, ROI 10x25 pixels). The specified area was chosen to calculate the enrichment factor over the diffusion band, which provides concentrated targets onto the probe-conjugated microbeads. The concentration enrichment step was followed with a 0 V step for 30 s and a washing step at -20 V for 30 s. A higher concentration (5 μM) was used to enhance the signal-to-noise ratio and reduce the error in the calculation of the enrichment factor. A background fluorescence signal was measured before loading the target solution and was subsequently subtracted. Figure 8.5 shows the fluorescence intensity profile over the diffusion band area. After the concentration step (10~130 s), the targets diffused back to the source reservoir or to SMCh B, resulting in a sudden increase in the fluorescence intensity of the diffusion band area at 130 s. The fluorescence intensity then decreased during the following 30 s at 0 V and rapidly dropped to the background level after a washing voltage of -20 V was applied. The corresponding fluorescence micrographs are shown in Figure 8.6. The enrichment factor was calculated by comparing the average value of five initial intensities before the concentration, and the peak intensity value after the concentration. Each experiment was repeated 3 times to yield an average enrichment factor of 20 ± 3.1 -fold.

Comparison of Sensitivity. The sensitivities of the microbead-based assays with or without hydrogel microplugs were compared. The same programmed switching of voltages (without the initial 0 V for 10 s) used for determination of the enrichment factors
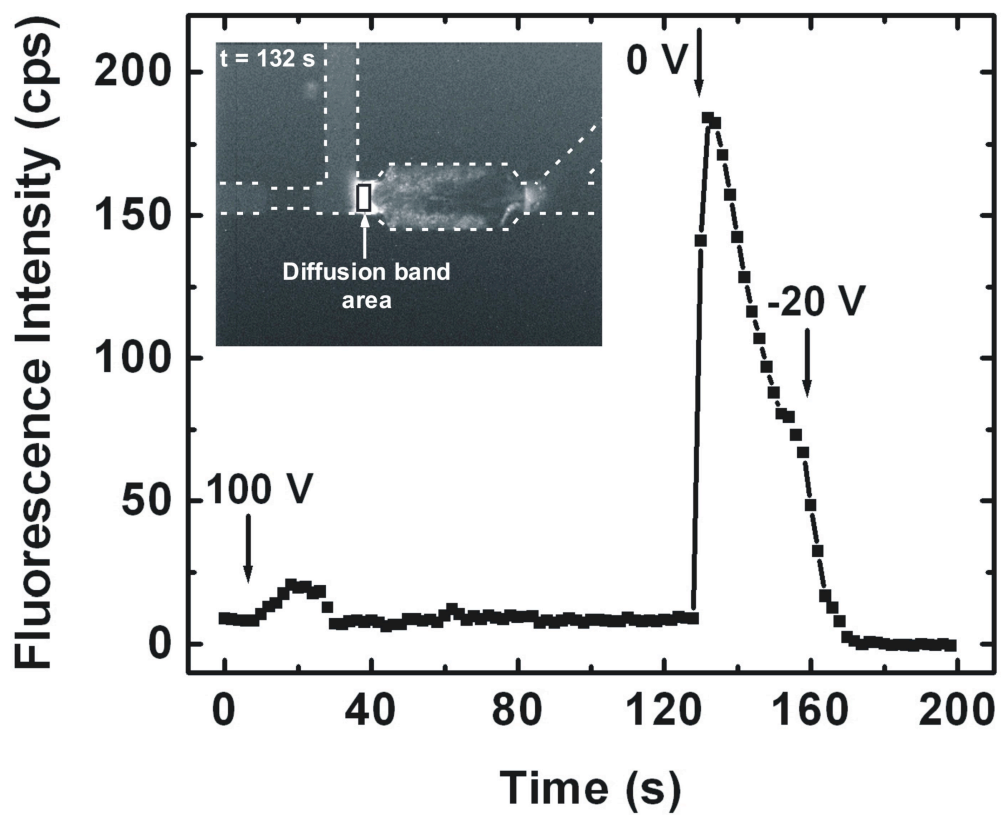
Figure 8.5. Fluorescence intensity profile over the diffusion band area obtained using a HEMA-based hydrogel microplug without probe-conjugated microbeads. Target solution: 5 μM. The diffusion band area represents a rectangular area (ROI 10x25 pixels) indicated by a black solid line in the inset.
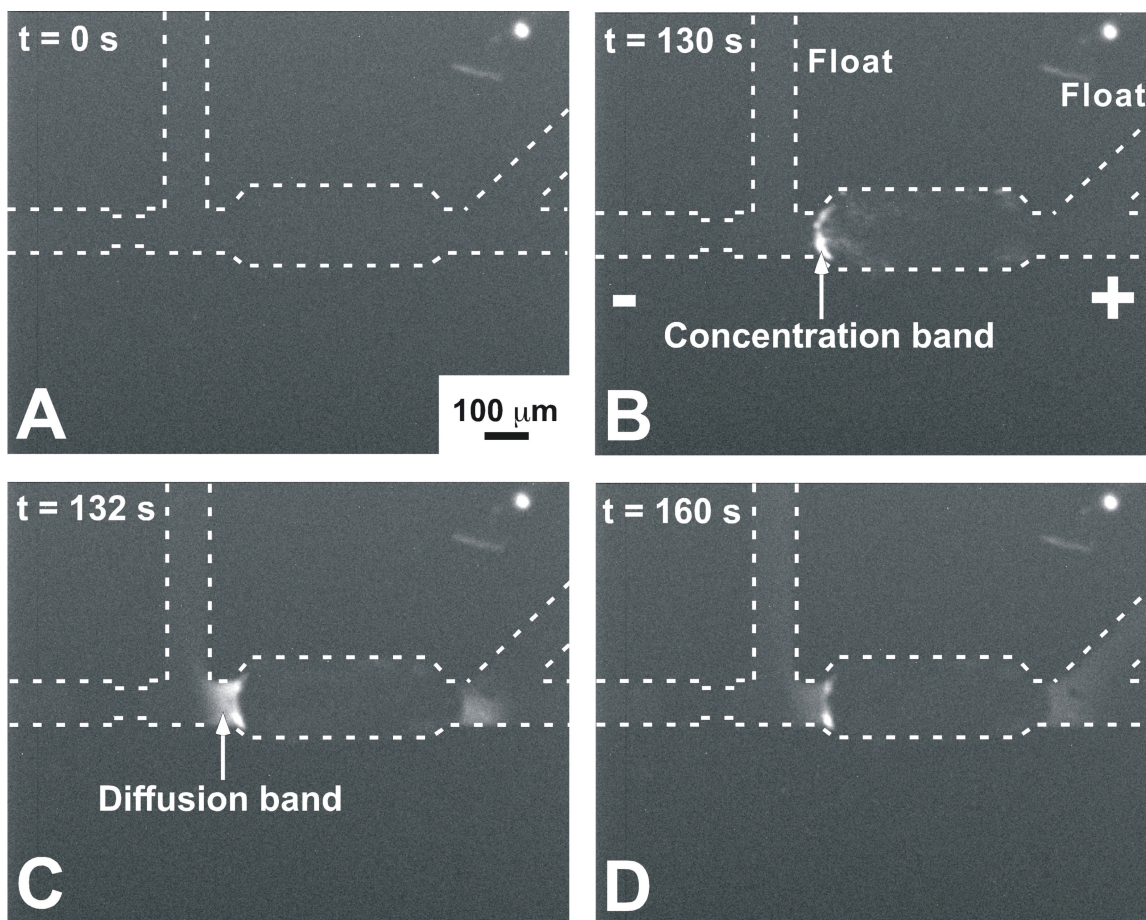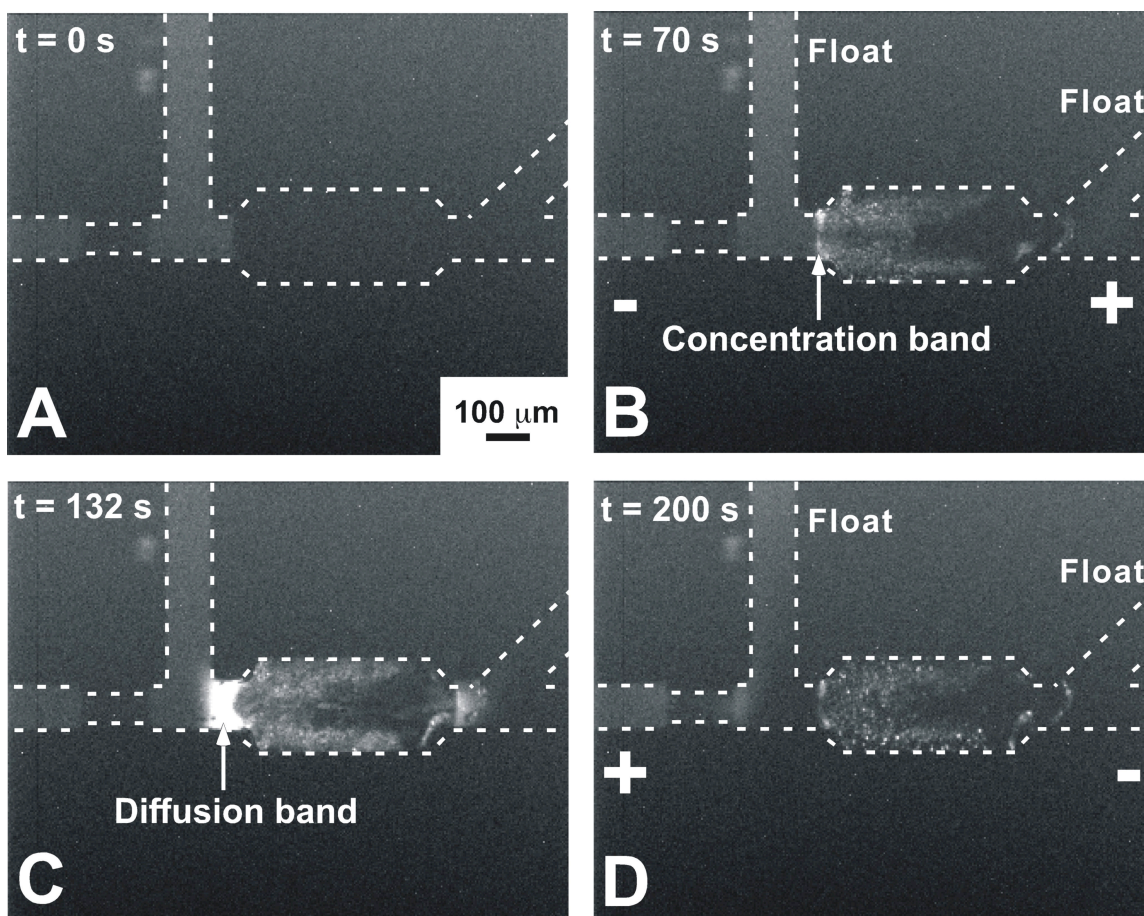
Figure 8.6. A series of fluorescence micrographs obtained during concentration of targets with a HEMA-based hydrogel microplug. Target solution: 5 µM. The concentration band represents a fluorescent band next to a hydrogel microplug. The diffusion band represents a fluorescent band next to the concentration band. Gray scale: 120~200.

was used for these assays. After loading the target solution in the source reservoir, 100 V was applied between the two reservoirs for 2 min to enable concentration of the target. Zero V was then applied for 30 s followed by a washing voltage of -20 V for 30 s to remove bulk target solution and nonspecifically adsorbed target that might be present. Keeping the voltage at 0 V for 30 s after the concentration step allows the concentrated targets to remain in the vicinity of the probe-conjugated microbeads for a longer time compared to the washing step (-20 V) (data not shown).

Figure 8.7 shows two fluorescence micrographs after the assays: micrographs of a microchip A (Figure 8.7A) and of a microchip B (Figure 8.7B). Clearly, the presence of the hydrogel plug resulted in a higher sensitivity for the microbead-based assay. Each experiment was repeated 3 times. The microfluidic devices having a hydrogel microplug showed 10 ± 0.4 times higher fluorescence signals at a concentration of 10 nM. This enhancement in sensitivity can be understood in terms of the enrichment factor achieved using a hydrogel microplug (~20-fold).

When the same experiments were repeated at a lower concentration (2.5 nM), the sensitivity enhancement was not significant. Figure 8.8A shows a fluorescence micrograph of microchip B without a hydrogel microplug after the assay. We only observed a fluorescence signal upstream from the probe-conjugated microbead bed. This indicates that the capturing efficiency of the probe-conjugated microbeads is high enough to capture most of target flowed during the assay and there is no significant amount of target reaching downstream of the microbead bed. The reason for the high efficiency of hybridization onto the probe-conjugated microbeads is probably due to the narrow fluid paths between packed microbeads which confine the targets in close proximity to the probes.[92] This would reduce the vertical diffusive transport distance and increase the number of target-probe collisions, thereby increasing the probability of hybridization.
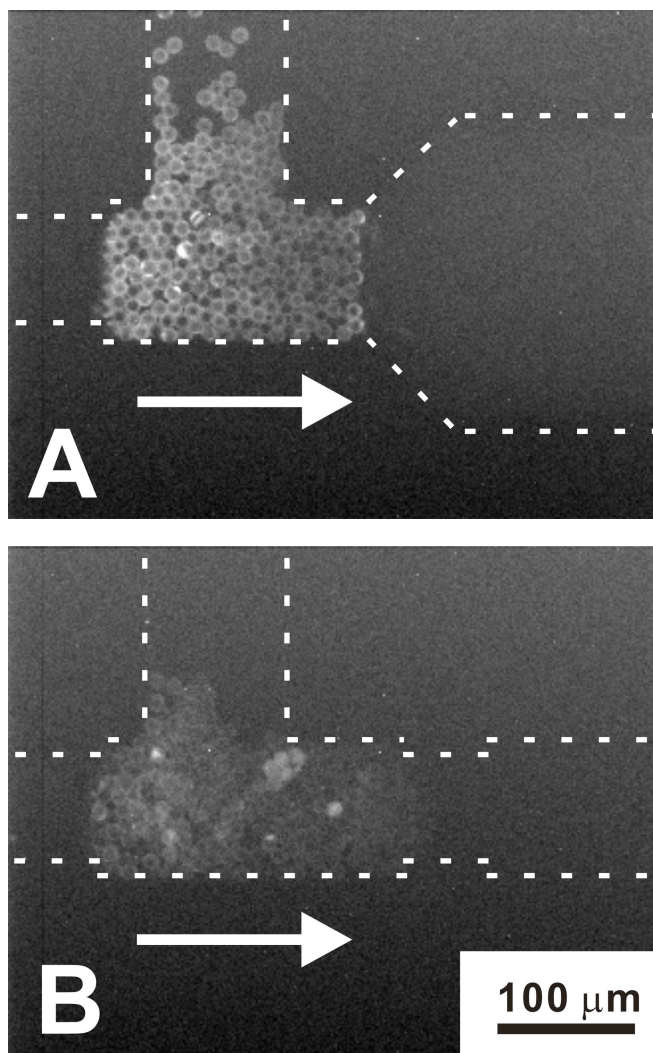
Figure 8.7. Fluorescence micrographs after the assay (A) with and (B) without a HEMA-based hydrogel microplug. Target solution: 10 nM. Gray scale: 125~215. The arrow indicates the initial flow direction of target ssDNA.
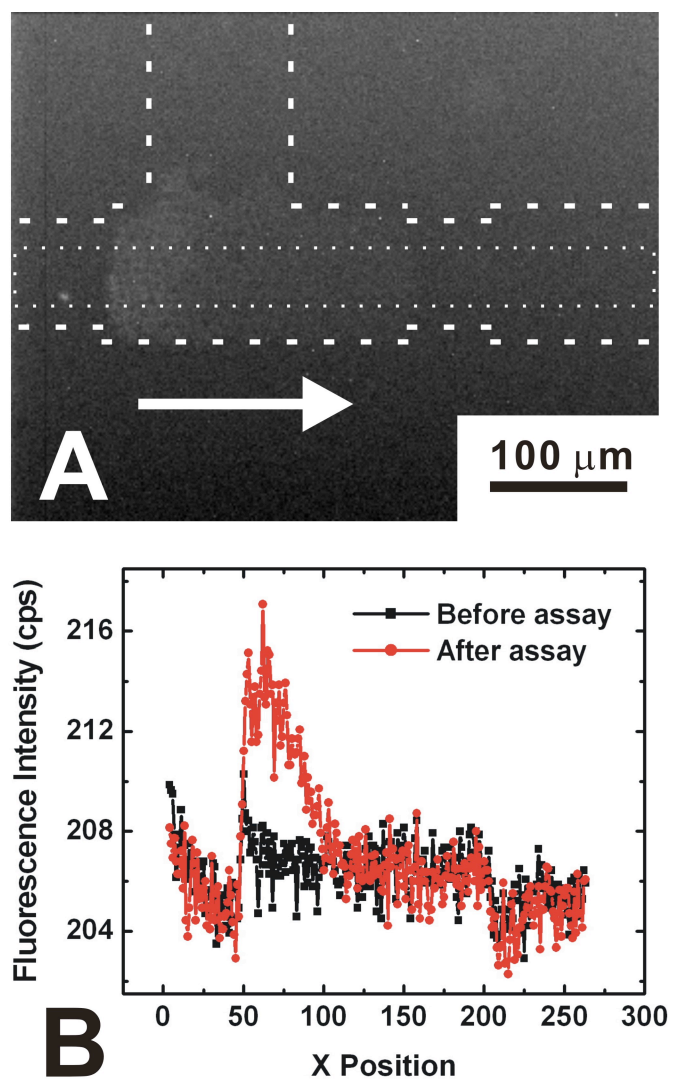
Figure 8.8. Fluorescence intensity along a microchannel packed with probe-conjugated microbeads. (A) Fluorescence micrograph after the assay. (B) Fluorescence intensity profile along the main microchannel. Target solution: 2.5 nM. Gray Scale: 125~215. The arrow indicates the initial flow direction of target ssDNA.

This high efficiency was confirmed by the observation that no significant fluorescent signal could be detected downstream of the bed after the assay (Figure 8.8B). The high efficiency of hybridization resulted in fewer targets arriving downstream of the microbead bed for concentration, and therefore there was no significant enhancement of sensitivity with the lower concentration of target solutions. This limitation of the system could be overcome by reducing the number of microbeads packed in front of a hydrogel microplug or locating the microbead bed in some place other than right in front of the hydrogel plug.

Another interesting phenomenon that we observed was that the hybridized targets were significantly denatured at -100 V in the presence of a hydrogel microplug while they were stable up to -150 V without a hydrogel (data not shown). This is probably due to the variation in the local field around the hydrogel microplug, resulting in different thermal (Joule heating), shear (electroosmosis), and electrical (electrophoresis) energies even with the application of the same electrical voltage.[189] This suggests that probe-conjugated microbeads could be used to investigate the local environment around the hydrogel microplug in a chip and ultimately as a tool for studying the concentration mechanism of the hydrogels. More importantly, the probe-conjugated microbeads were intact after the denaturation by application of the high washing voltage (-100 V), and could capture targets again (data not shown). This indicates that the probe-conjugated microbeads could be easily regenerated without the use of chemicals, which usually cause serious degradation of probe sites.[174] Furthermore, this could be used for single-nucleotide polymorphism (SNP) discrimination by simply applying appropriate washing voltages.[189]

8.5 CONCLUSION

135

In this study, we have demonstrated a sensitivity enhancement for microbead-based DNA detection using a hydrogel microplug in a microfluidic device. The hydrogel microplug provided ~10-fold enhancement in the sensitivity, which could be understood in terms of the enrichment factor (~20-fold) of the ssDNA concentration provided by the hydrogel. Higher sensitivity enhancement should be obtainable by optimizing the layout of the device: reducing the number of microbeads packed in front of the hydrogel microplug or relocating the bead bed. In addition, the probe-conjugated microbeads allowed rapid (few minutes) and sequence-specific capture of the targets. The electrokinetically controlled assay also provided the possibility of easy regeneration of probe sites on the microbeads as well as a simple washing procedure. Further, a complete understanding of the effect of hydrogel on the denaturation could be useful for SNP discrimination.

Chapter 9: Summary and Conclusion

This dissertation described development of two types of microdevices used for bioanalysis. The microdevices are DNA (or RNA) microarrays and bead-based microfluidic devices. There are two main aspects of this study. First, new strategies to fabricate DNA microarrays were demonstrated. The replication approach utilizing zip code masters was accurate and efficient, which allowed fabrication of replica DNA arrays having any configuration from a single, universal master array (Chapter 3). The replication strategy was combined even with in-situ enzymatic synthesis of DNA (Chapter 4 and 5) and extended to fabricate replica arrays of other materials like RNA (Chapter 6). Second, sensitive DNA sensors were developed. A microfluidic device packed with probe-conjugated microbeads was suggested to study parameters affecting the hybridization of DNA onto the beads under microfluidic flow conditions (Chapter 7). Integration of a hydrogel preconcentrator into a bead-based microfluidic device was also demonstrated to improve the limit of detection for DNA in the bead-based microfluidic devices (Chapter 8). A more detailed discussion of findings is found below.

Chapter 3 described an efficient and accurate method for production of DNA microarrays from a zip code master. The zip code approach provided a means to fabricate DNA arrays having any functional sequences just by using a single universal master modified with zip code oligonucleotides. Three consecutive replications from a single zip code master were achieved with no significant decrease of DNA density on the replicas. This approach was also used to replicate master arrays having three different zip codes (spot feature sizes as small as 100 μm) and the replica array showed no observable cross-reactivity. It can be envisioned to apply this zip code approach further to produce replicas

of any other materials that can be modified with a short oligonucleotide code; for example, cells, proteins, viruses, carbohydrates, and inorganic nanoparticles.

Chapter 4 and 5 demonstrated that DNA microarrays can be replicated even without using pre-synthesized DNA complements. Use of a T4 DNA polymerase reaction allowed in-situ synthesis of complementary oligonucleotides directly on master surfaces. Transfer of the synthesized DNA complements to a PDMS surface was demonstrated with micrometer-scale resolution. Importantly, spatial registration is preserved between the master and PDMS surface after transfer. Following the basic demonstration of the enzymatic synthesis approach, replication of 3 x 2 master arrays having different oligonucleotide sequences was achieved and the replicas were able to bind complementary oligonucleotides accurately. Even large-scale master arrays containing 2300 spots were successfully replicated. These results indicate that the enzymatic synthesis approach is robust and scaleable.

In Chapter 6, further extension of the replication strategy to other material (RNA) was demonstrated. RNA microarrays were fabricated by utilizing a surface T4 DNA ligase reaction. The RNA array components were formed by ligation of probe RNA strands to anchor DNA on a template DNA-immobilized master slide, and then directly transferred onto a PDMS surface. Multiple fabrications of RNA microarrays, more than 15 times, from a single master were achieved without significant degradation of activity of the resulting replica RNA array or the master DNA array. RNA microarrays having different RNA sequences were fabricated accurately. The fabricated RNA microarrays were active to hybridization.

Chapter 7 reported the study of hybridization of DNA onto probe-conjugated microbeads in a microfluidic device. The hybridization of DNA was described in terms of probe surface concentration, target concentration, and flow rate. The density of probes on

the microbeads (1.9×10^{12} probes/cm^2) was within the range that leads to rapid hybridization of DNA. The simple bead-based microfluidic device leaded to efficient target capture: a limit of detection of ~10^{-10} M (~10^{-16} mol) and a selectivity factor greater than 7.9×10^3 within a few minutes (4 min), resulting from the inherently high surface-area-to-volume ratio of beads, optimized probe surface density, and good mass-transfer characteristics.

Finally, Chapter 8 described a bead-based microchip integrated with a hydrogel preconcentrator enhancing the local concentration of target DNA in a microchannel. The microfluidic device consisted of probe-conjugated microbeads packed in front of a photopolymerized hydrogel plug. Electrokinetically transported target DNA strands were concentrated in front of the hydrogel microplug, which resulted in enrichment factor of ~20-fold within 2 min. The enrichment of target DNA near the bead bed allowed ~10-fold enhancement in the sensitivity of the microbead-based DNA detection.

References

1. Manz, A.; Grabner, N.; Widmer, H. M. <u>Miniaturized total chemical analysis systems: a novel concept for chemical sensing</u>. *Sens. Actuators B Chem.* **1990**, *1*, 244-248.

2. Janasek, D.; Franzke, J.; Manz, A. <u>Scaling and the design of miniaturized chemical-analysis systems</u>. *Nature* **2006**, *442*, 374-380.

3. Burns, M. A. <u>Everyone's a (future) chemist</u>. *Science* **2002**, *296*, 1818-1819.

4. Mitchell, P. <u>Microfluidics-downsizing large-scale biology</u>. *Nat. Biotechnol.* **2001**, *19*, 717-721.

5. Schena, M.; Shalon, D.; Davis, R. W.; Brown, P. O. <u>Quantitative monitoring of gene expression patterns with a complementary DNA microarray</u>. *Science* **1995**, *270*, 467-470.

6. Hoheisel, J. D. <u>Microarray technology: beyond transcript profiling and genotype analysis</u>. *Nat. Rev. Genet.* **2006**, *7*, 200-210.

7. Gilad, Y.; Borevitz, J. <u>Using DNA microarrays to study natural variation</u>. *Curr. Opin. Genet. Develop.* **2006**, *16*.

8. Myers, R. M.; Lumelsky, N.; Lerman, L. S.; Maniatis, T. <u>Detection of single base substitutions in total genomic DNA</u>. *Nature* **1985**, *313*, 495-498.

9. Huber, C. G.; Premstaller, A.; Xiao, W.; Oberacher, H.; Bonn, G. K.; Oefner, P. J. <u>Mutation detection by capillary denaturing high-performance liquid chromatography using monolithic colums</u>. *J. Biochem. Biophys. Meth.* **2001**, *47*, 5-19.

10. Niemeyer, C. M.; Blohm, D. <u>DNA microarrays</u>. *Angew. Chem. Int. Ed.* **1999**, *38*, 2865-2869.

11. Graves, D. J. <u>Powerful tools for genetic analysis come of age</u>. *Trends Biotechnol.* **1999**, *17*, 127-134.

12. Anderson, R. C.; Su, X.; Bogdan, G. J.; Fenton, J. <u>A miniature integrated device for automated multistep genetic assays</u>. *Nucleic Acids Res*. **2000**, *28*, e60.

13. Chin, C. D.; Linder, V.; Sia, S. K. <u>Lab-on-a-chip devices for global health: Past studies and future opportunities</u>. *Lab Chip* **2007**, *7*, 41-57.

14. Pease, A. C.; Solas, D.; Sullivan, E. J.; Cronin, M. T.; Holmes, C. P.; Fodor, S. P. A. <u>Light-generated oligonucleotide arrays for rapid DNA sequence analysis</u>. *Proc. Natl. Acad. Sci. U.S.A.* **1994**, *91*, 5022-5026.

15. McGall, G.; Labadie, J.; Brock, P.; Wallraff, G.; Nguyen, T.; Hinsberg, W. <u>Light-directed synthesis of high-density oligonucleotide arrays using semiconductor photoresists</u>. *Proc. Natl. Acad. Sci. U.S.A.* **1996**, *93*, 13555-13560.

16. Singh-Gasson, S.; Green, R. D.; Yue, Y. J.; Nelson, C.; Blattner, F.; Sussman, M. R.; Cerrina, F. <u>Maskless fabrication of light-directed oligonucleotide microarrays using a digital micromirror array</u>. *Nat. Biotechnol.* **1999**, *17*, 974-978.

17. Nuwaysir, E. F.; Huang, W.; Albert, T. J.; Singh, J.; Nuwaysir, K.; Pitas, A.; Richmond, T.; Gorski, T.; Berg, J.; Ballin, J.; McCormick, M.; Norton, J.; Pollock, T.; Sumwalt, T.; Butcher, L.; Porter, D.; Molla, M.; Hall, C.; Blattner, F.; Sussman, M. R.; Wallace, R. L.; Cerrina, F.; Green, R. D. <u>Gene expression analysis using oligonucleotide arrays produced by maskless photolithography</u>. *Genome Res*. **2002**, *12*, 1749-1755.

18. Albert, T. J.; Norton, J.; Ott, M.; Richmond, T.; Nuwaysir, K.; Nuwaysir, E. F.; Stengele, K.; Green, R. D. <u>Light-directed 5' → 3' synthesis of complex oligonucleotide microarrays</u>. *Nucleic Acids Res*. **2003**, *31*, e35.

19. Shalon, D.; Smith, S. J.; Brown, P. O. A DNA microarray system for analyzing complex DNA samples using two-color fluorescent probe hybridization. *Genome Res*. **1996**, *6*, 639-645.

20. Lee, T. M.; Carles, M. C.; Hsing, I. Microfabricated PCR-electrochemical device for simultaneous DNA amplification and detection. *Lab Chip* **2003**, *3*, 100-105.

21. Erill, I.; Campoy, S.; Rus, J.; Fonseca, L.; Ivorra, A.; Navarro, Z.; Plaza, J. A.; Aguilo, J.; Barbe, J. Development of a CMOS-compatible PCR chip: comparison of design and system strategies. *J. Micromech. Microeng*. **2004**, *14*, 1558-1568.

22. Erickson, D.; Liu, X.; Krull, U.; Li, D. Electrokinetically controlled DNA hybridization microfluidic chip enabling rapid target analysis. *Anal. Chem*. **2004**, *76*, 7269-7277.

23. Edman, C. F.; Raymond, D. E.; Wu, D. J.; Tu, E.; Sosnowski, R. G.; Butler, W. F.; Nerenberg, M.; Heller, M. Electric field directed nucleic acid hybridization on microchips. *Nucleic Acids Res*. **1997**, *25*, 4907-4914.

24. Yaralioglu, G. G.; Wygant, I. O.; Marentis, T. C.; Khuri-Yakub, B. T. Ultrasonic mixing in microfluidic channels using integrated transducers. *Anal. Chem*. **2004**, *76*, 3694-3698.

25. Liu, R. H.; Lenigk, R.; Druyor-Sanchez, R. L.; Yang, J.; Grodzinski, P. Hybridization enhancement using cavitation microstreaming. *Anal. Chem*. **2003**, *75*, 1911-1917.

26. Yuen, P. K.; Li, G.; Bao, Y.; Mueller, U. R. Microfluidic devices for fluidic circulation and mixing improve hybridization signal intensity on DNA arrays. *Lab Chip* **2003**, *3*, 46-50.

27. Lin, H.; Sun, L.; Crooks, R. M. Replication of a DNA microarray. *J. Am. Chem. Soc*. **2005**, *127*, 11210-11211.

28. Lin, H.; Kim, J.; Sun, L.; Crooks, R. M. <u>Replication of DNA microarrays from zip code masters</u>. *J. Am. Chem. Soc.* **2006**, *128*, 3268-3272.

29. Kim, J.; Crooks, R. M. <u>Transfer of surface polymerase reaction products to a secondary platform with conservation of spatial registration</u>. *J. Am. Chem. Soc.* **2006**, *128*, 12076-12077.

30. Kim, J.; Heo, J.; Crooks, R. M. <u>Hybridization of DNA to bead-immobilized probes confined within a microfluidic channel</u>. *Langmuir* **2006**, *22*, 10130-10134.

31. Dhopeshwarkar, R.; Sun, L.; Crooks, R. M. <u>Electrokinetic concentration enrichment within a microfluidic device using a hydrogel microplug</u>. *Lab Chip* **2005**, *5*, 1148-1154.

32. Safsten, P.; Klakamp, S. L.; Drake, A. W.; Karlsson, R.; Myszka, D. G. <u>Screening antibody-antigen interactions in parallel using Biacore A100</u>. *Anal. Biochem.* **2006**, *353*, 181-190.

33. Love, J. C.; Ronan, J. L.; Grotenbreg, G. M.; Van der Veen, A. G.; Ploegh, H. L. <u>A microengraving method for rapid selection of single cells producing antigen-specific antibodies</u>. *Nat. Biotechnol.* **2006**, *24*, 703-707.

34. Savchenko, A.; Kashuba, e.; Kashuba, V.; Snopok, B. <u>Imaging technique for the screening of protein-protein interactions using scattered light under surface plasmon resonance conditions</u>. *Anal. Chem.* **2007**, *79*, 1349-1355.

35. Angres, B. <u>Cell microarrays</u>. *Expert Rev. Mol. Diagn.* **2005**, *5*, 769-779.

36. Diaz-Mochon, J. J.; Tourniaire, G.; Bradley, M. <u>Microarray platforms for enzymatic and cell-based assays</u>. *Chem. Soc. Rev.* **2007**, *36*, 449-457.

37. Barbulovic-Nad, I.; Lucente, M.; Sun, Y.; Zhang, M.; Wheeler, A. R.; Bussmann, M. <u>Biomicroarray fabrication techniques - A review</u>. *Crit. Rev. Biotechnol.* **2006**, *26*, 237-259.

38. Wang, D. G.; Fan, J. B.; Siao, C. J.; Berno, A.; Young, P.; Sapolsky, r.; Ghandour, G.; Perkins, N.; Winchester, E.; Spencer, J.; Kruglyak, L.; Stein, L.; Hsie, L.; Topaloglou, T.; Hubbell, E.; Robinson, E.; Mittmann, M.; Morris, M. S.; Shen, N.; Kilburn, D.; Rioux, J.; Nusbaum, C.; Rozen, S.; Hudson, T. J.; Lipshutz, R.; Chee, M.; Lander, E. S. Large-scale identification, mapping, and genotyping of single-nucleotide polymorphisms in the human genome. *Science* **1998**, *280*, 1077-1082.

39. Ng, J. K.; Liu, W. Miniaturized platforms for the detection of single-nucleotide polymorphisms. *Anal. Bioanal. Chem.* **2006**, *386*, 427-434.

40. Lindroos, K.; Liljedahl, U.; Raitio, M.; Syvanen, A. C. Minisequencing on oligonucleotide microarrays: comparison of immobilisation chemistries. *Nucleic Acids Res.* **2001**, *29*, e69.

41. Ericsson, O.; Sivertsson, A.; Lundeberg, J.; Ahmadian, A. Microarray-based resequencing by apyrase-mediated allele-specific extension. *Electrophoresis* **2003**, *24*, 3330-3338.

42. Karaman, M. W.; Groshen, S.; Lee, C.; Pike, B. L.; Hacia, J. G. Comparisons of substitution, insertion and deletion probes for resequencing and mutational analysis using oligonucleotide microarrays. *Nucleic Acids Res.* **2005**, *33*, e33.

43. Malanoski, A. P.; Lin, B.; Wang, Z.; Schnur, J. M.; Stenger, D. A. Automated identification of multiple micro-organisms from resequencing DNA microarrays. *Nucleic Acids Res.* **2006**, *34*, 5300-5311.

44. Liu, Y.; Gong, Z.; Morin, N.; Pui, O.; Cheung, M.; Zhang, H.; Li, X. Electronic deoxyribonucleic acid (DNA) microarray detection of viable pathogenic Escherichia coli, Vibrio cholerae, and Salmonella typhi. *Anal. Chim. Acta* **2006**, *578*, 75-81.

45.   Kostic, T.; Weilharter, A.; Rubino, S.; Delogu, G.; Uzzau, S.; Rudi, K.; Sessitsch, A.; Bodrossy, L. <u>A microbial diagnostic microarray technique for the sensitive detection and identification of pathogenic bacteria in a background of nonpathogens</u>. *Anal. Biochem.* **2007**, *360*, 244-254.

46.   Chin, K.; Kong, A. <u>Application of DNA microarrays in pharmacogenomics and toxicogenomics</u>. *Pharm. Res.* **2002**, *19*, 1773-1778.

47.   Meloni, R.; Khalfallah, O.; Biguet, N. F. <u>DNA microarrays and pharmacogenomics</u>. *Pharmacol. Res.* **2004**, *49*, 303-308.

48.   Shou, J.; Dotson, C.; Qian, H.-R.; Tao, w.; Lin, C.; Lawrence, F.; N'Cho, M.; Kulkarni, N. H.; Bull, C. M.; Gelbert, L. M.; Onyia, J. E. <u>Optimized blood cell profiling method for genomic biomarker discovery using high-density microarray</u>. *Biomarkers* **2005**, *10*, 310-320.

49.   Pirrung, M. C. <u>How to Make a DNA Chip</u>. *Angew. Chem. Int. Ed.* **2002**, *41*, 1276-1289.

50.   Stoughton, R. B. <u>Applications of DNA microarrays in biology</u>. *Annu. Rev. Biochem.* **2005**, *74*, 53-82.

51.   Dufva, M. <u>Fabrication of high quality microarrays</u>. *Biomol. Eng.* **2005**, *22*, 173-184.

52.   Fodor, S. P. A.; Read, J. L.; Pirrung, M. C.; Stryer, L.; Lu, A. T.; Solas, D. <u>Light-directed, spatially addressable parallel chemical synthesis</u>. *Science* **1991**, *251*, 767-773.

53.   Butler, J. H.; Cronin, M.; Anderson, K. M.; Biddison, G. M.; Chatelain, F.; Cummer, M.; Davi, D. J.; Fisher, L.; Frauendorf, A. W.; Frueh, F. W.; Gjerstad, C.; Harper, T. F.; Kernahan, S. D.; Long, D. Q.; Pho, M.; Walker, J. A.; Brennan,

T. M. <u>In situ synthesis of oligonucleotide arrays by using surface tension</u>. *J. Am. Chem. Soc.* **2001**, *123*, 8887-8894.

54.   Hughes, T. R.; Mao, M.; Jones, A. R.; Burchard, J.; Marton, M. J.; Shannon, K. W.; Lefkowitz, S. M.; Ziman, M.; Schelter, J. M.; Meyer, M. R.; Kobayashi, S.; Davis, C.; Dai, H. Y.; He, Y. D. D.; Stephaniants, S. B.; Cavet, G.; Walker, W. L.; West, A.; Coffey, E.; Shoemaker, D. D.; Stoughton, R.; Blanchard, A. P.; Friend, S. H.; Linsley, P. S. <u>Expression profiling using microarrays fabricated by an ink-jet oligonucleotide synthesizer</u>. *Nat. Biotechnol.* **2001**, *19*, 342-347.

55.   Egeland, R. D.; Southern, E. M. <u>Electrochemically directed synthesis of oligonucleotides for DNA microarray fabrication</u>. *Nucleic Acids Res.* **2005**, *33*, e125.

56.   Piner, R. D.; Zhu, J.; Xu, F.; Hong, S. H.; Mirkin, C. A. <u>"Dip-pen" nanolithography</u>. *Science* **1999**, *283*.

57.   Lee, K. B.; Park, S. J.; Mirkin, C. A.; Smith, J. C.; Mrksich, M. <u>Protein nanoarrays generated by dip-pen nanolithography</u>. *Science* **2002**, *295*, 1702-1705.

58.   Xu, S.; Liu, G. Y. <u>Nanometer-scale fabrication by simulteneous nanoshaving and molecular self-assembly</u>. *Langmuir* **1997**, *13*, 127-129.

59.   Wadu-Mesthrige, K.; Xu, S.; Amro, N. A.; Liu, G. Y. <u>Fabrication and imaging of nanometer-sized protein patterns</u>. *Langmuir* **1999**, *15*, 8580-8583.

60.   Deegan, R. D.; Bakajin, O.; Dupont, T. F.; Huber, G.; Nagel, S. R.; Witten, T. A. <u>Capillary flow as the cuase of ring stains from dried liquid drops</u>. *Nature* **1997**, *389*, 827-829.

61.   Deng, Y.; Zhu, X.-Y. <u>Transport at the air/water interface is the reason for rings in protein microarrays</u>. *J. Am. Chem. Soc.* **2006**, *128*, 2768-2769.

62.   Okamoto, T.; Suzuki, T.; Yamamoto, N. <u>Microarray fabrication with covalent attachment of DNA using bubble ject technology</u>. *Nat. Biotechnol.* **2000**, *18*, 438-441.

63.   Allain, L. R.; Stratis-Cullum, D. N.; Vo-Dinh, T. <u>Investigation of microfabrication of biological sample arrays using piezoelectric and bubble-ject printing technologies</u>. *Anal. Chim. Acta* **2004**, *518*, 77-85.

64.   Xia, Y.; Whitesides, G. M. <u>Soft lithography</u>. *Angew. Chem. Int. Ed.* **1998**, *37*, 550-575.

65.   Xia, Y.; Whitesides, G. M. <u>Soft lithography</u>. *Annu. Rev. Mater. Sci.* **1998**, *28*, 153-184.

66.   Kane, R. S.; Takayama, S.; Ostuni, E.; Ingber, D. E.; Whitesides, G. M. <u>Patterning proteins and cells using soft lithography</u>. *Biomaterials* **1999**, *20*, 2363-2376.

67.   Dolnik, V.; Liu, S.; Jovanovich, S. <u>Capillary electrophoresis on microchip</u>. *Electrophoresis* **2000**, *21*, 41-54.

68.   Kutter, J. P. <u>Current developments in electrophoretic and chromatographic separation methods on microfabricated devices</u>. *Trends in Anal. Chem.* **2000**, *19*, 352-363.

69.   Wang, J. <u>From DNA biosensors to gene chips</u>. *Nucleic Acids Res.* **2000**, *28*, 3011-3016.

70.   Sanders, G. H. W.; Manz, A. <u>Chip-based microsystems for genomic and proteomic analysis</u>. *Trends in Anal. Chem.* **2000**, *19*, 364-378.

71.   Khandurina, J.; Guttman, A. <u>Bioanalysis in microfluidic devices</u>. *J. Chromatography A* **2002**, *943*, 159-183.

72. Chan, E. M.; Alivisatos, A. P.; Mathies, R. A. <u>High-temperature microfluidic synthesis of CdSe nanocrystals in nanoliter droplets</u>. *J. Am. Chem. Soc.* **2005**, *127*, 13854-13861.

73. Gunther, A.; Jensen, K. F. <u>Multiphase microfluidics: from flow characterics to chemical and materials synthesis</u>. *Lab Chip* **2006**, *6*, 1487-1503.

74. Okazaki, S. <u>Resolution limits of optical lithography</u>. *J. Vac. Sci. Technol. B* **1991**, *9*, 2829-2833.

75. Jeong, H. J.; Markle, D. A.; Owen, G.; Pease, F.; Grenville, A.; von Bunau, R. <u>The future of optical lithography</u>. *Solid State Technol.* **1994**, *37*, 39-47.

76. Kim, B.; Kwon, K.; Kwon, S.; Park, J.; Yoo, S. W.; Park, K.; Kim, B. <u>Modeling oxide etching in a magnetically enhanced reactive ion plasma using neural networks</u>. *J. Vac. Sci. Technol. B* **2002**, *20*, 2113-2119.

77. Fiorini, G. S.; Chiu, D. T. <u>Disposable microfluidic devices: fabrication, function, and application</u>. *Biotechniques* **2005**, *38*, 429-446.

78. Becker, H.; Gartner, C. <u>Polymer microfabrication methods for microfluidic analytical applications</u>. *Electrophoresis* **2000**, *21*, 12-26.

79. Duffy, D. C.; McDonald, J. C.; Schueller, O. J. A.; Whitesides, G. M. <u>Rapid prototyping of microfluidic systems in poly(dimethylsiloxane)</u>. *Anal. Chem.* **1998**, *70*, 4974-4984.

80. Duffy, D. C.; Schueller, O. J. A.; Brittain, S. T.; Whitesides, G. M. <u>Rapid prototyping of microfluidic swithes in poly(dimethylsiloxane) and their actuation by electro-osmotic flow</u>. *J. Micromech. Microeng.* **1999**, *9*, 211-217.

81. Anderson, J. R.; Chiu, D. T.; Jackman, R. J.; Cherniavskaya, O.; McDonald, J. C.; Wu, H.; Whitesides, S. H.; Whitesides, G. M. <u>Fabrication of topologically</u>

complex three-dimensional microfluidic systems in PDMS by rapid prototyping. *Anal. Chem.* **2000**, *72*, 3158-3164.

82. McDonald, J. C.; Whitesides, G. M. Poly(dimethylsiloxane) as a material for fabricating microfluidic devices. *Acc. Chem. Res.* **2002**, *35*, 491-499.

83. Sia, S. K.; Whitesides, G. M. Microfluidic devices fabricated in poly(dimethylsiloxane) for biological studies. *Electrophoresis* **2003**, *24*, 3563-3576.

84. Nkodo, A. E.; Garnier, J. M.; Tinland, B.; Ren, H.; Desruisseaux, C.; McCormick, L. C.; Drouin, G.; Slater, G. W. Diffusion coefficient of DNA molecules during free solution electrophoresis. *Electrophoresis* **2001**, *22*, 2424-2432.

85. Cheek, B. J.; Steel, A. B.; Torres, M. P.; Yu, Y.; Yang, H. Chemiluminescence detection for hybridization assays on the flow-thru chip, a three-dimensional microchannel biochip. *Anal. Chem.* **2001**, *76*, 5777-5783.

86. Hashimoto, M.; Barany, F.; Soper, S. A. Polymerase chain reaction/ligase detection reaction/hybridization assays using flow-through microfluidic devices for the detection of low-abundant DNA point mutations. *Biosens. Bioelectron.* **2006**, *21*, 1915-1923.

87. Seong, G. H.; Crooks, R. M. Efficient mixing and reactions within microfluidic channels using microbead-supported catalysts. *J. Am. Chem. Soc.* **2002**, *124*, 13360-13361.

88. Seong, G. H.; Zhan, W.; Crooks, R. M. Fabrication of microchambers defined by photopolymerized hydrogels and weirs within microfluidic systems: Application to DNA hybridization. *Anal. Chem.* **2002**, *74*, 3372-3377.

149

89. Fan, Z. H.; Mangru, S.; Granzow, R.; Heaney, P.; Ho, W.; Dong, Q.; Kumar, R. Dynamic DNA hybridization on a chip using paramagnetic beads. *Anal. Chem.* **1999**, *71*, 4851-4859.

90. Ali, M. F.; Kirby, R.; Goodey, A. P.; Rodriguez, M. D.; Ellington, A. D.; Neikirk, D. P.; McDevitt, J. T. DNA hybridization and discrimination of single-nucleotide mismatches using chip-based microbead arrays. *Anal. Chem.* **2003**, *75*, 4732-4739.

91. Kohara, Y.; Noda, H.; Okano, K.; Kambara, H. DNA probes on beads arrayed in a capillary, 'Bead-array', exhibited high hybridization performance. *Nucleic Acids Res.* **2002**, *30*, e87.

92. Verpoorte, E. Beads and chips: New recipes for analysis. *Lab Chip* **2003**, *3*, 60N-68N.

93. Kyriakou, G.; Davis, D. J.; Grant, R. B.; Watson, D. J.; Keen, A.; Tikhov, M. S.; Lambert, R. M. Electron impact-assisted carbon film growth on Ru(0001): Implications for next-generation EUV lithography. *J. Phys. Chem. C* **2007**, *111*, 4491-4494.

94. Joo, J.; Chow, B. Y.; Jacobson, J. M. Nanoscale patterning on insulating substrates by critical energy electron beam lithography. *Nano Lett.* **2006**, *6*, 2021-2025.

95. Klauser, R.; Huang, M.; Wang, S.; Chen, C.; Chuang, T. J.; Terfort, A.; Zharnikov, M. Lithography with a focused soft X-ray beam and a monomolecular resist. *Langmuir* **2004**, *20*, 2050-2053.

96. Beebe, D. J.; Moore, J. S.; Bauer, J. M.; Yu, Q.; Liu, R. H.; Devadoss, C.; Jo, B. Functional hydrogel structures for autonomous flow control inside microfluidic channels. *Nature* **2000**, *404*, 588-590.

97. Revzin, A.; Russell, R. J.; Yadavalli, V. K.; Koh, W.; Deister, C.; Hile, D. D.; Mellott, M. B.; Pishko, M. V. Fabrication of poly(ethylene glycol) hydrogel microstructures using photolithography. *Langmuir* **2001**, *17*, 5440-5447.

98. Dhopeshwarkar, R., *Electrokinetic concentration enrichment within a microfluidic device integrated with a hydrogel microplug*, in *Chemical Engineering*. 2007, Texas A&M University: College Station.

99. Xia, Y.; McClelland, J. J.; Gupta, R.; Qin, D.; Zhao, X.; Sohn, L. L.; Celotta, R. J.; Whitesides, G. M. Replica molding using polymeric materials: A practical step toward nanomanufacturing. *Adv. Mater*. **1997**, *9*, 147-149.

100. Favis, R.; Day, J. P.; Gerry, N. P.; Phelan, C.; Narod, S.; Barany, F. Universal DNA Array Detection of Small Insertions and Deletions in BRCA1 and BRCA2. *Nat. Biotechnol*. **2000**, *18*, 561-564.

101. Gerry, N. P.; Witowski, N. E.; Day, J.; Hammer, R. P.; Barany, G.; Barany, F. Universal DNA Microarray Method for Multiplex Detection of Low Abundance Point Mutations. *J. Mol. Biol*. **1999**, *292*, 251-262.

102. Yu, A. A.; Savas, T. A.; Taylor, G. S.; Guiseppe-Elie, A.; Smith, H. I.; Stellacci, F. Supramolecular nanostamping: Using DNA as movable type. *Nano Lett*. **2005**, *5*, 1061-1064.

103. Yu, A. A.; Sava, T.; Cabrini, S.; di Fabrizio, E.; Smith, H. I.; Stellacci, F. High resolution printing of DNA feature on poly(dimethyl methacrylate) substrate using supramolecular nano-stamping. *J. Am. Chem. Soc*. **2005**, *127*, 16774-16775.

104. Albrecht, C.; Blank, K.; Lalic-Myelthaler, M.; Hirler, S.; Mai, T.; Gilbert, I.; Schiffmann, S.; Bayer, T.; Clausen-Schaumann, H.; Gaub, H. E. DNA: A Programmable Force Sensor. *Science* **2003**, *301*, 367-370.

105. Blank, K.; Mai, T.; Gilbert, I.; Schiffmann, S.; Rankl, J.; Zivin, R.; Tackney, C.; Nicolaus, T.; Spinnler, K.; Oesterhelt, F.; Benoit, M.; Clausen-Schaumann, H.; Gaub, H. E. A Force-based Protein Biochip. *Proc. Natl. Acad. Sci. USA* **2003**, *100*, 11356-11360.

106. Lockhart, D. J.; Dong, H.; Byrne, M. C.; Follettie, M. T.; Gallo, M. V.; Chee, M. S.; Mittmann, M.; Wang, C.; Kobayashi, M.; Horton, H.; Brown, E. L. Expression Monitoring by Hybridization to High-density Oligonucleotide Arrays. *Nat. Biotechnol.* **1996**, *14*, 1675-1680.

107. Stegmaier, K.; Ross, K. N.; Colavito, S. A.; O'Malley, S.; Stockwell, B. R.; Golub, T. R. Gene Expression-based High-throughput Screening (GE-HTS) and Application to Leukemia Differentiation. *Nat. Genet.* **2004**, *36*, 257-263.

108. Hacia, J. G.; Brody, L. C.; Chee, M. S.; Fodor, S. P.; Collins, F. S. Detection of Heterozygous Mutations in BRCA1 Using High Density Oligonucleotide Arrays and Two-colour Fluorescence Analysis. *Nat. Genet.* **1996**, *14*, 441-447.

109. Golub, T. R.; Slonim, D. K.; Tamayo, P.; Huard, C.; Gaasenbeek, M.; Mesirov, J. P.; Coller, H.; Loh, M. L.; Downing, J. R.; Caligiuri, M. A.; Bloomfield, C. D.; Lander, E. S. Molecular Classification of Cancer: Class Discovery and Class Prediction by Gene Expression Monitoring. *Science* **1999**, *286*, 531-537.

110. Pirrung, M. C. Spatially Addressable Combinatorial Libraries. *Chem. Rev.* **1997**, *97*, 473-488.

111. Lombardi, S. From Genome Sequence to Genome Understanding. *PharmaGenomics* **2004**, *September*, 25-31.

112. Affara, N. A. Resource and Hardware Options for Microarray-based Experimentation. *Briefings in Functional Genomics & Proteomics* **2003**, *2*, 7-20.

113. McQuain, M. K.; Seale, K.; Peek, J.; Levy, S.; Haselton, F. R. <u>Effects of Relative Humidity and Buffer Additives on the Contact Printing of Microarrays by Quill Pins</u>. *Anal. Biochem.* **2003**, *320*, 281-291.

114. Okamoto, T.; Suzuki, T.; Yamamoto, N. <u>Microarray Fabrication with Covalent Attachment of DNA Using Bubble Jet Technology</u>. *Nat. Biotechnol.* **2000**, *18*, 438-441.

115. Flavell, A. J.; Bolshakov, V. N.; Booth, A.; Jing, R.; Russell, J.; Ellis, T. H. N.; Isaac, P. <u>A Microarray-based High Throughput Molecular Marker Genotyping Method: the Tagged Microarray Marker (TAM) Approach</u>. *Nucleic Acids Res.* **2003**, *31*, e115.

116. Lee, H. J.; Goodrich, T. T.; Corn, R. M. <u>SPR Imaging Measurements of 1-D and 2-D DNA Microarrays Created from Microfluidic Channels on Gold Thin Films</u>. *Anal. Chem.* **2001**, *73*, 5525-5531.

117. Lange, S. A.; Benes, V.; Kern, D. P.; Horber, J. K. H.; Bernard, A. <u>Microcontact Printing of DNA Molecules</u>. *Anal. Chem.* **2004**, *76*, 1641-1647.

118. Bullen, D.; Chung, S.-W.; Wang, X.; Zou, J.; Mirkin, C. A.; Liu, C. <u>Parallel Dip-pen Nanolithography with Arrays of Individually Addressable Cantilevers</u>. *Appl. Phys. Lett.* **2003**, *84*, 789-791.

119. Demers, L. M.; Ginger, D. S.; Park, S.-J.; Li, Z.; Chung, S.-W.; Mirkin, C. A. <u>Direct Patterning of Modified Oligonucleotides on Metals and Insulators by Dip-Pen Nanolithography</u>. *Science* **2002**, *296*, 1836-1838.

120. Yu, A. A.; Stellacci, F. <u>Stamping with high information density</u>. *J. Mater. Chem.* **2006**, *16*, 2868-2870.

121. Kim, S.; Lim, G.; Lee, S. E.; Lee, J.; Yun, K.; Park, J. <u>DNA chip replication for a personalized DNA chip</u>. *Biomol. Eng.* **2006**, *23*, 129-134.

122. Wang, K.; Koop, B. F.; Hood, L. A simple method using T4 DNA polymerase to clone polymerase chain reaction products. *BioTechniques* **1994**, *17*, 236-238.

123. Challberg, M. D.; Englund, P. T. Specific labeling of 3' termini with T4 DNA polymerase. *Methods Enzymol*. **1980**, *65*, 39-43.

124. Herne, T. M.; Tarlov, M. J. Characterization of DNA probes immobilized on gold surfaces. *J. Am. Chem. Soc*. **1997**, *119*, 8916-8920.

125. Conzone, S. D.; Pantano, C. G. Glass slides to DNA microarrays. *Mater*. *Today* **2004**, *7*, 20-26.

126. Kumar, A.; Goel, G.; Fehrenbach, E.; Puniya, A. K.; Singh, K. Microarrays: The technology, analysis, and application. *Eng*. *Life Sci*. **2005**, *5*, 215-222.

127. Campo, A. D.; Bruce, I. J. Substrate patterning and activation strategies for DNA chip fabrication. *Top*. *Curr*. *Chem*. **2005**, *260*, 77-111.

128. Singh-Gasson, S.; Green, R. D.; Yue, Y.; Nelson, C.; Blattner, F.; Sussman, M. R.; Cerrina, F. Maskless fabrication of light-directed oligonucleotide microarrays using a digital micromirror array. *Nat*. *Biotechnol*. **1999**, *17*, 974-978.

129. Vrana, K. E.; Freeman, W. M.; Aschner, M. Use of microarray technologies in toxicology research. *NeuroToxicology* **2003**, *24*, 321-332.

130. Demers, L. M.; Ginger, D. S.; Park, S. J.; Li, Z.; Chung, S. W.; Mirkin, C. A. Direct patterning of modified oligonucleotides on metals and insulators by dip-pen nanolithography. *Science* **2002**, *296*, 1836-1838.

131. Xu, S.; Liu, G. Nanometer-scale fabrication by simultaneous nanoshaving and molecular self-assembly. *Langmuir* **1997**, *13*, 127-129.

132. Schwartz, P. V. Meniscus force nanografting: Nanoscopic patterning of DNA. *Langmuir* **2001**, *17*, 5971-5977.

133. Lange, S. A.; Benes, V.; Kern, D. P.; Heinrich Hörber, J. K.; Bernard, A. Microcontact printing of DNA molecules. *Anal*. *Chem*. **2004**, *76*, 1641-1647.

134. McDonald, J. C.; Duffy, D. C.; Anderson, J. R.; Chiu, D. T.; Wu, H.; Schueller, O. J. A.; Whitesides, G. M. Fabrication of microfluidic systems in poly(dimethylsiloxane). *Electrophoresis* **2000**, *21*, 27-40.

135. Antson, D.-O.; Barbany, G.; Landegren, U.; Nilsson, M. RNA-templated DNA ligation for transcript analysis. *Nucleic Acids Res*. **2001**, *29*, 578-581.

136. Clepet, C.; Le Clainche, I.; Caboche, M. Improved full-length cDNA production based on RNA tagging by T4 DNA ligase. *Nucleic Acids Res*. **2004**, *32*, e6.

137. Lee, H. J.; Wark, A. W.; Li, Y.; Corn, R. M. Fabricating RNA microarrays with RNA-DNA surface ligation chemistry. *Anal*. *Chem*. **2005**, *77*, 7832-7837.

138. Goodrich, T. T.; Lee, H. J.; Corn, R. M. Direct detection of genomic DNA by enzymatically amplified SPR imaging measurements of RNA microarrays. *J*. *Am*. *Chem*. *Soc*. **2004**, *126*, 4086-4087.

139. Goodrich, T. T.; Lee, H. J.; Corn, R. M. Enzymatically amplified surface plasmon resonance imaging method using RNase H and RNA microarrays for the ultrasensitive detection of nucleic acids. *Anal*. *Chem*. **2004**, *76*, 6173-6178.

140. Cho, E. J.; Collett, J. R.; Szafranska, A. E.; Ellington, A. D. Optimization of aptamer microarray technology for multiple protein targets. *Anal*. *Chim*. *Acta* **2006**, *564*, 82-90.

141. McCauley, T. G.; Hamaguchi, N.; Stanton, M. Aptamer-based biosensor arrays for detection and quantification of biological macromolecules. *Anal*. *Biochem*. **2003**, *319*, 244-250.

142. Li, Y.; Lee, H. J.; Corn, R. M. Detection of protein biomarkers using RNA aptamer microarrays and enzymatically amplified surface plasmon resonance imaging. *Anal. Chem.* **2007**, *79*, 1082-1088.

143. Collett, J. R.; Cho, E. J.; Ellington, A. D. Production and processing of aptamer microarrays. *Methods* **2005**, *37*, 4-15.

144. Collett, J. R.; Cho, E. J.; Lee, J. F.; Levy, M.; Hood, A. J.; Wan, C.; Ellington, A. D. Functional RNA microarrays for high-throughput screening of antiprotein aptamers. *Anal. Biochem.* **2005**, *338*, 113-123.

145. Lee, H. J.; Wark, A. W.; Corn, R. M. Creating advanced multifunctional biosensors with surface enzymatic transformations. *Langmuir* **2006**, *22*, 5241-5250.

146. Li, Y.; Lee, H. J.; Corn, R. M. Fabrication and characterization of RNA aptamer microarrays for the study of protein-aptamer interactions with SPR imaging. *Nucleic Acids Res.* **2006**, *34*, 6416-6424.

147. Zammatteo, N.; Alexandre, I.; Ernest, I.; Le, L.; Brancart, F.; Remacle, J. Comparison between microwell and bead supports for the detection of human cytomegalovirus amplicons by sandwich hybridization. *Anal. Biochem.* **1997**, *253*, 180-189.

148. Sato, K.; Tokeshi, M.; Odake, T.; Kimura, H.; Ooi, T.; Nakao, M.; Kitamori, T. Integration of an immunosorbent assay system: Analysis of secretory human immunoglobulin A on polystyrene beads in a microchip. *Anal. Chem.* **2000**, *72*, 1144-1147.

149. Huang, S.; Stump, M. D.; Weiss, R.; Caldwell, K. D. Binding of biotinylated DNA to streptavidin-coated polystyrene latex: Effects of chain length and particle size. *Anal. Biochem.* **1996**, *237*, 115-122.

150. Walsh, M. K.; Wang, X.; Weimer, B. C. <u>Optimizing the immobilization of single-stranded DNA onto glass beads</u>. *J. Biochem. Bioph. Methods* **2001**, *47*, 221-231.

151. Kohara, Y. <u>Hybridization reaction kinetics of DNA probes on beads arrayed in a capillary enhanced by turbulent flow</u>. *Anal. Chem.* **2003**, *75*, 3079-3085.

152. Kwakye, S.; Baeumner, A. <u>A microfluidic biosensor based on nucleic acid sequence recognition</u>. *Anal. Bioanal. Chem.* **2003**, *376*, 1062-1068.

153. Gabig-Ciminska, M.; Holmgren, A.; Andresen, H.; Bundvig Barken, K.; Wümpelmann, M.; Albers, J.; Hintsche, R.; Breitenstein, A.; Neubauer, P.; Los, M.; Czyz, A.; Wegrzyn, G.; Silfversparre, G.; Jürgen, B.; Schweder, T.; Enfors, S.-O. <u>Electric chips for rapid detection and quantification of nucleic acids</u>. *Biosens. Bioelectron.* **2004**, *19*, 537-546.

154. Smistrup, K.; Kjeldsen, B. G.; Reimers, J. L.; Dufva, M.; Petersen, J.; Hansen, M. F. <u>On-chip magnetic bead microarray using hydrodynamic focusing in a passive magnetic separator</u>. *Lab Chip* **2005**, *5*, 1315-1319.

155. Goral, V. N.; Zaytseva, N. V.; Baeumner, A. J. <u>Electrochemical microfluidic biosensor for the detection of nucleic acid sequences</u>. *Lab Chip* **2006**, *6*, 414-421.

156. Steel, A. B.; Herne, T. M.; Tarlov, M. J. <u>Electrochemical quantitiation of DNA immobilized on gold</u>. *Anal. Chem.* **1998**, *70*, 4670-4677.

157. Peterson, A. W.; Heaton, R. J.; Georgiadis, R. M. <u>The effect of surface probe density on DNA hybridization</u>. *Nucleic Acids Res.* **2001**, *29*, 5163-5168.

158. Lemieux, B.; Aharoni, A.; Schena, M. <u>Overview of DNA chip technology</u>. *Mol. Breed.* **1998**, *4*, 277-289.

159. Gerhold, D.; Rushmore, T.; Caskey, C. T. <u>DNA chips: Promising toys have become powerful tools</u>. *Trends Biochem. Sci.* **1999**, *24*, 168-173.

160. Marx, J. <u>DNA arrays reveal cancer in its many forms</u>. *Science* **2000**, *289*, 1670-1672.

161. For DNA hybridization experiments with different concentrations of target solution, the following sequences of probes and targets were used to avoid quenching of fluorescein due to a proximal guanine base. The terminal bases on each sequence were exchanged with each other. The ratio of bases was unchanged. ss-DNA probe: 5' (Biotin-TEG) CGT TGA GGG GAC TTT CCC AGG C 3'; ss-DNA complementary target: 5' (6-FAM) TCC TGG GAA AGT CCC CTC AAC T 3'.

162. Calculated value (number of beads/μL x flow rate x packing time) assuming a 25 s packing time. Bead solution: 3.0×10^{-7} g/μL; number of beads/gram: 1.829×10^9; flow rate for packing beads: 10.0 μL/min.

163. Holden, M. A.; Kumar, S.; Beskok, A.; Cremer, P. S. <u>Microfluidic diffusion diluter: Bulging of PDMS microchannels under pressure-driven flow</u>. *J. Micromech. Microeng.* **2003**, *13*, 412-418.

164. Calculated using the binding capacity (0.021 μg biotin-FITC/mg microbeads), molecular weight of biotin-FITC (831 Daltons), and number of beads per gram (1.829×10^9). These values are provided by the manufacturer.

165. From the calculated surface area (1.5×10^{-13} cm^2/probe: width x length) to accommodate a 22-mer duplex DNA based on the size of the duplex having length of 3.4 nm/10 bases and diameter of 2.0 nm.

166. Watson, J. D.; Crick, F. H. C. <u>Molecular structure of nucleic acids: A structrue for deoxyibose nucleic acid</u>. *Nature* **1953**, *171*, 737-738.

167. Edman, C. F.; Raymond, D. E.; Wu, D. J.; Tu, E.; Sosnowski, R. G.; Butler, W. F.; Nerenberg, M.; Heller, M. Electric field directed nucleic acid hybridization on microchips. *Nucleic Acids Res*. **1997**, *25*, 4907-4914.

168. Liu, Y.; Rauch, C. B. DNA probe attachment on plastic surfaces and microfluidic hybridization array channel devices with sample oscillation. *Anal. Biochem*. **2003**, *317*, 76-84.

169. Yuen, P. K.; Li, G.; Bao, Y.; Müller, U. R. Microfluidic devices for fluidic circulation and mixing improve hybridization signal intensity on DNA arrays. *Lab Chip* **2003**, *3*, 46-50.

170. Calculated solution volume of bead bed (solution volume in the open chamber - total bead volume in the chamber) and of the open microchamber (π x radius^2 x channel height). Total bead volume in the chamber: 1.03 nL; radius of the chamber: 150 μm. channel height: 21 μm. .

171. Calculated total surface area of all beads in the microchamber (surface area per bead x number of beads in the chamber) and bottom surface area of the open microchamber (π x radius^2). Probes are assumed to be immobilized only on the bottom surface of the open chamber. Surface area per bead: 311.0 μm^2/bead; number of beads in the chamber: 2 x 10^3 beads; radius of the chamber: 150 μm.

172. Weber, S. G.; Purdy, W. C. The behaviour of an electrochemical detector used in liquid chromatography and continuous flow voltammetry. *Anal. Chim. Acta* **1978**, *100*, 531-544.

173. Sjölander, S.; Urbaniczky, C. Integrated fluid handling system for biomolecular interaction analysis. *Anal. Chem*. **1991**, *63*, 2338-2345.

174. Seong, G.; Zhan, W.; Crooks, R. M. Fabrication of microchambers defined by photopolymerized hydrogels and weirs within microfluidic systems: Application to DNA hybridization. *Anal. Chem.* **2002**, *74*, 3372-3377.

175. Hoffman, A. S. Hydrogels for biomedical applications. *Adv. Drug Delivery Rev.* **2002**, *43*, 3-12.

176. Ahn, S.; Walt, D. R. Detection of Salmonella spp. using microsphere-based, fiber-optic DNA microarrays. *Anal. Chem.* **2005**, *77*, 5041-5047.

177. Chen, Y.; Chen, Y.; Lii, H.; Z., L. Chemiluminescence detection of Epstein-Barr virus DNA with an oligonucleotide probe. *Clin. Chim. Acta* **2000**, *298*, 45-53.

178. Korimbocus, J.; Scaramozzino, N.; lacroix, B.; Crance, J. M.; Garin, D.; Vernet, G. DNA probe array for the simultaneous identification of Herpesviruses, Enteroviruses, and Flaviviruses. *J. Clin. Microbiol.* **2005**, 3779-3787.

179. Wang, J. Microchip devices for detecting terrorist weapons. *Anal. Chim. Acta* **2004**, *507*, 3-10.

180. Diamandis, E. P. Analytical methodology for immunoassays and DNA hybridization assays - Current status and selected systems - Critical review. *Clin. Chim. Acta* **1990**, *194*, 19-50.

181. Zhao, X.; Tapec-Dytioco, R.; Tan, W. Ultrasensitive DNA detection using highly fluorescent bioconjugated nanoparticles. *J. Am. Chem. Soc.* **2003**, *125*, 11474-11475.

182. Nam, J.; Stoeva, S. I.; Mirkin, C. A. Bio-bar-code-based DNA detection with PCR-like sensitivity. *J. Am. Chem. Soc.* **2004**, *126*, 5932-5933.

183. Saghatelian, A.; Guckian, K. M.; Thayer, D. A.; Ghadiri, M. R. DNA detection and signal amplification via an engineered allosteric enzyme. *J. Am. Chem. Soc.* **2003**, *125*, 344-345.

184. Patolsky, F.; Ranjit, K. T.; Lichtenstein, A.; Willner, I. <u>Dendritic amplification of DNA analysis by oligonucleotide-functionalized Au-nanoparticles</u>. *Chem. Commun.* **2000**, 1025-1026.

185. Dominguez, E.; Rincon, O.; Arantzazu, N. <u>Electrochemical DNA sensors based on enzyme dendritic architectures: an approach for enhanced sensitivity</u>. *Anal. Chem.* **2004**, *76*, 3132-3138.

186. Fan, Z. H.; Mangru, S.; Granzow, R.; Heaney, P.; Ho, W.; Dong, Q.; Kumar, R. <u>Dynamic DNA hybridization on a chip using paramagnetic beads</u>. *Anal. Chem.* **1999**, *71*, 4851-4859.

187. Charles, P. T.; Vora, G. J.; Andreadis, J. D.; Fortney, A. J.; Meador, C. E.; Dulcey, C. S.; Stenger, D. A. <u>Fabrication and surface characterization of DNA microarrays using amine- and thiol-terminated oligonucleotide probes</u>. *Langmuir* **2003**, *19*, 1586-1591.

188. Duffy, D. C.; McDonald, J. C.; Schueller, J. A.; Whitesides, G. M. <u>Rapid prototyping of microfluidic systems in poly(dimethylsiloxane)</u>. *Anal. Chem.* **1998**, *70*, 4974-4984.

189. Erickson, D.; Liu, X.; Venditti, R.; Li, D.; Krull, U. <u>Electrokinetically based approach for single-nucleotide polymorphism discrimination using a microfluidic device</u>. *Anal. Chem.* **2005**, *77*, 4000-4007.

Vita

Joohoon Kim was born in Seoul, Korea on February 20, 1976, the son of Soonhwa Park and Dalyeon Kim. He entered Seoul National University (SNU) in 1994. During his undergraduate period, he taught chemistry in the Women's Middle School affiliated with SNU as an internship teacher and obtained a teaching certificate. He received a Bachelor of Science degree in Chemistry Education and started his graduate studies in the Department of Chemistry (SNU) in 1998. He carried out two projects as a research assistant under the guidance of Professor Hasuck Kim: "Project of Developing New Energy Source" organized by LG-Caltex Oil Corp. and "G-7 Future Automobile Project" supported by Korea Automotive Technology Institute. After receiving a Master of Science degree in Chemistry in 2000, he served in the Air Force as an officer (Rank: 1st Lieut.) until 2003. Now, he is expected to receive his doctoral degree (Doctor of Philosophy, Ph.D.) under the guidance of Professor Richard M. Crooks from the University of Texas at Austin (Department of Chemistry and Biochemistry) in 2007. During his doctoral graduate studies, he published multiple journal articles and filed one US provisional patent. He was awarded a Graduate Fellowship from the American Chemical Society-Division of Analytical Chemistry (ACS-DAC) in 2007. Upon completion of his Ph.D., he is going to work as a postdoctoral fellow under the direction of Professor Milan Mrksich in the University of Chicago (Department of Chemistry) in September of 2007.

Permanent address: Seocho-gu Bangbae 3-Dong Raemian Tower 201-1105 Seoul Korea

This dissertation was typed by Joohoon Kim.